

Nonoptimal Microbial Response to Antibiotics Underlies Suppressive Drug Interactions

Tobias Bollenbach,¹ Selwyn Quan,³ Remy Chait,¹ and Roy Kishony^{1,2,*}

¹Department of Systems Biology, Harvard Medical School, 200 Longwood Avenue, Boston, MA 02115, USA

²School of Engineering and Applied Sciences, Harvard University, Cambridge, MA 02138, USA

³Department of Chemical and Systems Biology, Stanford University, 318 Campus Drive, Stanford, CA 94305, USA

*Correspondence: roy_kishony@hms.harvard.edu

DOI 10.1016/j.cell.2009.10.025

SUMMARY

Suppressive drug interactions, in which one antibiotic can actually help bacterial cells to grow faster in the presence of another, occur between protein and DNA synthesis inhibitors. Here, we show that this suppression results from nonoptimal regulation of ribosomal genes in the presence of DNA stress. Using GFP-tagged transcription reporters in *Escherichia coli*, we find that ribosomal genes are not directly regulated by DNA stress, leading to an imbalance between cellular DNA and protein content. To test whether ribosomal gene expression under DNA stress is nonoptimal for growth rate, we sequentially deleted up to six of the seven ribosomal RNA operons. These synthetic manipulations of ribosomal gene expression correct the protein-DNA imbalance, lead to improved survival and growth, and completely remove the suppressive drug interaction. A simple mathematical model explains the nonoptimal regulation of ribosomal genes under DNA stress as a side effect of their optimal regulation in different nutrient environments. These results reveal the genetic mechanism underlying an important class of suppressive drug interactions.

INTRODUCTION

Drug combinations can be an important tool for studying biological systems and revealing relationships between different cellular processes (Keith et al., 2005; Lehár et al., 2008, 2007; Tsui et al., 2004). The interaction between two drugs can be classified as additive, synergistic, or antagonistic according to their combined effect being equal, greater, or less than that expected based on their individual effects, Figure 1A (Bliss, 1939; Loewe, 1928, 1953; Pillai et al., 2005). Much attention has been given to synergistic drug combinations due to their increased potency. Antagonism, however, may have an advantage in slowing down and even reversing the evolution of resistance

(Chait et al., 2007; Hegreness et al., 2008; Michel et al., 2008; Yeh et al., 2006).

A particularly strong kind of antagonism, termed “suppression,” occurs when the combined inhibitory effect of two drugs is not only weaker than the expected additive sum, but also weaker than the effect of one of the drugs alone (Figure 1A; Pillai et al., 2005). We have previously reported that in the presence of a DNA synthesis-inhibiting antibiotic, the addition of a protein synthesis inhibitor increases the steady state growth rate of *Escherichia coli* (Figure 1B) and *Staphylococcus aureus* (Chait et al., 2007; Yeh et al., 2006). Many different pairings of DNA synthesis and translation inhibitors show this suppressive drug interaction (Yeh et al., 2006; see examples in Figures 1B and S1 available online), indicating that these interactions result from the effect of the drugs on bacterial physiology rather than from direct chemical interaction between the drugs. Considerable recent work has advanced our understanding of the effects of individual antibiotics on gene expression and cellular physiology (Brazas and Hancock, 2005; Davies et al., 2006; Drlica et al., 2008; Fajardo and Martinez, 2008; Goh et al., 2002; Hoffman et al., 2005; Kohanski et al., 2007, 2008; Kolodkin-Gal et al., 2008; Linares et al., 2006; Mason et al., 1995; Mesak et al., 2008; Piddock et al., 1990; Shaw et al., 2003; Yim et al., 2006; Yim et al., 2007), but the effects of drug combinations are less well understood and the mechanism that underlies suppressive drug interactions remains unknown.

It has been argued that many aspects of bacterial physiology have evolved to be ‘optimal’ - namely to maximize growth rate in a given condition (Dekel and Alon, 2005; Ibarra et al., 2002; Liebermeister et al., 2004). When protein synthesis inhibitors are added to DNA synthesis inhibitors, however, the cells actually grow faster. Thus, the overall rate of protein synthesis under DNA stress appears to be above the optimal value for maximum growth. This overall rate of protein synthesis is primarily determined by the number of ribosomes per cell, which is known to be tightly controlled (Gralla, 2005; Keener and Nomura, 1996; Moss, 2004; Paul et al., 2004). Precise regulation of ribosome synthesis is crucial for maximizing growth: under-production of ribosomes causes ineffective use of cellular resources, while over-production leads to an excess use of resources for protein synthesis at the expense of other cellular processes (Gralla, 2005; Keener and Nomura, 1996; Levy et al., 2007; Paul et al., 2004). As a result, in any particular environment, there exists

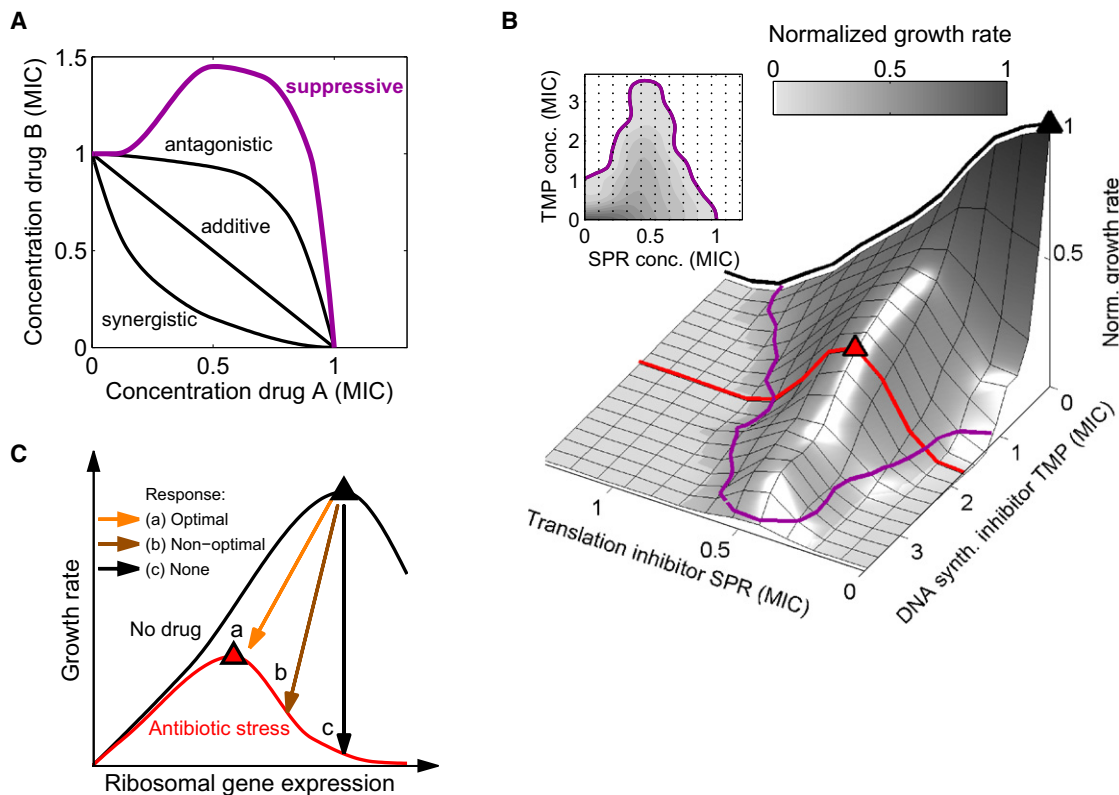


Figure 1. Suppression of DNA Synthesis Inhibitors by Translation Inhibitors Suggests the Hypothesis that Ribosomal Genes Are Not Optimally Regulated under DNA Stress

(A) Minimal Inhibitory Concentration (MIC) lines in the two-dimensional concentration space of two drugs. Two drugs are defined to interact additively if their combined effect is constant along linear lines of fixed total dosage (Loewe, 1928). Synergy and antagonism are defined as negative or positive deviations from this null line. A particularly strong type of antagonism—suppression—characterizes drug pairs whose combined effect is weaker than that of one of the drugs alone (magenta line).

(B) Suppressive interaction is seen in measurements of growth rates (gray levels) and MIC line (magenta) in a two-dimensional gradient of the translation inhibitor spiramycin (SPR) and the DNA synthesis inhibitor trimethoprim (TMP, inhibitor of DNA synthesis through folic acid deficiency). In the absence of DNA synthesis inhibitor (black line), growth rate is maximal without translation inhibition (black triangle) and reduces monotonically with the level of translation inhibitor. In contrast, at fixed finite concentration of DNA synthesis inhibitor (red line), growth rate increases initially as the translation inhibitor concentration increases, reaching a maximal value (red triangle) at intermediate translation inhibition level.

(C) Schematic expectation for growth rate as a function of ribosomal gene expression in absence (black line) or presence (red line) of an antibiotic. Arrows show possible ribosomal gene expression regulation in response to antibiotic addition. The comparison of panels (B) and (C) suggests the hypothesis that a nonoptimal, too high ribosome level in response to DNA synthesis inhibitors may cause this suppressive drug interaction. MICs for antibiotics are summarized in Table 1.

an optimal level of ribosomes that maximizes the bacterial growth rate (Figure 1C). The observation that, under DNA stress, reduction in protein synthesis allows faster growth suggests that ribosome level is not optimally regulated in these conditions.

The rate of ribosome synthesis in *E. coli* is determined by the transcription rate of the ribosomal RNA operons (*rrn* operons; Keener and Nomura, 1996; Paul et al., 2004), which code for the three different ribosomal RNAs. Feedback mechanisms at the level of translation adjust ribosomal protein synthesis to stoichiometrically match rRNA production (Keener and Nomura, 1996). The standard *E. coli* lab strain K12 MG1655 has seven almost identical copies of the *rrn* operons, which are among the most highly transcribed loci in the genome. Multiple copies are needed because the maximal transcription rate from a single *rrn* operon is insufficient for the ribosome synthesis required at high growth rates (Condon et al., 1995; Stevenson and Schmidt, 2004).

The *rrn* operons are regulated to achieve maximal growth in different nutrient environments. The levels of factors that reflect intracellular levels of resources such as amino acids and energy, including nucleoside triphosphates (NTPs), guanosine pentaphosphate and tetraphosphate (collectively referred to as ppGpp), affect *rrn* transcription (Cashel et al., 1996; Dennis et al., 2004; Gaal et al., 1997; Keener and Nomura, 1996; Paul et al., 2004; Schneider et al., 2002; Schneider and Gourse, 2004). Overproduction of protein depletes these resources and thus downregulates ribosome synthesis (Gralla, 2005; Paul et al., 2004). In many environmental conditions, this negative feedback loop is able to maintain ribosome concentration near its optimal level (the level that maximizes growth rate); in particular, ribosome synthesis is kept high in nutrient-rich environments and is shut down as a consequence of nutrient starvation (Cashel et al., 1996). However, it is unclear if the regulation of

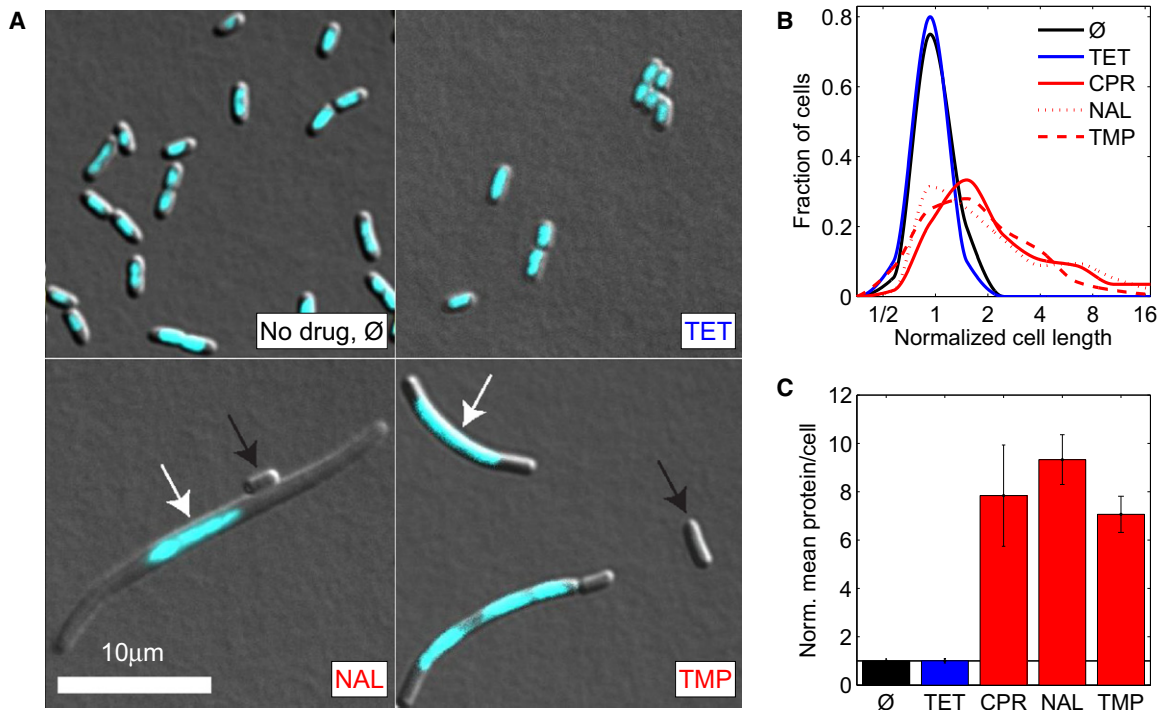


Figure 2. DNA Synthesis Inhibitors Lead to Increased Cell Size and Protein-DNA Ratio

(A) Microscopy images of DAPI stained (cyan) *E. coli* cells growing in absence of antibiotics (\emptyset) and in presence of translation inhibitor TET and DNA synthesis inhibitors NAL and TMP. Scale bar, 10 μ m. DNA synthesis inhibitors lead to a mixed population of cells that are larger and contain only one or few nucleoids (white arrows). A small fraction of cells has no nucleoid (black arrows).

(B) Histograms of cell lengths. Mean cell size and variability increases in presence of DNA synthesis inhibitors but not in presence of translation inhibitors.

(C) Mean total protein per cell (measured by a variant of the Lowry assay) in presence of different antibiotics normalized to no drug control. All antibiotic concentrations are tuned to achieve the same normalized growth rate (~0.35). See [Experimental Procedures](#).

ribosome synthesis leads to optimal expression levels (maximal growth) under all stress conditions, and in particular under DNA stress (Figure 1C).

The observation that, under DNA stress, inhibition of protein synthesis actually increases the rate of cellular growth suggests that the number of ribosomes per cell in these conditions is too high. Overexpression of ribosomes under these conditions would lead to an inefficient use of cellular resources and a growth rate that is lower than could be maximally achieved. Here, we test the hypothesis that the rate of ribosome synthesis in bacteria is nonoptimal under DNA stress, and that this nonoptimality causes the suppressive drug interactions in which translation inhibitors allow faster growth under DNA synthesis inhibition. We address this hypothesis by measuring cell composition, morphology and gene expression changes in response to antibiotics, by genetically manipulating ribosome synthesis, and by using a theoretical analysis of resource allocation in the cell.

RESULTS

Protein-DNA Ratio Is Skewed under DNA Stress

We first examined the changes in cell morphology and composition that result from treating cells with DNA synthesis inhibitors. These inhibitors cause DNA damage and trigger the SOS response, including expression of the cell division inhibitor *sulA*

(Huisman and D'Ari, 1981; Mesak et al., 2008; Walker, 1996). This prevents cell division before chromosome replication is completed (Huisman and D'Ari, 1981), leading to an increased average cell size (Walker, 1996) and cell size variability, in particular at sub-inhibitory antibiotic concentrations where exponential growth occurs at a reduced rate (Figure 2A,B). The increased cell size under DNA stress correlates with an elevated average amount of protein per cell (Figure 2C; measured by a modified Lowry assay, [Experimental Procedures](#)). Cellular DNA, however, is typically still restricted to only one or two nucleoids (Figure 2A) and, with increasing concentration of DNA synthesis inhibitor, the mean DNA content decreases per volume and even per cell (Georgopapadakou and Bertasso, 1991). The ratio of protein to DNA therefore significantly increases in the presence of DNA synthesis inhibitors. We hypothesized that this imbalance could be caused by excessive production of ribosomes in the cell, leading to overproduction of proteins and thus to reduced growth rates. We therefore examined whether and how ribosome synthesis is regulated in response to DNA synthesis inhibitors.

Ribosomal Gene Expression Is Not Specifically Regulated by DNA Stress

We used strains from a genome-wide GFP transcription reporter library (Zaslaver et al., 2006, 2004) to measure changes in the

expression level of promoters from almost 200 *E. coli* genes, representing key cellular functions including DNA stress response, metabolism and ribosome regulation and synthesis (Table S1). We obtained high time resolution measurements of optical density and GFP fluorescence of cultures growing in the presence of different antibiotics at a range of concentrations. We focused on measurements during exponential growth phase since our main interest in this work is to understand the combined effects of drugs on steady state growth. Growth rates (g) were determined from the increase in optical density over time (OD, Figure 3A). Changes in gene expression level (γ) were defined as the effect of the drug on the average GFP signal per OD during exponential phase ($\gamma = [\text{GFP}/\text{OD}] / [\text{GFP}/\text{OD}]_{\text{no drug}}$; Figure 3A and Experimental Procedures). By repeating the measurement at a range of drug concentrations, we determined expression level changes in response to antibiotics as a function of growth inhibition (see example for trimethoprim (TMP) in Figure 3B; antibiotics used in this study are summarized in Table 1). As expected, most SOS response genes were upregulated in response to DNA stress caused by any of three different DNA synthesis inhibitors (TMP, Figure 3B; ciprofloxacin [CPR] and nalidixic acid [NAL], Figure S2). On the other hand, most ribosomal genes were downregulated in response to these DNA synthesis inhibitors (Figures 3B, 3C, and S2). Consistent with the downregulation of ribosomal genes, the ppGpp-regulated ribosome inactivator gene *rmf* (Izutsu et al., 2001) was upregulated in response to TMP (Figure 3B).

How much are ribosomal genes downregulated under DNA synthesis stress? Ribosome production is normally reduced when the growth rate of the cell is reduced (Bremer and Dennis, 1996), but it is possible that the inhibition of DNA synthesis may also have a more specific effect on ribosome synthesis. To distinguish between nonspecific (growth-mediated) and specific effects of DNA synthesis inhibition on growth, we compared the change in expression of ribosomal genes in the presence of antibiotics that inhibit DNA synthesis to the change seen when growth rate is reduced using a poor growth medium. We found that, for equivalent reductions in cellular growth rate caused by these two mechanisms, the degree to which ribosomal gene expression is downregulated is essentially identical (Figures 3C and 3D). Thus, we see no evidence for specific regulation of ribosomal expression by DNA stress.

While DNA synthesis inhibitors did not specifically regulate ribosome production, the translation inhibitors spiramycin (SPR) and tetracycline (TET) elicit an upregulation of ribosomal gene expression (Figure 3D) which counters the effect of these drugs, consistent with previous studies (Fraenkel and Neidhardt, 1961; Kurland and Maaløe, 1962; Schneider et al., 2002). We next asked how this upregulation of ribosomal genes in response to protein synthesis inhibitors is affected by the presence of DNA synthesis inhibitors. We measured the regulation of 80 promoters including nine that control ribosomal genes (Table S1) in a two-dimensional concentration matrix of TMP and SPR (Experimental Procedures). For each promoter, we obtained its fold change in expression level as a function of the two drug dosages (Figures 4A and S3; Experimental Procedures; Kaplan et al., 2008; Tsui et al., 2004). We found that ribosomal gene expression levels in the presence of TMP are lower than

in its absence for any SPR level (Figure 4A) and the upregulation of ribosomal genes by SPR is significantly delayed (occurs at higher SPR concentrations) under TMP stress (arrow in Figure 4B). Consequently, the increase in growth resulting from the addition of a translation inhibitor in the presence of a DNA synthesis inhibitor occurs without substantial increase in ribosome production.

This delayed response allows a translation inhibitor to substantially reduce overall protein synthesis and restore the protein-DNA ratio to near its normal value (Piddock et al., 1990), plausibly explaining the ability of translation inhibitors to increase the survival and growth of cells suffering DNA synthesis inhibition. Hence, the results discussed so far are consistent with the hypothesis that the ribosome synthesis rate is not optimally controlled under prolonged DNA stress; that is, it is not sufficiently downregulated to maximize cellular growth rate. But how can we test this hypothesis more directly? The hallmark of nonoptimality is the possibility for improvement: if cellular production of ribosomes is indeed nonoptimal under DNA stress, we should be able to manipulate it to increase cellular survival and growth.

Manipulating Ribosome Synthesis Increases Growth Rate and Survival in the Presence of DNA Synthesis Inhibitors

To test whether direct manipulation of ribosome levels affects growth and survival in the presence of DNA synthesis inhibitors, we measured responses to antibiotics in strains that are engineered to decrease or increase ribosome synthesis. Following previous work (Asai et al., 1999; Condon et al., 1993), we constructed strains in which up to six of the seven *rrn* operons were incrementally deleted (designated $\Delta 1$, $\Delta 2$, $\Delta 3$, $\Delta 4$, $\Delta 5$, and $\Delta 6$; Experimental Procedures; Table S2; no plasmid-borne *rrn* operons were added to these strains). Our construction method removes the selection marker linked to each of the *rrn* operon deletions, allowing a direct comparison of the physiology of these strains with wild-type (Experimental Procedures). The relationship between the number of *rrn* operons and ribosome levels is not necessarily linear, since feedback regulation of ribosome synthesis partially compensates for deletions by increasing the expression of the remaining *rrn* operons (Condon et al., 1993). Nevertheless, ribosome levels and the rRNA concentration – an upper bound for ribosome level – is reduced by deleting *rrn* operons, particularly in rich growth media where *rrn* operon transcription rates are close to saturation and cannot be increased much further (Asai et al., 1999; Condon et al., 1993). We also examined strains deleted for the genes *relA* and *spoT*; these double-deletion mutants are devoid of ppGpp, a key negative regulator of ribosome synthesis (Xiao et al., 1991), and thus show increased *rrn* expression (Barker et al., 2001; Bartlett and Gourse, 1994). The *relA* *spoT* deletion strain has a longer lag time for the transition from stationary phase to exponential growth and a slightly reduced steady state growth rate (Figure S16; Gaal and Gourse, 1990).

We measured growth rates of these modified strains in normal conditions as well as under conditions where different antibiotics were added to the cultures. In the absence of antibiotics, the wild-type strain grows faster than all mutants with altered

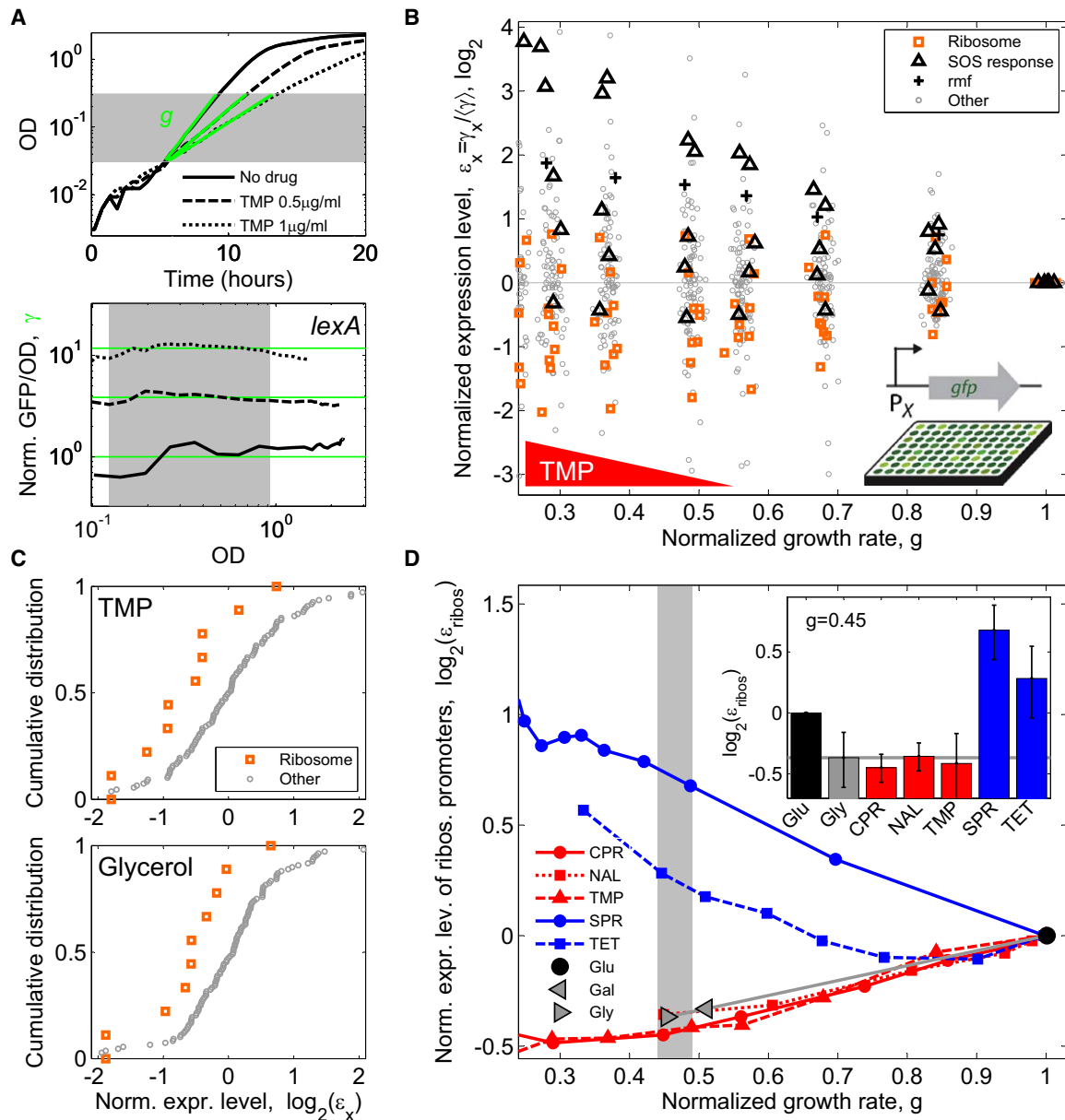


Figure 3. Ribosomal Gene Expression Is Downregulated under DNA Stress Only as Much as in the Normal Physiological Response to Slow Growth

(A) Example data demonstrating measurement of drug effect on growth rate and transcription reporters. Optical Density (OD) and GFP expression from various promoters (shown, as an example, is the promoter of *lexA* – the master regulator of the SOS response) are measured as a function of time for various drug concentrations (shown, 0, 0.5 and 1 $\mu\text{g}/\text{ml}$ TMP). Top: growth rates are defined by linear regression (green lines) to the OD curves (black). Bottom: Expression level γ (green lines) is defined as GFP fluorescence intensity per OD, averaged over an OD range of exponential growth (shaded region) and normalized to no drug control.

(B) Normalized expression levels ε_x of 110 promoters in *E. coli* as a function of growth rate in various concentrations of TMP. For each promoter x , ε_x is defined as expression level γ_x , normalized to the median expression level of all promoters $\langle \gamma \rangle$ (Experimental Procedures). SOS response promoters are upregulated (black triangles). Most ribosomal promoters are downregulated (orange squares) consistent with the upregulation of the ribosome inactivator *rmf* (black crosses). Random scatter added to growth rate to enhance visibility.

(C) Top: Cumulative distributions of normalized expression levels ε_x showing downregulation of ribosomal genes (orange) relative to all other promoters (gray) at a fixed concentration of TMP (normalized growth rate ~ 0.49). Bottom: a similar regulation is seen with no drug when the same change in growth rate is achieved by changing the carbon source from glucose to glycerol.

(D) Mean normalized expression level of ribosomal promoters $\varepsilon_{\text{ribos}}$ as a function of normalized growth rate for different DNA synthesis inhibitors (CPR, NAL, TMP; red), translation inhibitors (SPR, TET; blue), and in growth media with different carbon sources (glucose, galactose, glycerol; gray). Inset: $\varepsilon_{\text{ribos}}$ values at normalized growth rate of approximately 0.45 (panel [D], gray region); error bars show SEM. Ribosomal promoters are upregulated in response to translation inhibitors and downregulated in presence of DNA synthesis inhibitors. This downregulation, however, is similar to the growth-rate dependent downregulation that results from a change of carbon source (gray horizontal line).

Table 1. Antibiotics Used in This Study, Abbreviation, MIC in the Wild-Type MG1655 Strain, and Main Mode of Action

| Antibiotic | Abbreviation | MIC in LB ($\mu\text{g/ml}$) | MIC in M9 ($\mu\text{g/ml}$) | Mode of action |
|----------------|--------------|-----------------------------------|-----------------------------------|------------------------|
| Ciprofloxacin | CPR | 0.012 | 0.012 | DNA gyrase |
| Nalidixic acid | NAL | 6 | 6 | DNA gyrase |
| Trimethoprim | TMP | 0.42 | 1.5 | Folic acid synthesis |
| Spiramycin | SPR | 192 | 120 | Protein synthesis, 50S |
| Tetracycline | TET | 1.5 | 1.5 | Protein synthesis, 30S |
| Nitrofurantoin | NIT | 5 | 5 | Multiple mechanisms |

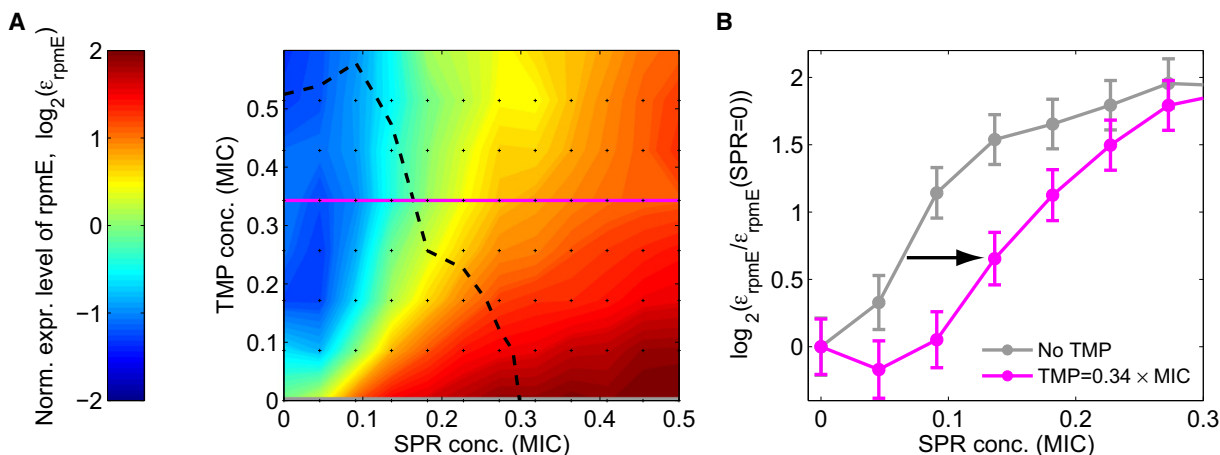
ribosome synthesis; genetically increasing or decreasing ribosome synthesis leads to reduced growth rates (Figure 5A). This observation confirms previous results (Asai et al., 1999) and is in agreement with the idea that ribosomal synthesis is optimally regulated to maximize growth in the absence of stress (Gralla, 2005; Paul et al., 2004).

In DNA stress conditions, however, the picture is profoundly different (Figures 5A, S4A, and S4B). As expected, all strains grow more slowly under DNA stress than in a stress-free environment (Figures 5A, CPR curve lower than no-drug curve). But, in the presence of the DNA synthesis inhibitors CPR and NAL, the strain with maximal growth is not the wild-type, but rather a strain with reduced ribosome synthesis ($\Delta 5$ at the drug concentration shown in Figures 5, S4A, and S4B). Complementing the deletion strains with a plasmid expressing one of the *rrn* operons (*rrnB*), partially revokes the increase in growth of these deletion mutants under DNA stress, confirming that this phenotype is

directly related to the reduction in *rrn* operons (Figure S13). Coincident with their increased growth rate compared to wild-type, the deletion stains also have a closer to normal cell size under DNA synthesis inhibition (Figure S5). Thus, in the presence of DNA synthesis inhibitors the expression of *rrn* genes in the wild-type appears to be higher than optimal.

We next tested if optimizing ribosome synthesis also allows cells to tolerate higher concentrations of DNA synthesis inhibitors. We determined changes of the minimal inhibitory concentration (MIC) in the *rrn* deletion mutants for a range of antibiotics (Experimental Procedures). Indeed, as we delete *rrn* operons we see an incremental increase in MIC for the DNA synthesis inhibitors CPR and NAL (TMP behaves differently in this assay; see below), compared to no change or even a decrease for antibiotics with other modes of action (Figure S4F).

In principle, the increased MIC for DNA synthesis inhibitors could be an indirect effect caused by the lower growth rate of the mutants with *rrn* operon deletions. To discriminate between such general growth rate effects and the specific effect of modified ribosomal expression in the *rrn* deletion strains, we reduced the growth rate of the wild-type by changing the carbon source in the growth medium, and asked if this change has a similar effect on the MIC as the *rrn* operon deletions (Experimental Procedures). We found that changing the growth rate in this way does not lead to a detectable change in MIC for CPR and NAL, but TMP shows a two-fold lower MIC when growth rate is reduced to a level comparable to that of the $\Delta 6$ mutant (data not shown). This allows us to rationalize the observation that, unlike the case for CPR and NAL, the MIC for TMP is not increased in the $\Delta 6$ strain (Figure S4F): the increased MIC due to the reduction in ribosomal synthesis may be masked by the reduction in MIC caused by the decreased growth rate. Overall, our results show that strains with genetically reduced ribosome synthesis survive better in the presence of DNA synthesis

**Figure 4. Upregulation of Ribosomal Promoters by Protein Synthesis Inhibitors Is Delayed under DNA Stress**

(A) Color map of normalized expression level ϵ_{rpmE} of ribosomal promoter *rpmE* in a two-dimensional concentration matrix (black dots) of DNA synthesis inhibitor (TMP) and translation inhibitor (SPR). Other ribosomal promoters behave similarly, Figure S3. Dashed line, line of constant growth rate (isobole; $g = 0.38$). (B) Relative change in expression level $\epsilon_{\text{rpmE}}(\text{SPR}) / \epsilon_{\text{rpmE}}(\text{SPR} = 0)$ as a function of SPR concentration, at no TMP (TMP = 0, gray), and at a fixed TMP concentration (TMP = 0.34 MIC, magenta). Upregulation requires higher SPR concentration in the presence of TMP (arrow). Error-bars in (B) were estimated from the standard deviation of replicate measurements done on different days (see Figure S17).

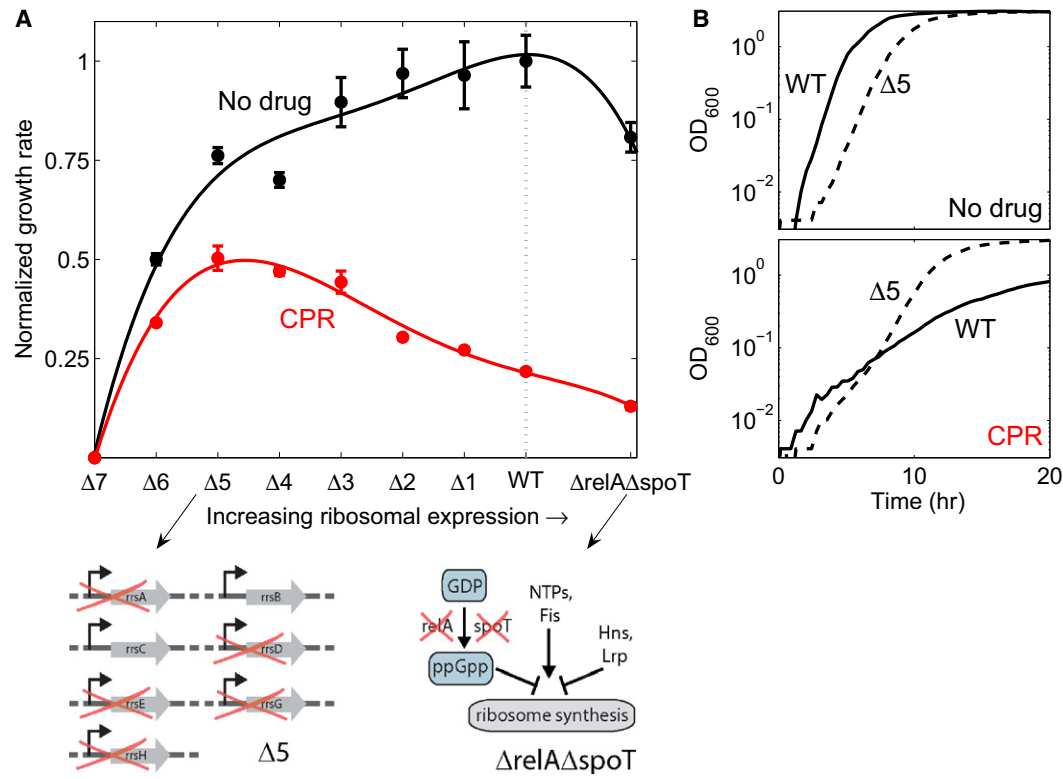


Figure 5. Wild-Type Regulation of Ribosomal Expression Level under DNA Stress Is Nonoptimal: Genetically Manipulating Ribosome Synthesis Can Increase Survival and Growth

(A) Normalized growth rates of wild-type (WT) and strains with incremental deletions of one to six of the seven *rrn* operons as well as for $\Delta \text{relA}\Delta\text{spoT}$ strain, in rich medium (LB) in the absence (black) and presence of the DNA synthesis inhibitor CPR (red). Lines, 4th order polynomial fit to guide the eye. Schematic on left: strain $\Delta 5$ in which 5 of 7 *rrn* operons are deleted. Schematic on right: $\Delta \text{relA}\Delta\text{spoT}$ strain which is devoid of ppGpp, a key negative regulator of ribosome synthesis, while other factors regulating ribosome synthesis remain. While wild-type expression level is optimized for maximal growth under no drug conditions, it is not optimized for maximal growth under DNA synthesis inhibition: Reduced ribosome synthesis in *rrn* deletion strains increases growth.

(B) Sample data showing the growth curves (OD versus time) for WT (solid line) and $\Delta 5$ strain (dashed line) in no drug or under CPR at the concentration of (A).

inhibitors, and thus that the wild-type regulation of ribosome synthesis is nonoptimal for growth in these conditions.

Reducing Ribosome Synthesis Removes the Suppressive Drug Interactions between DNA Synthesis Inhibitors and Translation Inhibitors

If nonoptimality in the regulation of ribosome synthesis under DNA stress is the cause for the suppressive interactions between inhibitors of DNA synthesis and translation (Figure 1), then these suppressive drug interactions should disappear in the genetically altered strains. To test this prediction, we measured growth rates of the wild-type and the strains with genetically altered ribosome expression levels in a two-dimensional drug matrix of a DNA synthesis and a translation inhibitor (Experimental Procedures). Strikingly, we find that genetically reducing ribosome synthesis reduces the magnitude of the suppressive drug interaction and can even remove it entirely. Indeed, in contrast to the wild-type, the $\Delta 6$ strain shows an almost additive interaction (linear MIC line in Figure 6A compared to nonmonotonic line in 6B; see also definition of drug interactions in Figure 1A). We observed this phenomenon for different antibiotic pairs that inhibit DNA synthesis and translation, for differently constructed

rrn deletion strains (Figure S12), and for strains grown in both rich and minimal growth medium (Figures 6A, 6B, and S1). Further, complementing the deletion strains with a plasmid expressing one of the *rrn* operons (*rrnB*), partially restores the suppressive interaction between the drugs (Figure S14). Together, these results support the notion that the suppressive drug interaction is caused by nonoptimal regulation of ribosome synthesis: the reduced ribosome synthesis rate in the $\Delta 6$ strain is closer to the optimal level for maximal growth rate under DNA stress and, consequently, the addition of an antibiotic that inhibits translation no longer has a beneficial effect.

Conversely, we tested whether impairing the downregulation of ribosome synthesis can amplify suppressive drug interactions. We can force ribosome synthesis in the presence of TMP even further above its optimal level by using a *relA spoT* deletion mutant. In this ppGpp-deficient mutant, the downregulation of ribosome synthesis in response to TMP is impaired since it cannot elicit the wild-type upregulation of ppGpp in response to TMP (Khan and Yamazaki, 1972; Smith and Midgley, 1973). Indeed, we found that the impaired regulation of ribosome synthesis in a *relA spoT* deletion mutant amplifies the suppressive drug interaction between the DNA synthesis inhibitor TMP

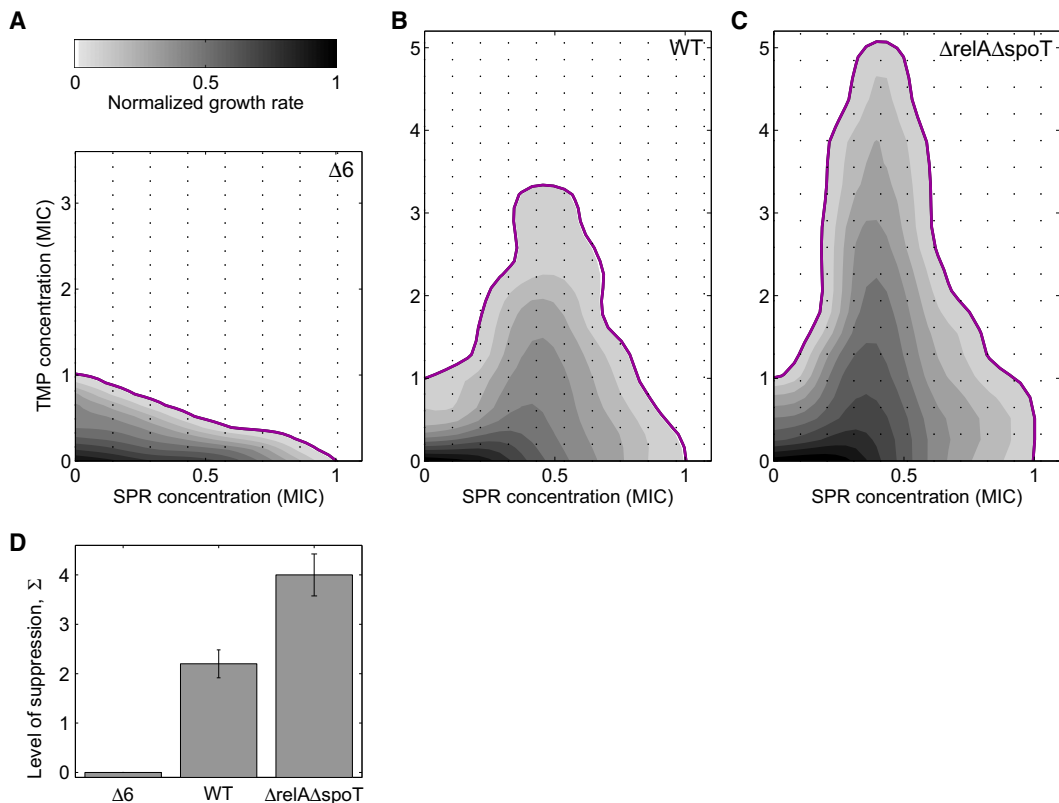


Figure 6. Genetically Optimizing Ribosome Synthesis Removes Suppressive Drug Interaction between Inhibitors of DNA Synthesis and Translation

Growth rates (gray levels) and MIC line (magenta) of $\Delta 6$ (A), WT (B), and $\Delta relA\Delta spoT$ strain (C) in two-dimensional concentration matrices (black dots) of DNA synthesis inhibitor (TMP) and translation inhibitor (SPR). The suppressive drug interaction (B) disappears when ribosome synthesis is reduced (A) and is amplified when downregulation of ribosome synthesis is impaired (C). The disappearance of suppression is incremental with number of *rrn* deletions and does not depend on the specific DNA synthesis or translation inhibitor used, Figure S1. (D) Quantified level of suppression in the three strains. The level of suppression Σ is defined as $\Sigma = (\text{MIC}_{\max} - \text{MIC}_0)/\text{MIC}_0$, where MIC_{\max} is the maximal TMP MIC over all SPR concentrations and MIC_0 the TMP MIC in absence of SPR. Cultures grown in rich medium (LB).

and the translation inhibitor SPR (compare Figure 6C to 6B). A very similar effect is observed in a *relA* deletion mutant (Figure S7). The observation that increasing ribosomal expression amplifies suppression while decreasing ribosomal expression reduces it (Figure 6D) provides persuasive evidence that this drug interaction is due to nonoptimal regulation of ribosome expression.

A Simple Mathematical Model of Ribosome Synthesis Regulation Captures Nonoptimal Response to DNA Stress and Suppressive Drug Interactions

Why is ribosome synthesis so inappropriately regulated in response to DNA synthesis inhibitors? To explore this issue, we developed a coarse-grained mathematical model of ribosome synthesis regulation in bacterial growth (Figure 7A and Supplemental Data). This model describes the interdependencies of the cellular concentrations of DNA, proteins, ribosomes, resources, and cellular growth at steady state. Resources enter the cell at a fixed rate and are distributed between the production of proteins, ribosomes and DNA. In the model, ribosome synthesis

is regulated based on the intracellular concentration of these resources. We optimize this regulation function to maximize the growth rate at different resource uptake rates, corresponding to different nutrient environments in the absence of antibiotics. We then assume that this same regulation function based on intracellular resource concentrations also applies when antibiotics are present. The effect of antibiotics is modeled as a reduction in the rate of translation or DNA synthesis. We further assume that a threshold amount of protein per replication origin must be produced to initiate DNA replication and cell division (Donachie, 1968; Donachie and Blakely, 2003). For simplicity, we assume in the model that the cellular protein concentration is constant so that the cell size is proportional to the total amount of protein per cell (this approximation may not be true in general). Importantly, most parameters that enter into the model are known or fully constrained by experimental data (Bremer and Dennis, 1996; Table S3). This simple model quantitatively reproduces the changes in cell composition and growth rate that have been observed in different nutrient environments (Bremer and Dennis, 1996; Figure S6).

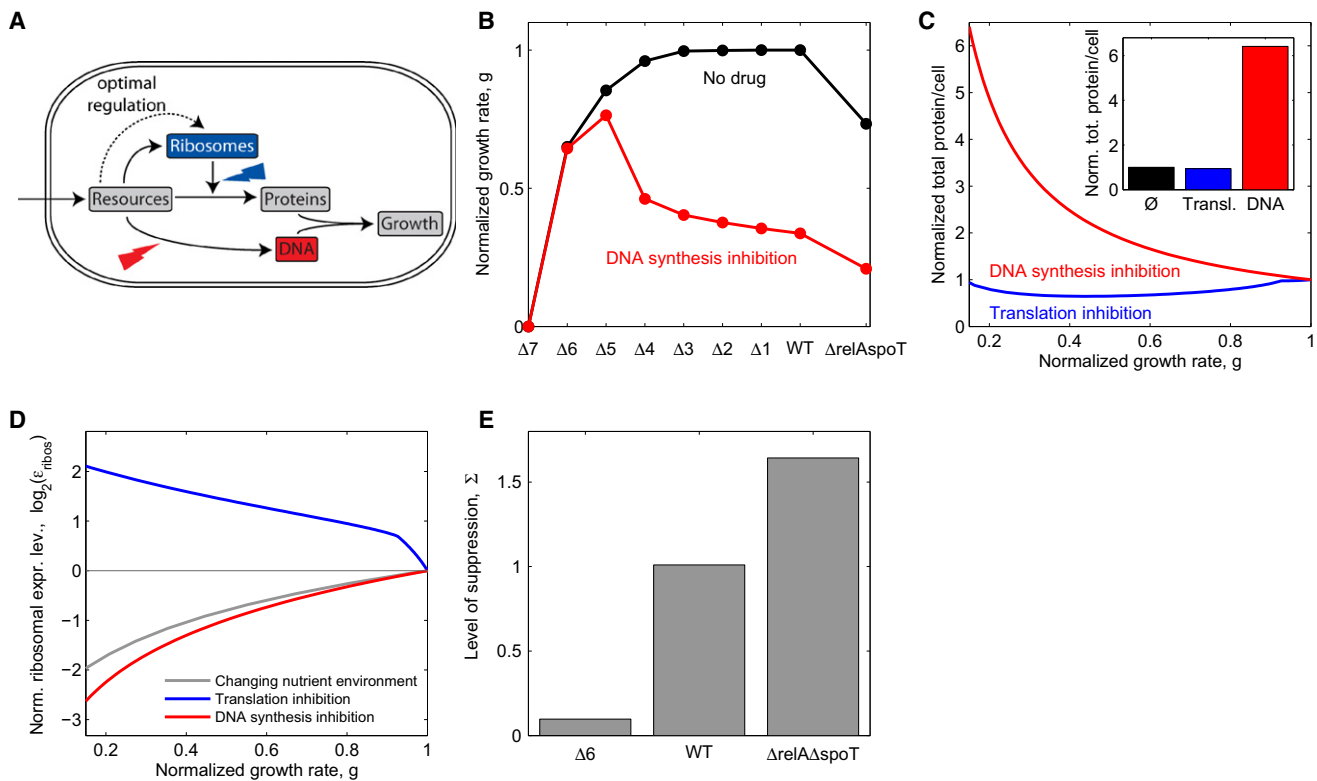


Figure 7. Mathematical Model with Optimal Growth Rate-Dependent Regulation of Ribosome Synthesis Yields Nonoptimal Response to DNA Synthesis and Thereby Suppression by Translation Inhibitors

(A) Schematic depiction of a very simplified model of bacterial growth capturing resource allocation to DNA, ribosomes and proteins. Ribosome synthesis is assumed to be optimally regulated by resource concentration. See [Supplemental Data](#) for the complete mathematical model.

(B) Growth rate obtained from the model for WT, *rrn* operon deletions and *relA spoT* deletions in the absence of antibiotics (black line) and in the presence of DNA synthesis inhibitor (red line), cf. [Figure 5A](#).

(C) Change of total protein per cell under translation inhibition (blue) or DNA synthesis inhibition (red), cf. [Figure 2C](#). Inset shows total protein per cell at $g = 0.15$.

(D) Normalized ribosomal expression level $\varepsilon_{\text{ribos}}$ (corresponds to ribosomal protein fraction η in the model, see [Supplemental Data](#)) as a function of growth rate under reduced nutrient availability (gray), translation inhibition (blue), or DNA synthesis inhibition (red). Ribosome synthesis is similarly downregulated in response to reduced nutrient availability or DNA synthesis inhibition and is upregulated in response to translation inhibition, cf. [Figure 3D](#).

(E) Quantified level of suppression in the different strains, cf. [Figure 6D](#). Parameters as in [Table S3](#) with resource influx $v_a = 15 \text{ h}^{-1}$ which leads to a growth rate $g = 1.3 \text{ h}^{-1}$ in absence of antibiotics, for details see [Supplemental Data](#).

The model and its resource-based optimization of ribosome production faithfully describes our key experimental observations and in particular leads to nonoptimal regulation under DNA stress. Specifically, it correctly captures the up- and down-regulation of ribosome synthesis in the presence of translation and DNA synthesis inhibitors, respectively (cf. Figures 3D and 7D). As in our experimental results, this reduction in the level of ribosomal synthesis under DNA synthesis inhibition is similar to the reduction seen when growth is attenuated by nutrient deprivation (red versus gray lines in [Figure 7D](#); compare to experiments in [Figure 3D](#)). This reduction in expression of ribosomal synthesis is insufficient, leading to a skewed protein-DNA ratio (cf. Figures 2 and 7C) and to sub-maximal growth rate (cf. Figures 5A and 7B). Importantly, this simple model also reproduces the suppressive drug interaction between DNA synthesis and translation inhibitors, its attenuation as a result of *rrn* operon deletions, and its amplification as a result of *relA spoT* deletions (cf. Figures 6D and 7E).

DISCUSSION

We showed that ribosome synthesis is not specifically regulated by DNA synthesis inhibiting drugs, leading to a skewed DNA to protein ratio and sub-maximal growth rate. Genetically reducing ribosome synthesis allows cells to grow faster under DNA stress. Importantly, this genetic optimization of ribosome production based on intracellular resource concentrations in normal conditions can lead to nonoptimal resource allocation between DNA and protein synthesis under DNA synthesis inhibition, and thereby to decreased growth. This explanation, while fully consistent with our data, does not exclude the possibility that other mechanisms contribute to the suppressive interactions between DNA synthesis inhibitors and translation inhibitors. For example, reduced protein synthesis leads to reduced growth rate and

thereby to a smaller number of replication forks, which ultimately may reduce the impact of DNA synthesis inhibitors, especially of gyrase inhibitors which cause double strand breaks and cell death through oxidative stress (Dwyer et al., 2007; Kolodkin-Gal et al., 2008). Upregulation of drug efflux pumps may also play a role (Poole, 2005).

Our result that regulation of ribosomal gene expression in response to sustained DNA stress is not optimal for maximal growth in laboratory conditions raises the question of whether this response might be optimized for another goal or for other more natural conditions. The lack of specific regulation of ribosomal genes under DNA stress is particularly puzzling given *E. coli*'s ability to specifically regulate genes through the SOS response (Friedman et al., 2005; Michel, 2005; Radman, 1975; Tippin et al., 2004). There are several ways in which the observed lack of specific response to DNA stress could actually be beneficial in natural conditions. First, it is possible that in the natural environment in which the organism evolved, DNA synthesis inhibition is usually encountered at the same time as nutrient deprivation, removing the need for a specific mechanism to downregulate protein synthesis (Cashel et al., 1996; Gralla, 2005; Paul et al., 2004). Indeed, gene regulation responses can exploit correlations between environmental changes, even if they do not occur simultaneously (Mitchell et al., 2009; Tagkopoulos et al., 2008). Second, it is possible that DNA stress is usually short-lived in the natural environment, and so the global response to DNA damage and the formation of larger, filamentous cells could be optimized to ensure a fast recovery when the stress is relieved (Guan and Burnham, 1992). Finally, it is possible that phenotypic variability between cells, which increases under DNA stress (Figure 2A,B), plays a role in the survival strategy under these conditions (Balaban et al., 2004; Guido et al., 2007; Kussell and Leibler, 2005; Pearl et al., 2008). In any case, while the lack of specific regulation of ribosomal genes under DNA stress could be optimal in some conditions, it is clearly nonoptimal in the laboratory condition.

In summary, we showed that nonoptimal regulation of ribosome synthesis is at the heart of the suppressive drug interactions between protein and DNA synthesis inhibitors. Understanding the underlying mechanism of the interaction allowed us to genetically manipulate whether and to what extent these two drug classes interact. More generally, these results show that cellular systems, even those critical for growth and survival, are not always optimally regulated, and that tight optimal control in some conditions can lead to nonoptimal regulation in other conditions. Such nonoptimal regulation may open possibilities for new ways to manipulate cellular growth in the lab and in the clinic.

EXPERIMENTAL PROCEDURES

Media, Strains, and Drugs

Experiments were conducted as indicated in rich Luria-Bertani (LB) broth or M9 minimal medium with different carbon sources (glucose, galactose, glycerol) at 0.4%. Glucose M9 was supplemented with 0.2% amicase. Drug solutions were made from powder stocks, filter-sterilized, stored at -20°C in the dark and added as indicated. All strains used were derived from *E. coli* K-12 strain MG1655 (Supplemental Data and Table S2).

Growth Rate and MIC Assays

Overnight cultures were diluted ~2000-fold and grown on an automated robotic system (Caliper) at 30°C with rapid shaking in 96-well microtiter plates (Costar) containing 200 µl medium per well. Absorbance at 600nm (A_{600} , proportional to optical density OD_{600} , proportionality constant 3.1) and GFP fluorescence were recorded by a plate reader (Victor III or EnVision, Perkin-Elmer) at intervals of ~30 min for at least 24 hr, and background subtracted. Growth rates were calculated using Matlab by linear regression of $\log(OD_{600})$ (Matlab function "regress") during exponential growth ($0.01 < A_{600} < 0.1$). The measurement error was evaluated as the 95% confidence interval of the linear regression (error bars in Figure 5A). Growth was annotated as no data if the regression error was greater than 20%. Also removed are some cases where resistant mutants occurred, in particular for CPR and NAL; these were identified by large variations between replicates and by no growth for 12 hr or longer followed by fast growth. Two-dimensional drug concentration matrices were set up on one 96-well plate (11 × 8 format) or on four plates (22 × 16 format) leaving one column per plate for controls. To reduce noise, a smoothed function was fitted to the measured growth rates by using a smoothing cubic spline, and linearly interpolated isoboles were plotted (Matlab functions "csaps" and "contour").

MIC was defined as the lowest concentration at which background subtracted A_{600} did not exceed 0.02 after 24 hr. MICs were first determined crudely in logarithmic antibiotic concentration gradients with two-fold dilutions and then more accurately with linear gradients ranging from zero to about two times the MIC.

Gene Expression Assay

GFP reporter strains were grown in glucose M9 medium supplemented with 0.2% amicase. GFP background was subtracted as described (Zaslaver et al., 2006). We defined the expression level as the mean GFP/A_{600} in the interval $0.04 < A_{600} < 0.3$, Figure 3A. Only promoters with a clearly detectable GFP signal were used for analysis, reducing the total number to 110 promoters, Figure 3B. Expression level changes γ relative to the drug-free control were normalized to the median expression level change $\langle\gamma\rangle$ of all promoters in the same drug environment. Changes in the median expression level of all promoters reflect nonspecific effects such as pH changes or changes of the reporter plasmid copy number. We verified that the effect of plasmid copy number on the measured expression level is independent of the GFP promoter, by comparing to strains in which the same GFP reporters were integrated into the chromosome (Supplemental Data).

DNA and Protein Assay

Cultures were grown to $OD_{600}\sim 0.2$ in glucose M9 medium, DAPI stained (5 µg/ml, 5 min), mounted on agar pads, and imaged (Figure 2A). Cell lengths were measured manually using ImageJ (<http://rsbweb.nih.gov/ij/>) for ~100 cells in each condition (Figure 2B). To calculate protein per cell, we combined 8 identical 200 µl cultures and determined the total protein concentration using the D_c protein assay (Biorad). Cell concentration was estimated by colony plate count. We slightly over-estimate protein per cell because cells devoid of DNA (less than 10% of cells) do not form colonies. Error bars in Figure 2C represent the error $N^{1/2}$ for the cell count N .

SUPPLEMENTAL DATA

Supplemental Data include Supplemental Experimental Procedures, three tables, and seventeen figures and can be found with this article online at [http://www.cell.com/supplemental/S0092-8674\(09\)01315-4](http://www.cell.com/supplemental/S0092-8674(09)01315-4).

ACKNOWLEDGMENTS

We thank U. Alon, J. Collins, M. Elowitz, M. Ernebjerg, A. Gassett, A. Hilfinger, E. Kelsic, M. Kohanski, D. Landgraf, R. Milo, A. Palmer, D. Rudner, M. Springer, M. Staller, C. Squires, E. Toprak, I. Wapinski, R. Ward, P. Yeh, and all members of the Kishony lab for discussions, comments, and technical help; and M. Traxler for his gift of strains. This work was supported in part by

National Institutes of Health Grant R01GM081617 (to R.K.). T.B. acknowledges funding from the Alexander von Humboldt foundation.

Received: March 23, 2009

Revised: June 15, 2009

Accepted: October 14, 2009

Published: November 12, 2009

REFERENCES

- Asai, T., Condon, C., Voulgaris, J., Zaporojets, D., Shen, B., Al-Omar, M., Squires, C., and Squires, C.L. (1999). Construction and initial characterization of *Escherichia coli* strains with few or no intact chromosomal rRNA operons. *J. Bacteriol.* 181, 3803–3809.
- Balaban, N.Q., Merrin, J., Chait, R., Kowalik, L., and Leibler, S. (2004). Bacterial persistence as a phenotypic switch. *Science* 305, 1622–1625.
- Barker, M.M., Gaal, T., and Gourse, R.L. (2001). Mechanism of regulation of transcription initiation by ppGpp. II. Models for positive control based on properties of RNAP mutants and competition for RNAP. *J. Mol. Biol.* 305, 689–702.
- Bartlett, M.S., and Gourse, R.L. (1994). Growth rate-dependent control of the *rnbB* P1 core promoter in *Escherichia coli*. *J. Bacteriol.* 176, 5560–5564.
- Bliss, C.I. (1939). The toxicity of poisons applied jointly. *Ann. Appl. Biol.* 26, 585–615.
- Brazas, M.D., and Hancock, R.E. (2005). Using microarray gene signatures to elucidate mechanisms of antibiotic action and resistance. *Drug Discov. Today* 10, 1245–1252.
- Bremer, H., and Dennis, P.P. (1996). Modulation of Chemical Composition and Other Parameters of the Cell by Growth Rate. In *Escherichia coli and Salmonella*, F.C. Neidhardt, ed. (Washington, D.C.: ASM Press), pp. 1553–1569.
- Cashel, M., Gentry, D.R., Hernandez, V.J., and Vinella, D. (1996). The Stringent Response. In *Escherichia coli and Salmonella*, F.C. Neidhardt, ed. (Washington, D.C.: ASM Press), pp. 1458–1496.
- Chait, R., Craney, A., and Kishony, R. (2007). Antibiotic interactions that select against resistance. *Nature* 446, 668–671.
- Condon, C., French, S., Squires, C., and Squires, C.L. (1993). Depletion of functional ribosomal RNA operons in *Escherichia coli* causes increased expression of the remaining intact copies. *EMBO J.* 12, 4305–4315.
- Condon, C., Liveris, D., Squires, C., Schwartz, I., and Squires, C.L. (1995). rRNA operon multiplicity in *Escherichia coli* and the physiological implications of *rnb* inactivation. *J. Bacteriol.* 177, 4152–4156.
- Davies, J., Spiegelman, G.B., and Yim, G. (2006). The world of subinhibitory antibiotic concentrations. *Curr. Opin. Microbiol.* 9, 445–453.
- Dekel, E., and Alon, U. (2005). Optimality and evolutionary tuning of the expression level of a protein. *Nature* 436, 588–592.
- Dennis, P.P., Ehrenberg, M., and Bremer, H. (2004). Control of rRNA synthesis in *Escherichia coli*: a systems biology approach. *Microbiol. Mol. Biol. Rev.* 68, 639–668.
- Donachie, W.D. (1968). Relationship between cell size and time of initiation of DNA replication. *Nature* 219, 1077–1079.
- Donachie, W.D., and Blakely, G.W. (2003). Coupling the initiation of chromosome replication to cell size in *Escherichia coli*. *Curr. Opin. Microbiol.* 6, 146–150.
- Drlica, K., Malik, M., Kerns, R.J., and Zhao, X. (2008). Quinolone-mediated bacterial death. *Antimicrob. Agents Chemother.* 52, 385–392.
- Dwyer, D.J., Kohanski, M.A., Hayete, B., and Collins, J.J. (2007). Gyrase inhibitors induce an oxidative damage cellular death pathway in *Escherichia coli*. *Mol. Syst. Biol.* 3, 91.
- Fajardo, A., and Martinez, J.L. (2008). Antibiotics as signals that trigger specific bacterial responses. *Curr. Opin. Microbiol.* 11, 161–167.
- Fraenkel, D.G., and Neidhardt, F.C. (1961). Use of chloramphenicol to study control of RNA synthesis in bacteria. *Biochim. Biophys. Acta* 53, 96–110.
- Friedman, N., Vardi, S., Ronen, M., Alon, U., and Stavans, J. (2005). Precise temporal modulation in the response of the SOS DNA repair network in individual bacteria. *PLoS Biol.* 3, e238.
- Gaal, T., Bartlett, M.S., Ross, W., Turnbough, C.L., Jr., and Gourse, R.L. (1997). Transcription regulation by initiating NTP concentration: rRNA synthesis in bacteria. *Science* 278, 2092–2097.
- Gaal, T., and Gourse, R.L. (1990). Guanosine 3'-diphosphate 5'-diphosphate is not required for growth rate-dependent control of rRNA synthesis in *Escherichia coli*. *Proc. Natl. Acad. Sci. USA* 87, 5533–5537.
- Georgopapadakou, N.H., and Bertasso, A. (1991). Effects of quinolones on nucleoid segregation in *Escherichia coli*. *Antimicrob. Agents Chemother.* 35, 2645–2648.
- Goh, E.B., Yim, G., Tsui, W., McClure, J., Surette, M.G., and Davies, J. (2002). Transcriptional modulation of bacterial gene expression by subinhibitory concentrations of antibiotics. *Proc. Natl. Acad. Sci. USA* 99, 17025–17030.
- Gralla, J.D. (2005). *Escherichia coli* ribosomal RNA transcription: regulatory roles for ppGpp, NTPs, architectural proteins and a polymerase-binding protein. *Mol. Microbiol.* 55, 973–977.
- Guan, L., and Burnham, J.C. (1992). Postantibiotic effect of Cl-960, enoxacin and ciprofloxacin on *Escherichia coli*: effect on morphology and haemolysin activity. *J. Antimicrob. Chemother.* 29, 529–538.
- Guido, N.J., Lee, P., Wang, X., Elston, T.C., and Collins, J.J. (2007). A pathway and genetic factors contributing to elevated gene expression noise in stationary phase. *Biophys. J.* 93, L55–L57.
- Hegreness, M., Shores, N., Damian, D., Hartl, D., and Kishony, R. (2008). Accelerated evolution of resistance in multidrug environments. *Proc. Natl. Acad. Sci. USA* 105, 13977–13981.
- Hoffman, L.R., D'Argenio, D.A., MacCoss, M.J., Zhang, Z., Jones, R.A., and Miller, S.I. (2005). Aminoglycoside antibiotics induce bacterial biofilm formation. *Nature* 436, 1171–1175.
- Huisman, O., and D'Ari, R. (1981). An inducible DNA replication-cell division coupling mechanism in *E. coli*. *Nature* 290, 797–799.
- Ibarra, R.U., Edwards, J.S., and Palsson, B.O. (2002). *Escherichia coli* K-12 undergoes adaptive evolution to achieve *in silico* predicted optimal growth. *Nature* 420, 186–189.
- Izutsu, K., Wada, A., and Wada, C. (2001). Expression of ribosome modulation factor (RMF) in *Escherichia coli* requires ppGpp. *Genes Cells* 6, 665–676.
- Kaplan, S., Bren, A., Zaslaver, A., Dekel, E., and Alon, U. (2008). Diverse two-dimensional input functions control bacterial sugar genes. *Mol. Cell* 29, 786–792.
- Keener, J., and Nomura, M. (1996). Regulation of Ribosome Synthesis. In *Escherichia Coli and Salmonella*, F.C. Neidhardt, ed. (Washington, D.C.: ASM Press), pp. 1417–1431.
- Keith, C.T., Boris, A.A., and Stockwell, B.R. (2005). Multicomponent therapeutics for networked systems. *Nat. Rev. Drug Discov.* 4, 71–78.
- Khan, S.R., and Yamazaki, H. (1972). Trimethoprim-induced accumulation of guanosine tetraphosphate (ppGpp) in *Escherichia coli*. *Biochem. Biophys. Res. Commun.* 48, 169–174.
- Kohanski, M.A., Dwyer, D.J., Hayete, B., Lawrence, C.A., and Collins, J.J. (2007). A common mechanism of cellular death induced by bactericidal antibiotics. *Cell* 130, 797–810.
- Kohanski, M.A., Dwyer, D.J., Wierzbowski, J., Cottarel, G., and Collins, J.J. (2008). Mistranslation of membrane proteins and two-component system activation trigger antibiotic-mediated cell death. *Cell* 135, 679–690.
- Kolodkin-Gal, I., Sat, B., Kesht, A., and Engelberg-Kulka, H. (2008). The communication factor EDF and the toxin-antitoxin module mazEF determine the mode of action of antibiotics. *PLoS Biol.* 6, e319.
- Kurland, C.G., and Maaløe, O. (1962). Regulation of ribosomal and transfer RNA synthesis. *J. Mol. Biol.* 4, 193–210.
- Kussell, E., and Leibler, S. (2005). Phenotypic diversity, population growth, and information in fluctuating environments. *Science* 309, 2075–2078.

- Lehár, J., Krueger, A., Zimmermann, G., and Borisy, A. (2008). High-order combination effects and biological robustness. *Mol. Syst. Biol.* 4, 215.
- Lehár, J., Zimmermann, G.R., Krueger, A.S., Molnar, R.A., Ledell, J.T., Heilbut, A.M., Short, G.F., 3rd, Giusti, L.C., Nolan, G.P., Magid, O.A., et al. (2007). Chemical combination effects predict connectivity in biological systems. *Mol. Syst. Biol.* 3, 80.
- Levy, S., Ihmels, J., Carmi, M., Weinberger, A., Friedlander, G., and Barkai, N. (2007). Strategy of transcription regulation in the budding yeast. *PLoS ONE* 2, e250.
- Liebermeister, W., Klipp, E., Schuster, S., and Heinrich, R. (2004). A theory of optimal differential gene expression. *Biosystems* 76, 261–278.
- Linares, J.F., Gustafsson, I., Baquero, F., and Martinez, J.L. (2006). Antibiotics as antimicrobial signaling agents instead of weapons. *Proc. Natl. Acad. Sci. USA* 103, 19484–19489.
- Loewe, S. (1928). Die quantitativen Probleme der Pharmakologie. *Ergeb. Physiol.* 27, 47–187.
- Loewe, S. (1953). The problem of synergism and antagonism of combined drugs. *Arzneimittelforschung* 3, 285–290.
- Mason, D.J., Power, E.G., Talsania, H., Phillips, I., and Gant, V.A. (1995). Antibacterial action of ciprofloxacin. *Antimicrob. Agents Chemother.* 39, 2752–2758.
- Mesak, L.R., Miao, V., and Davies, J. (2008). Effects of subinhibitory concentrations of antibiotics on SOS and DNA repair gene expression in *Staphylococcus aureus*. *Antimicrob. Agents Chemother.* 52, 3394–3397.
- Michel, B. (2005). After 30 years of study, the bacterial SOS response still surprises us. *PLoS Biol.* 3, e255.
- Michel, J.B., Yeh, P.J., Chait, R., Moellering, R.C., Jr., and Kishony, R. (2008). Drug interactions modulate the potential for evolution of resistance. *Proc. Natl. Acad. Sci. USA* 105, 14918–14923.
- Mitchell, A., Romano, G.H., Groisman, B., Yona, A., Dekel, E., Kupiec, M., Dahan, O., and Pilpel, Y. (2009). Adaptive prediction of environmental changes by microorganisms. *Nature* 460, 220–224.
- Moss, T. (2004). At the crossroads of growth control; making ribosomal RNA. *Curr. Opin. Genet. Dev.* 14, 210–217.
- Paul, B.J., Ross, W., Gaal, T., and Gourse, R.L. (2004). rRNA transcription in *Escherichia coli*. *Annu. Rev. Genet.* 38, 749–770.
- Pearl, S., Gabay, C., Kishony, R., Oppenheim, A., and Balaban, N.Q. (2008). Nongenetic individuality in the host-phage interaction. *PLoS Biol.* 6, e120.
- Piddock, L.J., Walters, R.N., and Diver, J.M. (1990). Correlation of quinolone MIC and inhibition of DNA, RNA, and protein synthesis and induction of the SOS response in *Escherichia coli*. *Antimicrob. Agents Chemother.* 34, 2331–2336.
- Pillai, S.K., Moellering, R.C., and Eliopoulos, G.M. (2005). Antimicrobial combinations. In *Antibiotics in Laboratory Medicine*, V. Lorian, ed. (Philadelphia: Lippincott Williams and Wilkins), pp. 365–440.
- Poole, K. (2005). Efflux-mediated antimicrobial resistance. *J. Antimicrob. Chemother.* 56, 20–51.
- Radman, M. (1975). SOS repair hypothesis: phenomenology of an inducible DNA repair which is accompanied by mutagenesis. *Basic Life Sci.* 5A, 355–367.
- Schneider, D.A., Gaal, T., and Gourse, R.L. (2002). NTP-sensing by rRNA promoters in *Escherichia coli* is direct. *Proc. Natl. Acad. Sci. USA* 99, 8602–8607.
- Schneider, D.A., and Gourse, R.L. (2004). Relationship between growth rate and ATP concentration in *Escherichia coli*: a bioassay for available cellular ATP. *J. Biol. Chem.* 279, 8262–8268.
- Shaw, K.J., Miller, N., Liu, X., Lerner, D., Wan, J., Bittner, A., and Morrow, B.J. (2003). Comparison of the changes in global gene expression of *Escherichia coli* induced by four bactericidal agents. *J. Mol. Microbiol. Biotechnol.* 5, 105–122.
- Smith, R.J., and Midgley, J.E. (1973). The effect of trimethoprim on macromolecular synthesis in *Escherichia coli*. Regulation of ribonucleic acid synthesis by 'Magic Spot' nucleotides. *Biochem. J.* 136, 249–257.
- Stevenson, B.S., and Schmidt, T.M. (2004). Life history implications of rRNA gene copy number in *Escherichia coli*. *Appl. Environ. Microbiol.* 70, 6670–6677.
- Tagkopoulos, I., Liu, Y.C., and Tavazoie, S. (2008). Predictive behavior within microbial genetic networks. *Science* 320, 1313–1317.
- Tippin, B., Pham, P., and Goodman, M.F. (2004). Error-prone replication for better or worse. *Trends Microbiol.* 12, 288–295.
- Tsui, W.H., Yim, G., Wang, H.H., McClure, J.E., Surette, M.G., and Davies, J. (2004). Dual effects of MLS antibiotics: transcriptional modulation and interactions on the ribosome. *Chem. Biol.* 11, 1307–1316.
- Walker, G.C. (1996). The SOS Response of *Escherichia coli*. In *Echerichia coli and Salmonella*, F.C. Neidhardt, ed. (Washington, D.C.: ASM Press), pp. 1400–1416.
- Xiao, H., Kalman, M., Ikehara, K., Zemel, S., Glaser, G., and Cashel, M. (1991). Residual guanosine 3',5'-bispyrophosphate synthetic activity of *relA* null mutants can be eliminated by *spoT* null mutations. *J. Biol. Chem.* 266, 5980–5990.
- Yeh, P., Tscharum, A.I., and Kishony, R. (2006). Functional classification of drugs by properties of their pairwise interactions. *Nat. Genet.* 38, 489–494.
- Yim, G., Wang, H.H., and Davies, J. (2006). The truth about antibiotics. *Int. J. Med. Microbiol.* 296, 163–170.
- Yim, G., Wang, H.H., and Davies, J. (2007). Antibiotics as signalling molecules. *Philos. Trans. R. Soc. Lond. B Biol. Sci.* 362, 1195–1200.
- Zaslaver, A., Bren, A., Ronen, M., Itzkovitz, S., Kikoin, I., Shavit, S., Liebermeister, W., Surette, M.G., and Alon, U. (2006). A comprehensive library of fluorescent transcriptional reporters for *Escherichia coli*. *Nat. Methods* 3, 623–628.
- Zaslaver, A., Mayo, A.E., Rosenberg, R., Bashkin, P., Sberro, H., Tsalyuk, M., Surette, M.G., and Alon, U. (2004). Just-in-time transcription program in metabolic pathways. *Nat. Genet.* 36, 486–491.

Supplemental Data

**Nonoptimal Microbial Response
to Antibiotics Underlies Suppressive
Drug Interactions**

Tobias Bollenbach, Selwyn Quan, Remy Chait, and Roy Kishony

Supplemental Experimental Procedures

Strain construction

In the ribosomal RNA deletion strains, each of the seven *rrn* operons was entirely deleted by the PCR allelic exchange method (Datsenko and Wanner, 2000) to give seven kanamycin marked *rrn* deletion strains. Deletions spanned the *rrn* promoters and terminators. Ribosomal RNA deletions were then combined into a strain with all *rrn* operons removed from the chromosome by a successive series of P1 transduction and kanamycin resolution steps with FLP resolvase (pCP20). A tRNA plasmid (ptRNA67) was introduced at the Δ 5 stage. Deletions were confirmed by PCR and Southern blots. All *rrn* deletion strains used in this study including the Δ 6 strain show little variation in morphology and form uniform colonies which is a sign of genetic stability. Δ 4 and Δ 6 strains with different remaining *rrn* operons show similar results in our key experiments (Figures S11 and S12) and the effects of *rrn* deletion can be partially revoked by genetic complementation (Figures S13, S14) indicating that random second site mutations that might have occurred in the construction of these strains do not significantly affect our results.

The Δ *relA* and Δ *relA* Δ *spoT* strains are from (Traxler et al., 2008). For the Δ *relA* Δ *spoT* strain, we verified the absence of suppressor mutations in *rpoBC* and *rpoD* before and after our experiment (Figure S15) using a standard control that is based on the fact that these strains cannot grow on minimal medium (Xiao et al., 1991) while suppressor mutations in *rpoBC* and *rpoD* allow for growth on minimal medium (Barker et al., 2001; Bartlett et al., 1998; Hernandez and Cashel, 1995; Zhou and Jin, 1998). Strain specifications are given in Table S2.

Chromosomal integration of promoter-GFP constructs

To verify that effects of reporter plasmid copy number changes on the measured expression level are independent of promoter, we integrated promoter-GFP constructs (*lexA*, *folA*, and *hisL*) into the *phoA* locus of strain TB10 (Johnson et al., 2004) by using λ Red-mediated recombination (Yu et al., 2000); we used primers

AAGAAGTTATTGAAGCATCCTCGTCAGTAAAAAGTTAATCTTTAACAGACC
AGAACAGCCCGTTGCG and
CAGCAAAAAAAACCACCCGGCAGCGAAAATTCACTGCCGGCGCGGTTTAG
GATCTATCAACAGGAGTCCAAGCG where the underlined sequence is homologous to the integration site. We verified successful integration events by colony PCR. Integrated constructs were moved into MG1655 by P1 transduction. Measuring fluorescence intensity, we find that the ratio of GFP expressed from the plasmid to GFP expressed from the chromosome is ~5 and increases as growth rate is decreased by adding antibiotics or changing carbon source, consistent with an increase in plasmid copy number. This increase is identical for the three promoters tested and is thus well corrected by normalization to the median expression level change.

Supplemental Figure Legends

Figure S1. Disappearance of suppression is incremental with number of *rrn* deletions and does not depend on growth medium, or the specific DNA synthesis or translation inhibitor used. (A,B) Growth rates of WT and *rrn* deletion strains in a two-dimensional concentration gradient of DNA synthesis inhibitor TMP and translation inhibitor SPR in rich LB medium (A) and glucose M9 minimal medium (B). MIC line shown in magenta. (C,D) As A,B, using DNA synthesis inhibitor CPR and translation inhibitor TET. The suppressive drug interaction (WT) is reduced in magnitude and eventually disappears as ribosome synthesis is reduced ($\Delta 4$, $\Delta 5$, $\Delta 6$). Small black dots, concentrations at which growth rate was sampled. For raw growth curve data, see Figures S8 and S9.

Figure S2. Regulation of ribosomal promoters for the DNA synthesis inhibitors CPR and NAL. (A) Normalized expression levels ε_x of 110 promoters in *E. coli* as a function of median growth rate in various concentrations of CPR (Experimental Procedures). Ribosomal promoters, orange squares; SOS response promoters, black triangles; *rmf* promoter, black crosses. Random scatter added to growth rate for visibility. (B) Cumulative distributions of normalized expression levels ε_x at single concentrations of CPR and NAL (normalized growth rate ~ 0.45). Ribosomal promoters, orange; other promoters, gray.

Figure S3. Regulation of ribosomal promoters in drug combination of DNA synthesis inhibitor and translation inhibitor. (A) Normalized expression level ε_x of ribosomal promoters *rpmE*, *rpsT*, *rrsA*, *rpsU* and the mean normalized expression level of all nine ribosomal promoters investigated here (Table S1) in a two-dimensional concentration matrix of TMP and SPR (Experimental Procedures). Small black dots, concentrations at which expression level was sampled. (B) Change in expression level $\varepsilon_x(\text{SPR}) / \varepsilon_x(\text{SPR}=0)$ as a function of SPR concentration, at no TMP (TMP=0, grey), and at a fixed TMP concentration (TMP=0.34 MIC, magenta). Up-regulation requires higher SPR concentration in the presence of TMP. Error-bars in B for promoters *rpmE*, *rpsT*, *rrsA*, *rpsU* were estimated from the standard deviation of replicate measurements done on different days (see Figure S17). Error-bars for the mean normalized expression level of all nine ribosomal promoters investigated here (rightmost panel) show the standard error of the mean.

Figure S4. Increased growth rate and survival resulting from reduced ribosome synthesis is specific to DNA synthesis inhibitors. (A-E) Normalized growth rates of strains with incremental deletions of *rrn* operons arranged in order of increasing ribosomal expression under different antibiotics. Growth rate increases with decreasing ribosome synthesis from WT levels, under DNA synthesis inhibitors CPR (A) and NAL (B). Growth rate is unaffected or decreases with decreasing ribosome synthesis for translation inhibitors SPR (C)

and TET (D) as well as nitrofurantoin NIT (E) which acts by multiple mechanisms. Lines, 4th order polynomial fits. (F) MICs of antibiotics for $\Delta 6$ strain relative to WT strain. Error bars show the standard deviation of replicates or the concentration resolution of the MIC determination, whichever is larger. Cultures grown in rich medium (LB).

Figure S5. Reduced ribosome synthesis leads to smaller cell size under DNA synthesis inhibitors at the same relative growth inhibition. (A) DIC images of WT cells and cells with reduced ribosome synthesis ($\Delta 6$) growing in presence of DNA synthesis inhibitor (NAL) at the same relative growth inhibition ($g \sim 0.3$ which corresponds to absolute growth rate 0.2h^{-1} for WT and 0.1h^{-1} for $\Delta 6$); scale bar, $10 \mu\text{m}$. (B) Cumulative distribution of cell lengths. Cell size of $\Delta 6$ (squares) is slightly larger than that of WT (circles) in the absence of drugs but smaller in the presence of DNA synthesis inhibitor (NAL) at the same relative growth inhibition. This cell size difference is similar or even more pronounced if size distributions of $\Delta 6$ and WT are compared at the same absolute growth rate or at the same drug concentration.

Figure S6. Mathematical model with optimal regulation of ribosome synthesis quantitatively reproduces the changes in cell composition and growth rate that occur in different nutrient environments. Comparison of model results to experimental data as growth rate changes in different nutrient environments. Lines show model results, symbols experimental data (Bremer and Dennis, 1996). (A) Total protein per cell. (B) DNA per cell. (C) Fraction of total protein that is ribosomal protein. (D) Peptide chain elongation rate (translation rate per ribosome; circles) and DNA chain elongation rate (DNA synthesis rate per replication fork; squares).

Figure S7. Suppression relative to that seen for WT is amplified for a $\Delta relA$ strain to a similar extent as for a $\Delta relA \Delta spoT$ strain. Growth rates of WT (A), $\Delta relA$ (B), and $\Delta relA \Delta spoT$ (C) strain in two-dimensional concentration gradients of DNA synthesis inhibitor (TMP) and translation inhibitor (SPR); MIC line, magenta. The suppressive drug interaction (A) is amplified in the $\Delta relA$ strain (B) and in the $\Delta relA \Delta spoT$ strain (C). *relA* deletions impair the cell's capability to synthesize ppGpp while not completely removing it like *relA spoT* deletions (Xiao et al., 1991). Since $\Delta relA$ strains are less associated with the rapid occurrence of suppressor mutations in *rpoBC* and *rpoD* that are known to occur in $\Delta relA \Delta spoT$ strains (Barker et al., 2001; Bartlett et al., 1998; Hernandez and Cashel, 1995; Zhou and Jin, 1998), these results support that our conclusions are not affected by suppressor mutations. Small black dots, concentrations at which growth rate was sampled. Note that absolute TMP MICs for the $\Delta relA$ and $\Delta relA \Delta spoT$ strains are about two-fold lower than those of the WT. For raw growth curve data, see Figure S10. Cultures grown in rich medium (LB).

Figure S8. Raw growth curves of WT and mutants with reduced ribosome synthesis in two-dimensional drug matrix of TMP and SPR. (A) Comparison of growth curves of WT and $\Delta 6$ strain in identical two-dimensional concentration gradients of TMP and SPR in rich LB medium (Experimental Procedures). Each small box shows $\log(\text{OD}_{600})$ versus time, see magnified box on bottom left for scales. (B) As A, comparing WT and $\Delta 5$ strain in glucose M9 minimal medium (Experimental Procedures). (C) Repeat of $\Delta 6$ in A with higher drug concentration resolution and lower SPR concentrations to verify absence of suppression.

Figure S9. Raw growth curves of WT and mutants with reduced ribosome synthesis in two-dimensional drug matrix of CPR and TET. (A,B) Growth curves of WT (A) and $\Delta 6$ strain (B) in identical two-dimensional concentration gradients of CPR and TET in glucose M9 minimal medium (Experimental Procedures). Each small box shows $\log(\text{OD}_{600})$ versus time, see magnified box on bottom left for scales. (C,D) As A,B, in rich medium (LB).

Figure S10. Raw growth curves of WT and mutants with impaired regulation of ribosome synthesis in two-dimensional drug matrix of TMP and SPR. Growth curves of WT (A), ΔrelA strain (B), and $\Delta \text{relA} \Delta \text{spoT}$ strain (C) in identical two-dimensional concentration gradients of TMP and SPR in rich LB medium. Each small box shows $\log(\text{OD}_{600})$ versus time, see magnified box on bottom left for scales. The decrease in MIC for TMP in the $\Delta \text{relA} \Delta \text{spoT}$ strain was verified in independent experiments with higher concentration resolution along the TMP axis.

Figure S11. Deletions of different sets of 4 or 6 *rrn* operons have similar effects on growth rate in the absence and in the presence of DNA synthesis inhibitors. (A) Optical density (OD_{600}) as a function of time for wild type MG1655 (black), two different $\Delta 4$ strains ($\Delta \text{rrnGBAD}$, dashed green line; $\Delta \text{rrnGADE}$, dotted green line), and two different $\Delta 6$ strains ($\Delta \text{rrnGADEHB}$, dashed magenta line; $\Delta \text{rrnGADBHC}$, dotted magenta line) in the absence of antibiotics. (B) As A, in the presence of a fixed concentration of the DNA synthesis inhibitor CPR. Results are similar if NAL is used instead of CPR (not shown). Note that all $\Delta 4$ and $\Delta 6$ strains have increased MICs for CPR and NAL (not shown). These results show that the growth rate phenotypes of the *rrn* deletion strains we report are reproducible across differently constructed *rrn* deletion strains. Consequently, they are unlikely to be caused by second site mutations that could occur in the construction of these strains. Cultures grown in rich medium (LB).

Figure S12. Deletions of different sets of 4 or 6 *rrn* operons have similar effects on suppressive drug interactions between DNA synthesis inhibitors and translation inhibitors. (A) Normalized growth rates in a two-dimensional drug matrix of TMP and SPR for the wild type strain MG1655 (see Figure 6B). (B) As A, for two different $\Delta 4$ strains as indicated. (C) As A, for two different $\Delta 6$ strains as indicated. While there are small differences in the shape of the MIC line, both $\Delta 4$ strains show a strongly reduced magnitude of the suppressive drug

interaction compared to WT and suppression is completely absent in both $\Delta 6$ strains. These results demonstrate that the suppression phenotypes of the *rrn* deletion strains we observe are reproducible across differently constructed *rrn* deletion strains. Consequently they are unlikely to be caused by second site mutations that could occur in the construction of these strains. Cultures grown in rich medium (LB).

Figure S13. Complementation with a plasmid-borne *rrn* operon partially reverses the effects of *rrn* deletions on growth rate, in the presence and absence of a DNA synthesis inhibitor. (A) Optical density (OD_{600}) as a function of time for wild type MG1655 (solid line), a $\Delta 6$ strain ($\Delta rrnGADEHB$, dashed line) and the same $\Delta 6$ strain with plasmid pKK3535 that carries an *rrnB* operon (dotted line) in the absence of antibiotics. (B) As A, in the presence of a fixed concentration of the DNA synthesis inhibitor NAL (near the MIC of the wild type). (C) As B, but at a higher concentration of NAL (slightly above the MIC of the wild type). Results are similar if CPR is used instead of NAL (not shown). (D-F) As A-C, but using a different $\Delta 6$ strain ($\Delta rrnGADBHC$, dashed line) complemented with plasmid pK4-16 that carries an *rrnB* operon (dotted line). (G-J) As A-C, but using two different $\Delta 4$ strains ($\Delta rrnGADE$, dashed black line; $\Delta rrnGBAD$, dashed gray line) complemented with plasmid pKK3535 (black and gray dotted lines). These results indicate that the observed effects of *rrn* deletions on growth rate in these different environments are mostly due to changes in the ribosome level and are not caused by second site mutations that could occur in the construction of these strains. Cultures grown in rich medium (LB).

Figure S14. Addition of a plasmid-borne *rrn* operon to a $\Delta 6$ strain partially restores the suppressive drug interaction between DNA synthesis inhibitors and translation inhibitors. (A) Normalized growth rates in a two-dimensional drug matrix of TMP and SPR for wild type MG1655 as in Figure 6B. (B) As A, for a $\Delta 6$ strain ($\Delta rrnGADEHB$). (B) As B, for the same $\Delta 6$ strain bearing plasmid pK4-16, which carries an *rrnB* operon. These results show that the effects of *rrn* deletions on the magnitude of the suppressive drug interactions between DNA synthesis inhibitors and translation inhibitors are mostly due to changes in the ribosome level and are not caused by potential second site mutations that could possibly occur in the construction of these strains. Cultures grown in rich medium (LB).

Figure S15. Absence of growth of $\Delta relA\Delta spoT$ strain on minimal media plates indicates absence of suppressor mutations in RNA polymerase genes in this strain. Strains $\Delta relA\Delta spoT$ and $\Delta relA$ were taken from wells with different concentrations of TMP and SPR (see schematic on right; cf. Figure 6C) after growth for 24h in this two drug environment and streaked on LB plates (left column) and glucose M9 minimal media plates (not supplemented with amino acids, right column). WT MG1655 grown in the absence of antibiotics was streaked on all plates as a positive control. Samples were taken from the following environments: (A) no drug, (B) highest concentration of TMP alone with

visible growth after 24h ($OD_{600} > 0.06$), (C) highest concentration of SPR alone with visible growth after 24h, (D) two-drug environment of TMP and SPR at highest overall TMP concentration with visible growth after 24h (see schematic on right). In all cases, the $\Delta relA \Delta spoT$ strain grows on LB but does not grow on minimal medium (Xiao et al., 1991). This confirms that suppressor mutations in *rpoBC* and *rpoD*, which can arise quickly in $\Delta relA \Delta spoT$ mutants (Barker et al., 2001; Bartlett et al., 1998; Hernandez and Cashel, 1995; Zhou and Jin, 1998), do not occur at an appreciable rate in the course of our experiment. Differences in colony densities reflect samples from wells with different degrees of growth. LB plates were incubated at 37°C for 24h, M9 plates for 48h to ensure detection of slowly growing colonies.

Figure S16. A *relA spoT* deletion strain has an increased lag time while its steady state growth rate is only slightly reduced compared to WT. Eight replicates of growth curves (optical density as a function of time) for both WT MG1655 (black lines) and the $\Delta relA \Delta spoT$ mutant (gray lines) are shown. Green lines are curves representing exponential growth with the median growth rate of all replicates for the WT, and for the $\Delta relA \Delta spoT$ strain. The shown values for the growth rates are median +/- standard deviation of replicates. Note that the $\Delta relA \Delta spoT$ strain has a clearly increased lag time but only a slightly reduced steady state growth rate. Cultures grown in rich medium (LB).

Figure S17. Day-to-day variability of gene expression measurements. Black circles show the standard deviation of the expression level γ (see Figure 3A) from seven replicate measurements (done on different days) of the promoters shown in Table S1 plotted as a function of the average expression level γ of each promoter. The red line indicates the maximum standard deviation as a function of the expression level which is used to estimate the error-bars in Figures 4B and S3B. Replicate measurements were done in the absence of antibiotics.

Supplemental Tables

Table S1: Transcriptional promoter-GFP reporter strains used in this study.

| Promoter | Description |
|---------------|---|
| <i>ampC</i> * | Beta-lactamase/D-ala carboxypeptidase; penicillin resistance, penicillin-binding protein (PBP) |
| <i>amyA</i> * | cytoplasmic alpha-amylase |
| <i>argA</i> * | N-alpha-acetylglutamate synthase (amino-acid acetyltransferase) (1st module) |
| <i>argQ</i> * | arginine tRNA 2 (duplicate of argV,Y,Z) |
| <i>aroH</i> * | 3-deoxy-D-arabinoheptulosonate-7-phosphate synthase (DAHP synthetase), tryptophan repressible |
| <i>aroL</i> * | shikimate kinase II |
| <i>asnA</i> | asparagine synthetase A |
| <i>aspC</i> | aspartate aminotransferase, PLP-dependent |
| <i>aspU</i> | aspartate tRNA 1 (duplicate of aspT,V) |
| <i>atpI</i> * | membrane-bound ATP synthase subunit, F1-F0-type proton-ATPase |
| <i>bacA</i> * | bacitracin resistance; possibly phosphorylates undecaprenol |
| <i>bioB</i> * | biotin synthetase (2nd module) |
| <i>bolA</i> * | activator of morphogenic pathway (BolA family), important in general stress response |
| <i>brnQ</i> * | LIVCS family, branched chain amino acid transporter system II (LIV-II) |
| <i>btuB</i> * | outer membrane porin, transporter for vitamin B12/cobalamin, receptor for E colicins, and bacteriophage BF23 (1st module) |
| <i>chpR</i> | part of proteic killer gene system, suppressor of inhibitory function of ChpA |
| <i>clpP</i> * | proteolytic subunit of clpA-clpP ATP-dependent serine protease, heat shock protein F21.5 |
| <i>cls</i> | cardiolipin synthase |
| <i>cmr</i> | MFS superfamily transporter, multidrug/chloramphenicol efflux transporter (1st module) |
| <i>cpsG</i> * | phosphomannomutase in colanic acid gene cluster |
| <i>cpxR</i> * | response regulator in two-component regulatory system with CpxA, regulates expression of protein folding and degrading factors (OmpR family) (1st module) |
| <i>creD</i> * | tolerance to colicin E2 |
| <i>cspA</i> * | major cold shock protein 7.4, transcription antiterminator of hns, |
| <i>cspB</i> * | Qin prophage; cold shock protein; may regulate transcription |
| <i>cspD</i> * | similar to CspA but not cold shock induced, nucleic acid-binding domain |
| <i>cusR</i> * | response regulator in two-component regulatory system with CusS, transcriptional regulation of copper resistance (1st module) |
| <i>cyoA</i> * | cytochrome o ubiquinol oxidase subunit II |
| <i>cysB</i> * | transcriptional regulator for biosynthesis of L-cysteine (LysR family) (1st module) |
| <i>cysP</i> * | ABC superfamily (peri_bind) thiosulfate transport protein |
| <i>cysT</i> * | cysteine tRNA |
| <i>dacA</i> * | D-alanyl-D-alanine carboxypeptidase, penicillin-binding protein 5 (1st module) |
| <i>dgkA</i> * | diacylglycerol kinase |
| <i>dinG</i> | LexA regulated (SOS) repair enzyme (2nd module) |
| <i>dinJ</i> * | damage-inducible protein J |
| <i>dinP</i> * | DNA polymerase IV, devoid of proofreading, damage-inducible protein P (1st module) |
| <i>dnaK</i> * | chaperone Hsp70 in DNA biosynthesis/cell division (1st module) |
| <i>dnaX</i> * | DNA polymerase III, tau and gamma subunits; DNA elongation factor III (1st module) |
| <i>dps</i> * | stress response DNA-binding protein; starvation induced resistance to H2O2, ferritin-like |

| | |
|---------------|--|
| <i>edd</i> * | 6-phosphogluconate dehydratase |
| <i>emrA</i> * | multidrug resistance secretion protein |
| <i>emrE</i> * | DLP12 prophage; MFP family auxillary multidrug transport protein, methylviologen and ethidium resistance |
| <i>emrR</i> | transcriptional repressor of for multidrug resistance pump (MarR family) |
| <i>evgA</i> * | response regulator (activator) in two-component regulatory system with EvgS, regulates multidrug resistance (LuxR/UhpA family) |
| <i>fabZ</i> | (3R)-hydroxymyristol acyl carrier protein dehydratase |
| <i>fadB</i> * | multifunctional multimodular FadB: 3-hydroxybutyryl-coa epimerase (EC 5.1.2.3); delta(3)-cis-delta(2)-trans-enoyl-coa-isomerase (EC 5.3.3.8); enoyl-coa-hydrtatase (4.2.1.17) (1st module) |
| <i>fecA</i> * | outer membrane porin, receptor for ferric citrate, in multi-component regulatory system with cytoplasmic Fecl (sigma factor) and membrane bound FecR (1st module) |
| <i>fecI</i> * | sigma (19) factor of RNA polymerase, affected by FecR and outer membrane receptor FecA (TetR/ArcR family) |
| <i>fepA</i> * | outer membrane porin, receptor for ferric enterobactin (enterochelin) and colicins B and D (1st module) |
| <i>flgM</i> | anti-FliA (anti-sigma) factor; also known as RflB protein |
| <i>fliA</i> * | sigma F (sigma 28) factor of RNA polymerase, transcription of late flagellar genes (class 3a and 3b operons) |
| <i>folA</i> * | dihydrofolate reductase type I; trimethoprim resistance |
| <i>fsr</i> * | MFS family fosmidomycin transport protein (2nd module) |
| <i>ftsZ</i> * | tubulin-like GTP-binding protein and GTPase, forms circumferential ring in cell division |
| <i>galE</i> * | UDP-galactose 4-epimerase (1st module) |
| <i>glgS</i> * | glycogen biosynthesis, rpoS dependent |
| <i>glnU</i> * | glutamine tRNA 1 (duplicate of glnW) |
| <i>gltB</i> * | glutamate synthase, large subunit (2nd module) |
| <i>gltJ</i> * | ABC superfamily (membrane), glutamate/aspartate transporter |
| <i>glyA</i> * | serine hydroxymethyltransferase (2nd module) |
| <i>gnd</i> * | gluconate-6-phosphate dehydrogenase, decarboxylating (1st module) |
| <i>gyrB</i> | DNA gyrase, subunit B (type II topoisomerase) (1st module) |
| <i>hdeA</i> * | conserved protein |
| <i>hipB</i> * | transcriptional repressor which interacts with HipA |
| <i>hisL</i> * | his operon leader peptide |
| <i>hisQ</i> * | ABC superfamily (membrane) histidine and lysine/arginine/ornithine transport system |
| <i>hisS</i> * | histidine tRNA synthetase (operon includes yfgL, see D. Kahne, Science, 2001) |
| <i>hslJ</i> | Heat shock protein hslJ |
| <i>htpG</i> * | chaperone Hsp90, heat shock protein C 62.5 |
| <i>htpX</i> * | Heat shock protein, integral membrane protein |
| <i>htrA</i> * | periplasmic serine protease Do, heat shock protein (2nd module) |
| <i>icdA</i> * | isocitrate dehydrogenase in e14 prophage, specific for NADP+ (2nd module) |
| <i>iciA</i> * | inhibitor of replication initiation, also transcriptional regulator of dnaA and argK (affects arginine transport) (LysR family) |
| <i>ilex</i> * | isoleucine tRNA 2 |
| <i>ilvL</i> * | ilvGEDA operon leader peptide |
| <i>inaA</i> * | pH inducible protein involved in stress response, protein kinase-like |
| <i>lacZ</i> * | Beta-galactosidase, lac operon |
| <i>lexA</i> * | transcriptional repressor for SOS response (signal peptidase of LexA family) |
| | dihydrolipoamide dehydrogenase, FAD/NAD(P)-binding ; component of 2-oxodehydrogenase and pyruvate complexes; L protein of glycine cleavage complex second part (2nd module) |
| <i>lpdA</i> * | diaminopimelate decarboxylase, PLP-binding (2nd module) |
| <i>lysA</i> * | |

| | |
|---------------|---|
| <i>macA</i> * | putative membrane protein |
| <i>malZ</i> * | maltodextrin glucosidase (2nd module) |
| <i>marR</i> * | transcriptional repressor for antibiotic resistance and oxidative stress |
| <i>mazG</i> * | conserved protein |
| <i>mdtH</i> * | putative MFS superfamily transport protein |
| <i>menF</i> | isochorismate synthase (isochorismate hydroxymutase 2), menaquinone biosynthesis |
| <i>mesJ</i> * | cell cycle protein |
| <i>metA</i> | homoserine transsuccinylase |
| <i>metJ</i> | transcriptional repressor for methionine biosynthesis (MetJ family) |
| <i>minC</i> * | cell division inhibitor; activated MinC inhibits FtsZ ring formation |
| <i>mrcB</i> * | bifunctional multimodular MrcB: tglycosyl transferase of penicillin-binding protein 1b (2nd module) |
| <i>mscL</i> * | mechanosensitive channel |
| <i>msrA</i> * | peptide methionine sulfoxide reductase |
| <i>murA</i> * | UDP-N-acetylglucosamine 1-carboxyvinyltransferase |
| <i>murC</i> * | L-alanine adding enzyme, UDP-N-acetyl-muramate:alanine ligase (1st module) |
| <i>napF</i> | Fe-S ferredoxin-type protein: electron transfer |
| <i>nfnB</i> * | dihydropteridine reductase/oxygen-insensitive NAD(P)H nitroreductase |
| <i>nhaA</i> * | NhaA family of transport protein, Na ⁺ /H ⁺ antiporter (1st module) |
| <i>nrfA</i> * | nitrite reductase periplasmic cytochrome c(552): |
| <i>nuoA</i> * | NADH dehydrogenase I chain A |
| <i>ompN</i> * | outer membrane protein N, non-specific porin (1st module) |
| <i>osmC</i> * | resistance protein, osmotically inducible |
| <i>pabC</i> | 4-amino-4-deoxychorismate lyase (aminotransferase) (2nd module) |
| <i>pepQ</i> | proline dipeptidase (2nd module) |
| <i>pfkA</i> | 6-phosphofructokinase I |
| <i>pgpB</i> | phosphatidylglycerophosphate phosphatase B |
| <i>pheL</i> * | leader peptide of chorismate mutase-P-prephenate dehydratase |
| <i>plsB</i> * | glycerolphosphate acyltransferase (2nd module) |
| <i>pmbA</i> | peptide maturation protein, maturation of antibiotic MccB17, see tld genes ? |
| <i>pmrD</i> | polymyxin resistance protein B |
| <i>polA</i> * | DNA polymerase I, 3' --> 5' polymerase, 5' --> 3' and 3' --> 5' exonuclease (1st module) |
| <i>polB</i> * | DNA polymerase II and 3' --> 5' exonuclease |
| <i>priA</i> * | primosomal protein N' (= factor Y) directs replication fork assembly at D-loops, ATP-dependent (2nd module) |
| <i>priC</i> * | primosomal replication protein N'' |
| <i>proB</i> | gamma-glutamate kinase |
| <i>psiF</i> * | induced by phosphate starvation |
| <i>ptsG</i> * | multimodular PtsG: PTS family enzyme IIC, glucose-specific (1st module) |
| <i>pykF</i> * | pyruvate kinase I (formerly F), fructose stimulated (2nd module) |
| <i>rbfA</i> * | ribosome-binding factor, role in processing of 10S rRNA |
| <i>recA</i> * | DNA strand exchange and recombination protein with protease and nuclease activity (1st module) |
| <i>recN</i> * | protein used in recombination and DNA repair (2nd module) |
| <i>ribA</i> | GTP cyclohydrolase II |
| <i>rmf</i> * | ribosome modulation factor (involved in dimerization of 70S ribosomes) |
| <i>rnhA</i> * | RNase HI, degrades RNA of DNA-RNA hybrids |
| <i>rob</i> * | transcriptional activator for resistance to antibiotics, organic solvents and heavy metals (AraC/XylS family) (right origin binding protein) (1st module) |
| <i>rpiA</i> * | ribosephosphate isomerase, constitutive |

| | |
|---------------|---|
| <i>rplL</i> * | 50S ribosomal subunit protein L7/L12 |
| <i>rplN</i> * | 50S ribosomal subunit protein L14 |
| <i>rplT</i> * | 50S ribosomal subunit protein L20, also posttranslational autoregulator |
| <i>rplY</i> | 50S ribosomal subunit protein L25 |
| <i>rpmB</i> * | 50S ribosomal subunit protein L28 |
| <i>rpmE</i> * | 50S ribosomal subunit protein L31 |
| <i>rpmI</i> * | 50S ribosomal subunit protein A |
| <i>rpoD</i> * | sigma D (sigma 70) factor of RNA polymerase , major sigma factor during exponential growth (2nd module) |
| <i>rpoE</i> | sigma E (sigma 24) factor of RNA polymerase, response to periplasmic stress (TetR/ArcR family) |
| <i>rpoH</i> * | sigma H (sigma 32) factor of RNA polymerase; transcription of heat shock proteins induced by cytoplasmic stress |
| <i>rpoS</i> * | sigma S (sigma 38) factor of RNA polymerase, major sigmafactor during stationary phase |
| <i>rpsA</i> * | 30S ribosomal subunit protein S1 (3rd module) |
| <i>rpsB</i> * | 30S ribosomal subunit protein S2 |
| <i>rpsT</i> * | 30S ribosomal subunit protein S20 |
| <i>rpsU</i> * | 30S ribosomal subunit protein S21 |
| <i>rriA</i> * | 23S rRNA |
| <i>rriB</i> * | 23S rRNA |
| <i>rrsA</i> * | 16S rRNA |
| <i>rsd</i> * | regulator of sigma D, has binding activity to the major sigma subunit of RNAP |
| <i>sbcB</i> * | exonuclease I, 3' --> 5' specific; deoxyribophosphodiesterase |
| <i>sbmA</i> * | ABC superfamily (membrane module of atp&memb) transporter (2nd module) |
| <i>sbmC</i> * | DNA gyrase inhibitor |
| <i>sdhC</i> * | succinate dehydrogenase , cytochrome b556 |
| <i>serA</i> * | D-3-phosphoglycerate dehydrogenase |
| <i>serC</i> * | 3-phosphoserine aminotransferase / phosphohydroxythreonine transaminase |
| <i>serU</i> * | serine tRNA 2 |
| <i>slp</i> * | outer membrane protein, induced after carbon starvation |
| <i>smpA</i> * | small membrane protein A |
| <i>soxS</i> * | transcriptional activator of superoxide response regulon (AraC/XylS family) |
| <i>sspA</i> * | stringent starvation protein A, regulator of transcription |
| <i>sufI</i> * | suppressor of <i>ftsI</i> , putative periplasmic protein, cupredoxin-like |
| <i>thiC</i> * | 5'-phosphoryl-5-aminoimidazole = 4-amino-5-hydroxymethyl-2-methylpyrimidine-P tol protein required for outer membrane integrity, uptake of group A colicins, C-terminal is coreceptor with F pilus for filamentous phages, role in translocation of filamentous phage DNA to cytoplasm (1st module) |
| <i>tolA</i> * | outer membrane channel; specific tolerance to colicin E1; segregation of daughter chromosomes, role in organic solvent tolerance |
| <i>tolC</i> * | transcriptional repressor for tryptophan biosynthesis (TrpR family) |
| <i>trpR</i> * | L-tartrate dehydratase |
| <i>ttdA</i> * | tyrosine aminotransferase , tyrosine repressible, PLP-dependent |
| <i>tyrB</i> * | ABC superfamily (membrane) sn-glycerol 3-phosphate transport protein |
| <i>ugpA</i> * | component of DNA polymerase V , signal peptidase with UmuC |
| <i>umuD</i> * | universal stress protein A |
| <i>uspA</i> * | UvrA with UvrBC is a DNA excision repair enzyme (2nd module) |
| <i>uvrA</i> * | UvrC with UvrAB is a DNA excision repair enzyme (1st module) |
| <i>uvrC</i> * | DNA-dependent ATPase I and helicase II (1st module) |
| <i>uvrD</i> * | flavodoxin-like protein, trp repressor binding protein |
| <i>wrbA</i> * | exonuclease VII, large subunit |
| <i>xseA</i> | |

| | |
|---------------|---|
| <i>yaeL</i> * | putative protease |
| <i>yajR</i> * | putative MFS family transport protein (1st module) |
| <i>yceE</i> * | putative MFS family transport protein (1st module) |
| <i>yddA</i> * | bifunctional multimodular YddA: putative ABC superfamily (membrane) transport protein (1st module) |
| <i>ydeA</i> * | MFS family, L-arabinose/isopropyl-beta-D-thiogalactopyranoside export protein, contributes to control of arabinose regulon (2nd module) |
| <i>ydeB</i> * | inner membrane protein involved in multiple antibiotic resistance |
| <i>ydhE</i> * | putative MATE family transport protein (1st module) |
| <i>ydiM</i> * | putative MFS family transport protein (1st module) |
| <i>yebG</i> * | DNA damage-inducible gene in SOS regulon, dependent on cyclic AMP and H-NS |
| <i>yebQ</i> * | putative MFS family transport protein (1st module) |
| <i>yjcR</i> * | putative multidrug resistance efflux pump protein, membrane protein |
| <i>ynfM</i> | putative MFS family transport protein (1st module) |
| <i>yojH</i> * | NA |
| <i>yojI</i> * | putative ABC superfamily (atp module of atp&membrane) transport protein (2nd module) |

* Promoters with low GFP signal. These were excluded from the analysis shown in Figure 3.

* Promoters used for the two-dimensional drug concentration gradient of Figure 4.

Table S2: Strains used in this study.

| Strain | Type | Source |
|---------------------------|-------------------------------------|-------------------------|
| WT | MG1655 | - |
| WT (reporter strains) | MG1655 / pUA66 or pUA139 | (Zaslaver et al., 2006) |
| Δ1 | MG1655 $\Delta rrnE$ | This study (S. Quan) |
| Δ2 | MG1655 $\Delta rrnGB$ | This study (S. Quan) |
| Δ3 | MG1655 $\Delta rrnGBA$ | This study (S. Quan) |
| Δ4* | MG1655 $\Delta rrnGADE$ | This study (S. Quan) |
| Δ4 | MG1655 $\Delta rrnGBAD$ | This study (S. Quan) |
| Δ5 | MG1655 $\Delta rrnGADEH$ / ptRNA67 | This study (S. Quan) |
| Δ6* | MG1655 $\Delta rrnGADBHC$ / ptRNA67 | This study (S. Quan) |
| Δ6 | MG1655 $\Delta rrnGADEHB$ / ptRNA67 | This study (S. Quan) |
| $\Delta relA \Delta spoT$ | MG1655 $\Delta relA \Delta spoT$ | (Traxler et al., 2008) |
| $\Delta relA$ | MG1655 $\Delta relA$ | (Traxler et al., 2008) |

*Assay strain used unless otherwise indicated.

Supplemental References

- Barker, M. M., Gaal, T., and Gourse, R. L. (2001). Mechanism of regulation of transcription initiation by ppGpp. II. Models for positive control based on properties of RNAP mutants and competition for RNAP. *J Mol Biol* 305, 689-702.
- Bartlett, M. S., Gaal, T., Ross, W., and Gourse, R. L. (1998). RNA polymerase mutants that destabilize RNA polymerase-promoter complexes alter NTP-sensing by rrn P1 promoters. *J Mol Biol* 279, 331-345.
- Bionumbers (2009). <http://bionumbers.hms.harvard.edu/>.
- Blattner, F. R., Plunkett, G., 3rd, Bloch, C. A., Perna, N. T., Burland, V., Riley, M., Collado-Vides, J., Glasner, J. D., Rode, C. K., Mayhew, G. F., et al. (1997). The complete genome sequence of Escherichia coli K-12. *Science* 277, 1453-1474.
- Bremer, H., and Churchward, G. (1977). An examination of the Cooper-Helmstetter theory of DNA replication in bacteria and its underlying assumptions. *J Theor Biol* 69, 645-654.
- Bremer, H., and Dennis, P. P. (1996). Modulation of Chemical Composition and Other Parameters of the Cell by Growth Rate, In *Escherichia coli and Salmonella*, F. C. Neidhardt, ed. (Washington, D.C.: ASM Press), pp. 1553-1569.
- Cooper, S., and Helmstetter, C. E. (1968). Chromosome replication and the division cycle of Escherichia coli B/r. *J Mol Biol* 31, 519-540.
- Datsenko, K. A., and Wanner, B. L. (2000). One-step inactivation of chromosomal genes in Escherichia coli K-12 using PCR products. *Proc Natl Acad Sci U S A* 97, 6640-6645.
- Donachie, W. D. (1968). Relationship between cell size and time of initiation of DNA replication. *Nature* 219, 1077-1079.
- Donachie, W. D., and Blakely, G. W. (2003). Coupling the initiation of chromosome replication to cell size in Escherichia coli. *Curr Opin Microbiol* 6, 146-150.
- Georgopapadakou, N. H., and Bertasso, A. (1991). Effects of quinolones on nucleoid segregation in Escherichia coli. *Antimicrob Agents Chemother* 35, 2645-2648.
- Hernandez, V. J., and Cashel, M. (1995). Changes in conserved region 3 of Escherichia coli sigma 70 mediate ppGpp-dependent functions in vivo. *J Mol Biol* 252, 536-549.

Johnson, J. E., Lackner, L. L., Hale, C. A., and de Boer, P. A. (2004). ZipA is required for targeting of DMinC/DicB, but not DMinC/MinD, complexes to septal ring assemblies in *Escherichia coli*. *J Bacteriol* 186, 2418-2429.

Paul, B. J., Ross, W., Gaal, T., and Gourse, R. L. (2004). rRNA transcription in *Escherichia coli*. *Annu Rev Genet* 38, 749-770.

Traxler, M. F., Summers, S. M., Nguyen, H. T., Zacharia, V. M., Hightower, G. A., Smith, J. T., and Conway, T. (2008). The global, ppGpp-mediated stringent response to amino acid starvation in *Escherichia coli*. *Mol Microbiol* 68, 1128-1148.

Xiao, H., Kalman, M., Ikehara, K., Zemel, S., Glaser, G., and Cashel, M. (1991). Residual guanosine 3',5'-bispyrophosphate synthetic activity of *relA* null mutants can be eliminated by *spoT* null mutations. *J Biol Chem* 266, 5980-5990.

Yu, D., Ellis, H. M., Lee, E. C., Jenkins, N. A., Copeland, N. G., and Court, D. L. (2000). An efficient recombination system for chromosome engineering in *Escherichia coli*. *Proc Natl Acad Sci U S A* 97, 5978-5983.

Zaslaver, A., Bren, A., Ronen, M., Itzkovitz, S., Kikoin, I., Shavit, S., Liebermanmeister, W., Surette, M. G., and Alon, U. (2006). A comprehensive library of fluorescent transcriptional reporters for *Escherichia coli*. *Nat Methods* 3, 623-628.

Zhou, Y. N., and Jin, D. J. (1998). The *rpoB* mutants destabilizing initiation complexes at stringently controlled promoters behave like "stringent" RNA polymerases in *Escherichia coli*. *Proc Natl Acad Sci U S A* 95, 2908-2913.

Figure S1

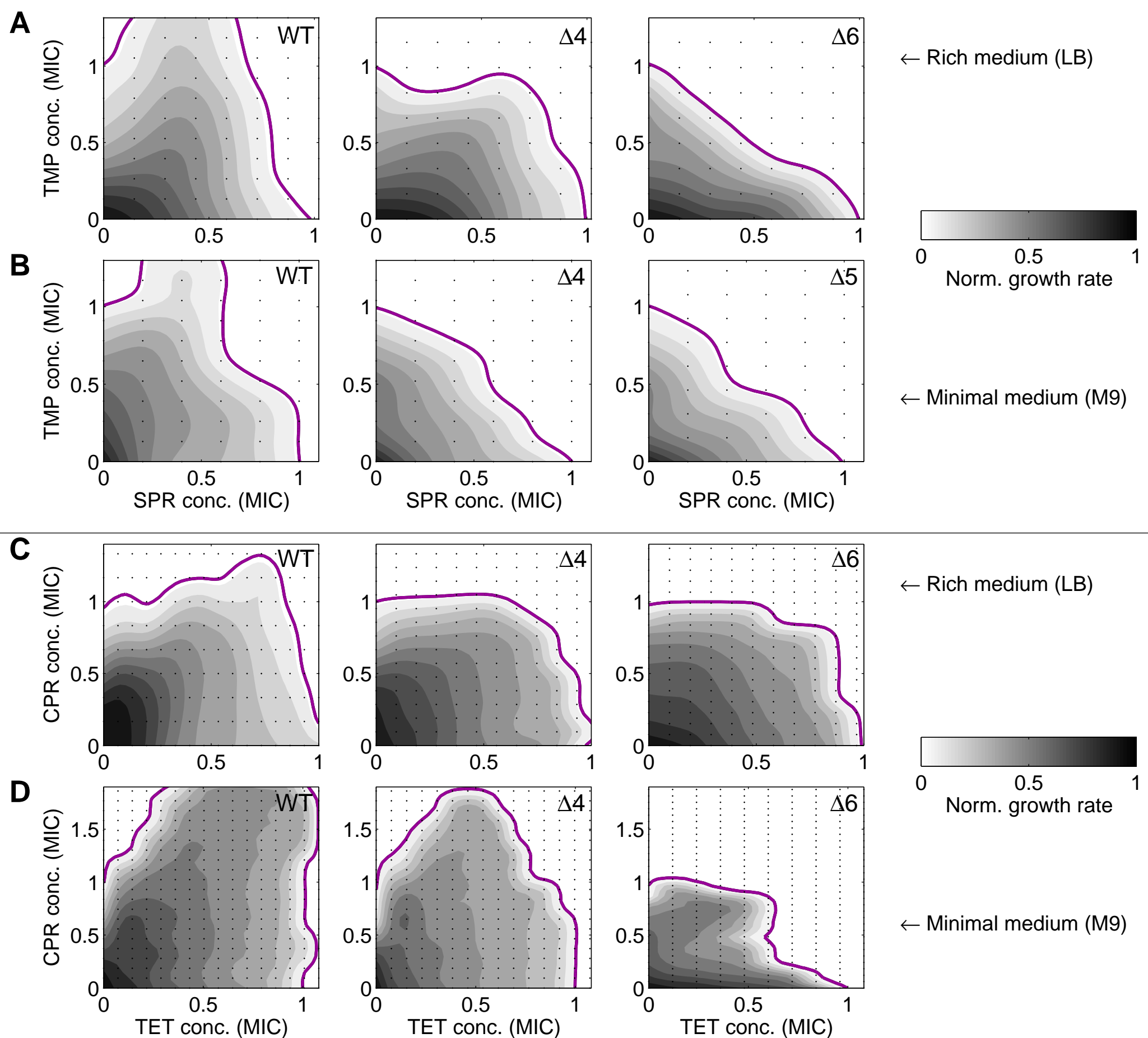


Figure S2

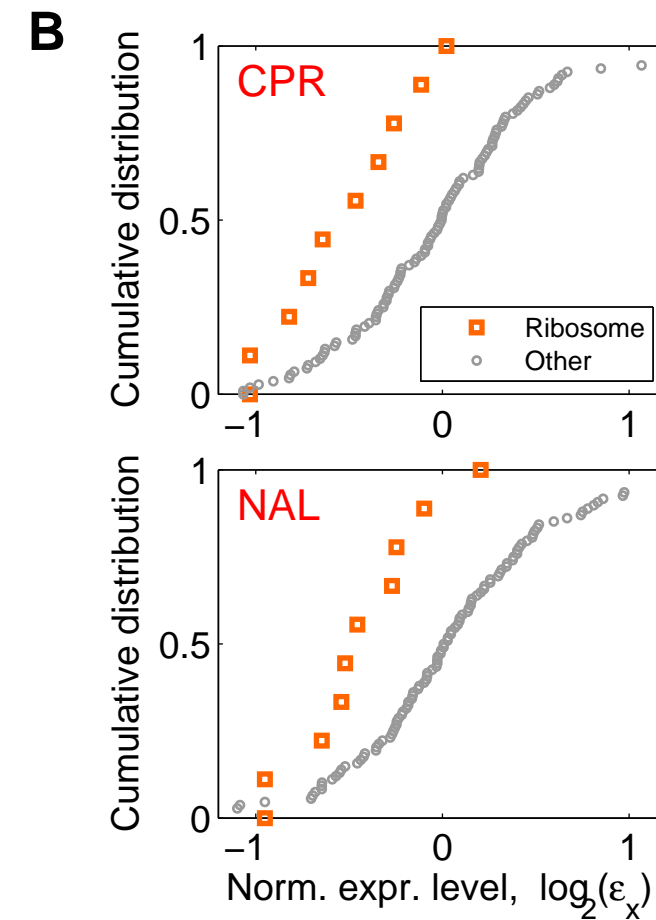
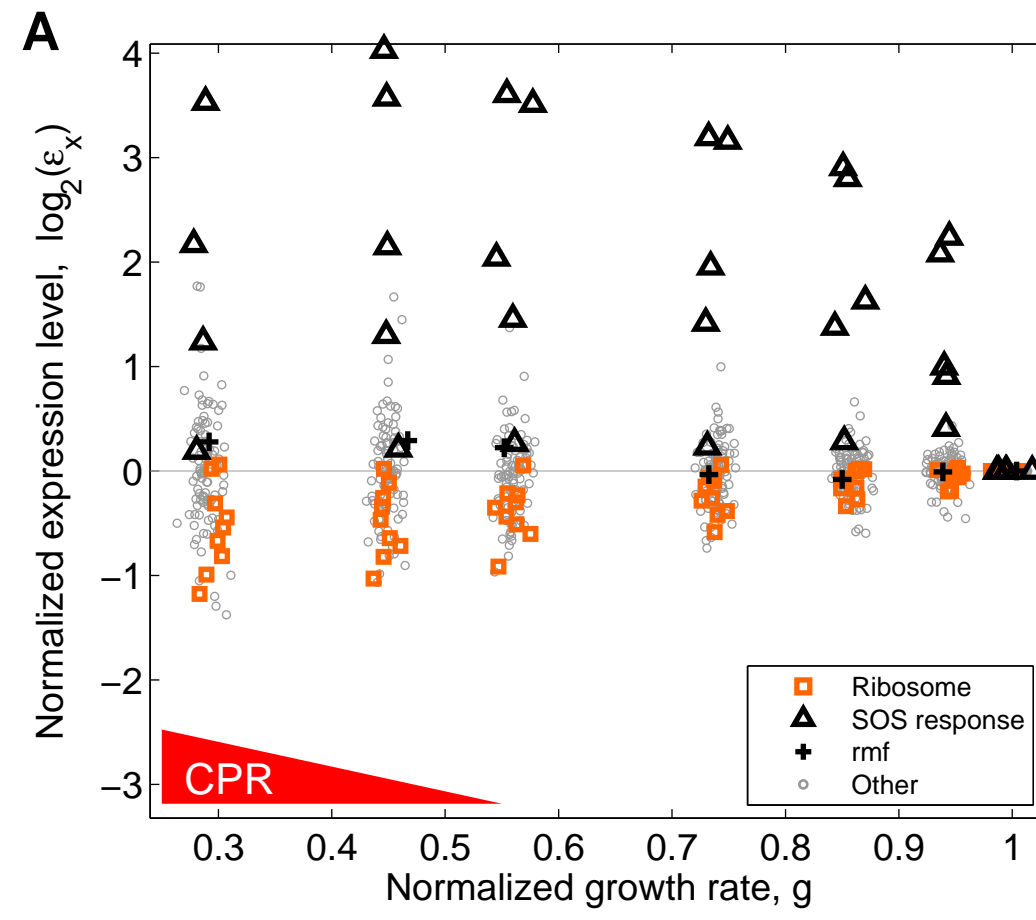


Figure S3

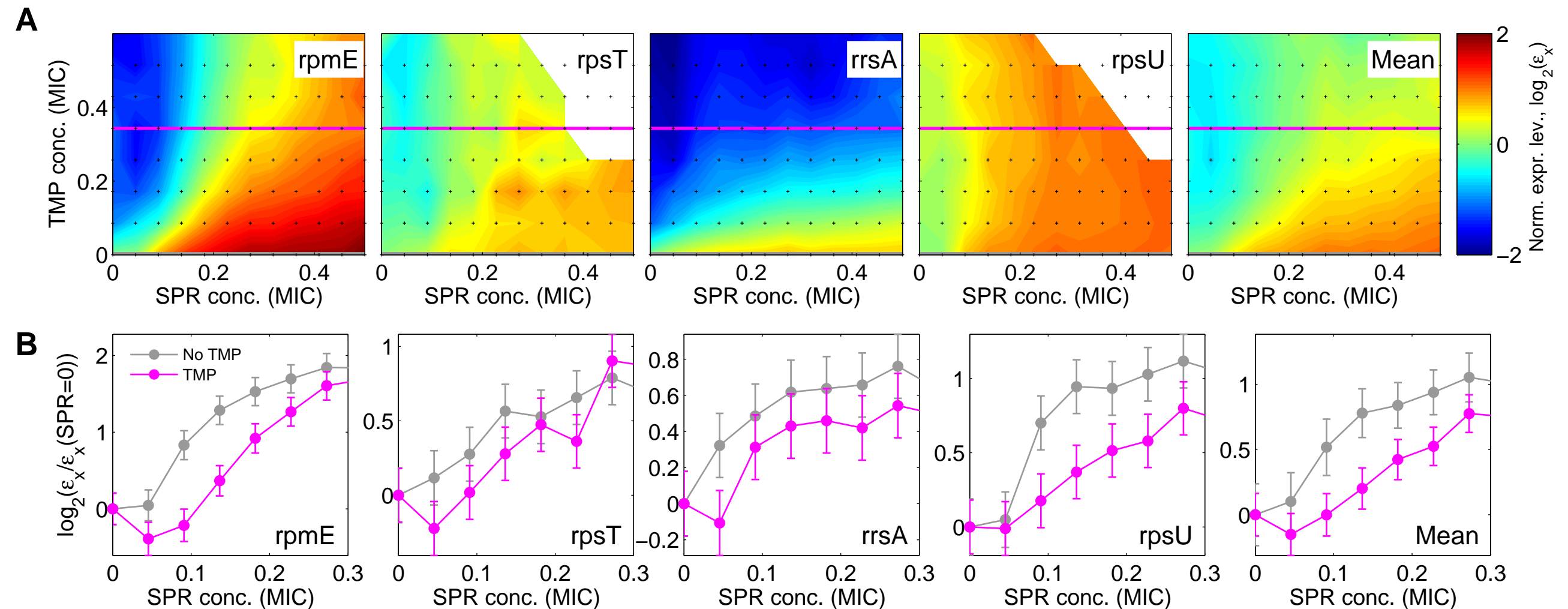


Figure S4

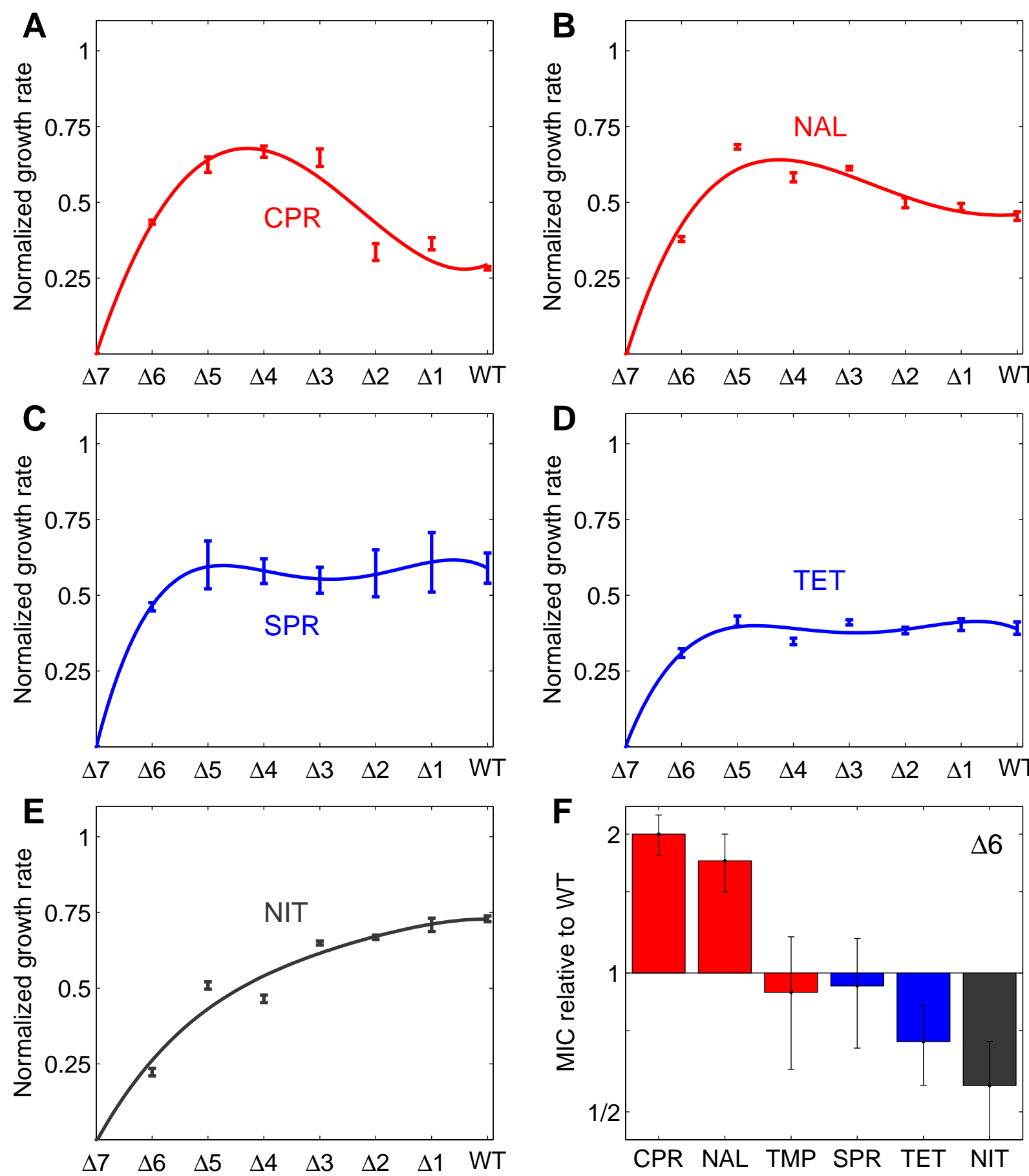
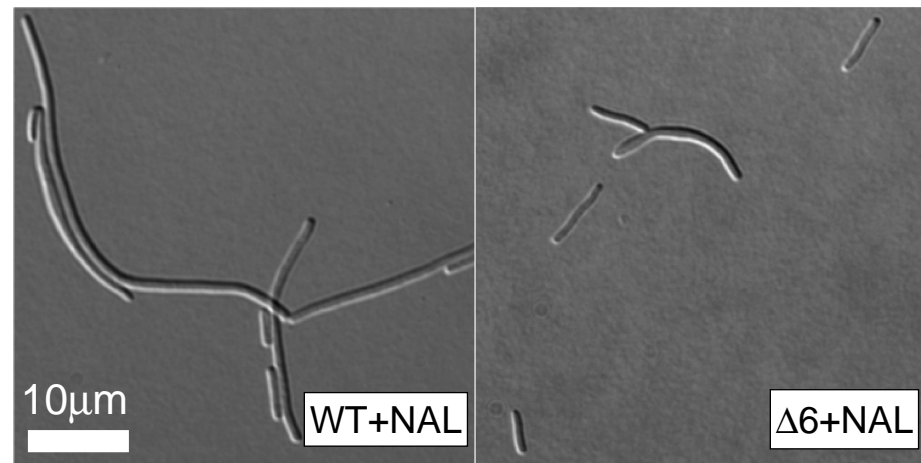


Figure S5

A



B

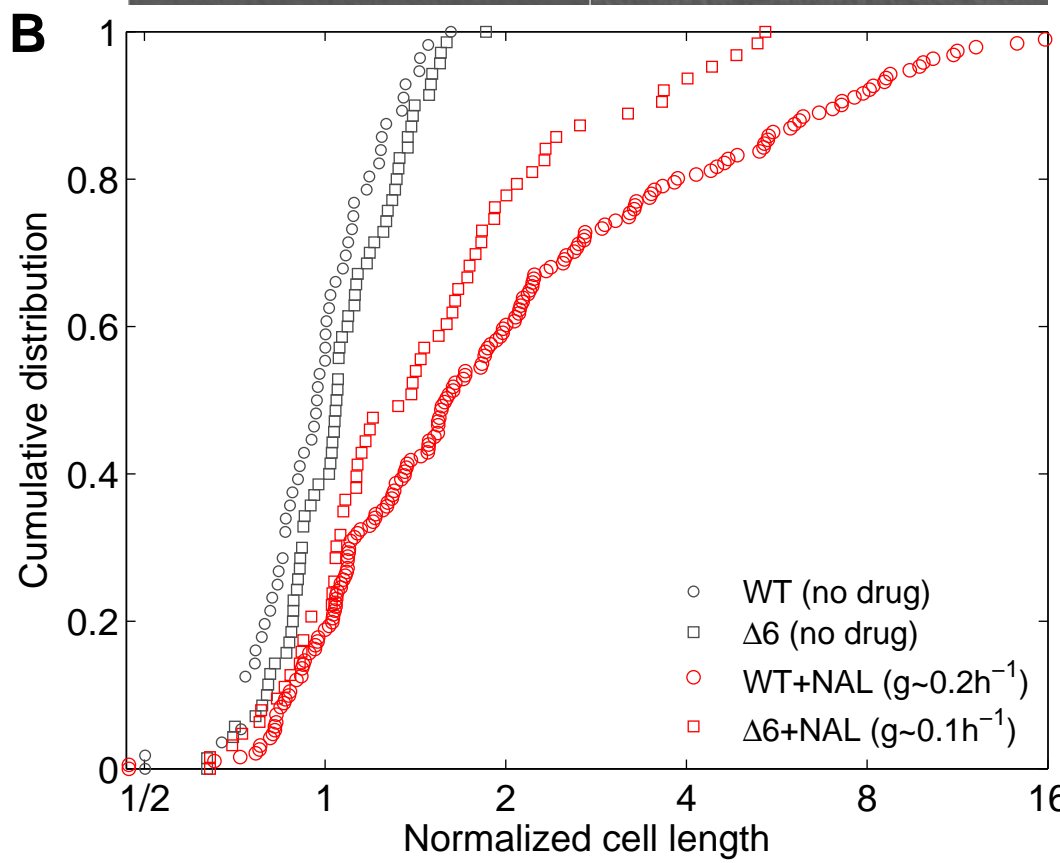


Figure S6

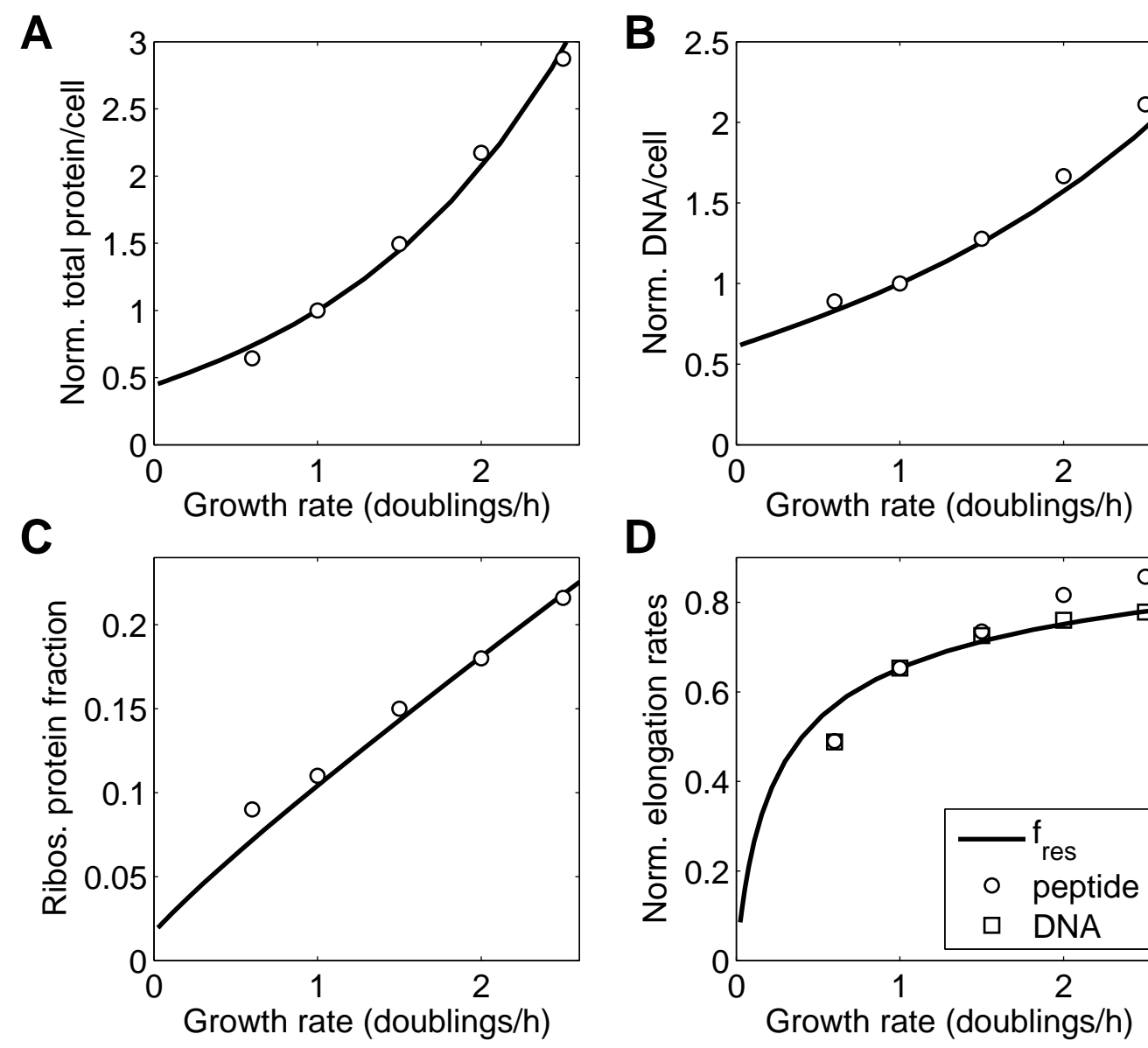


Figure S7

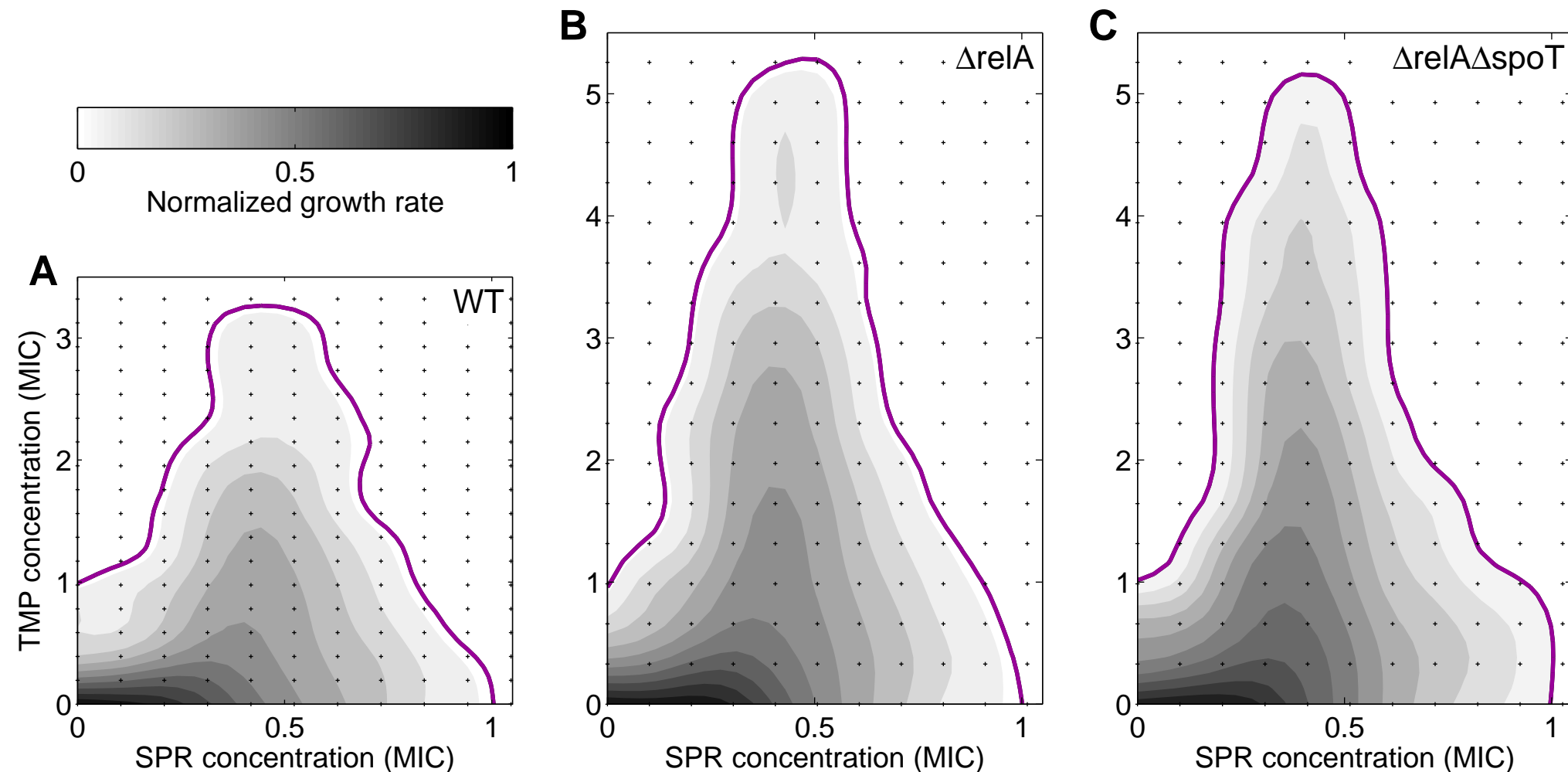


Figure S8

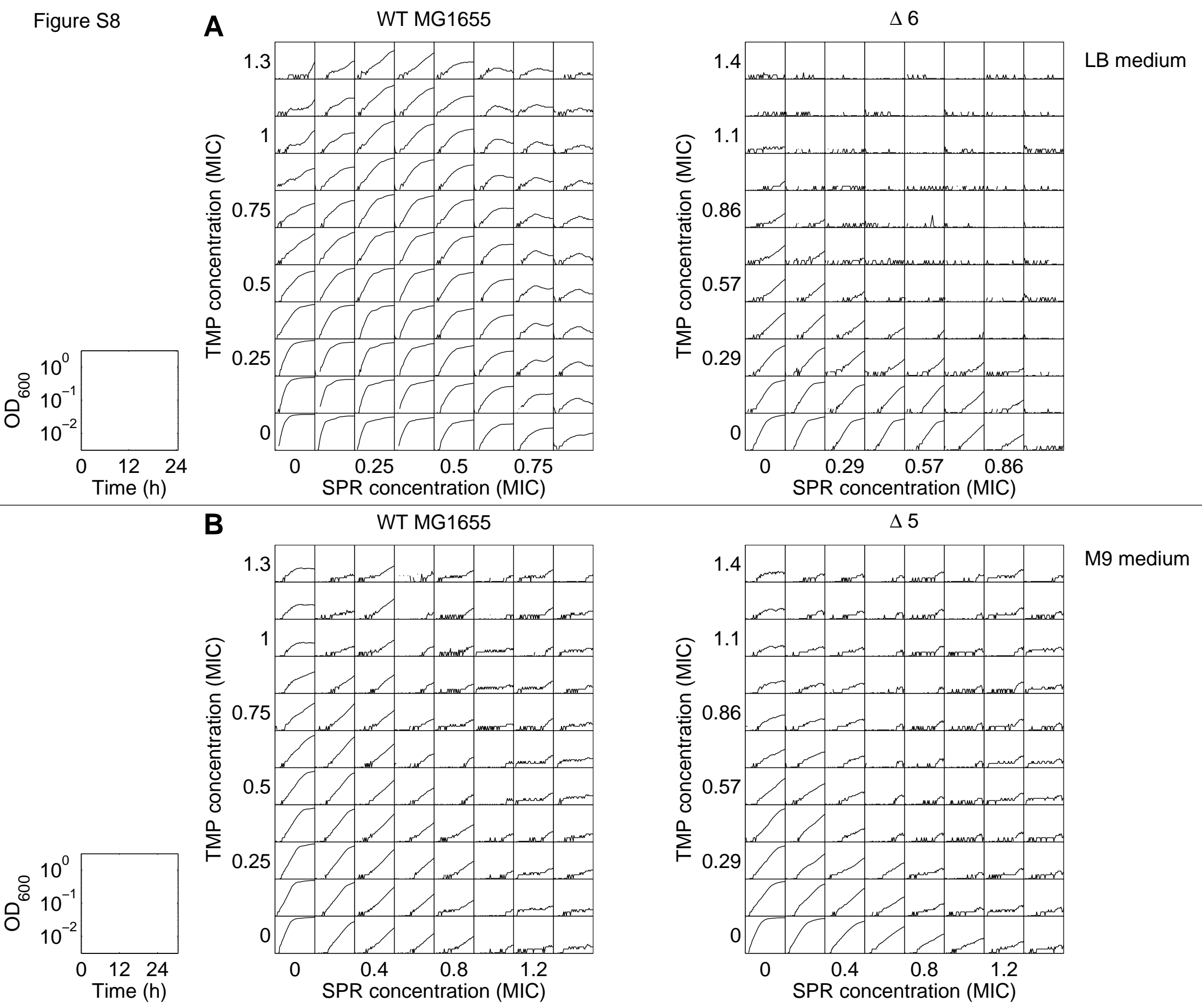
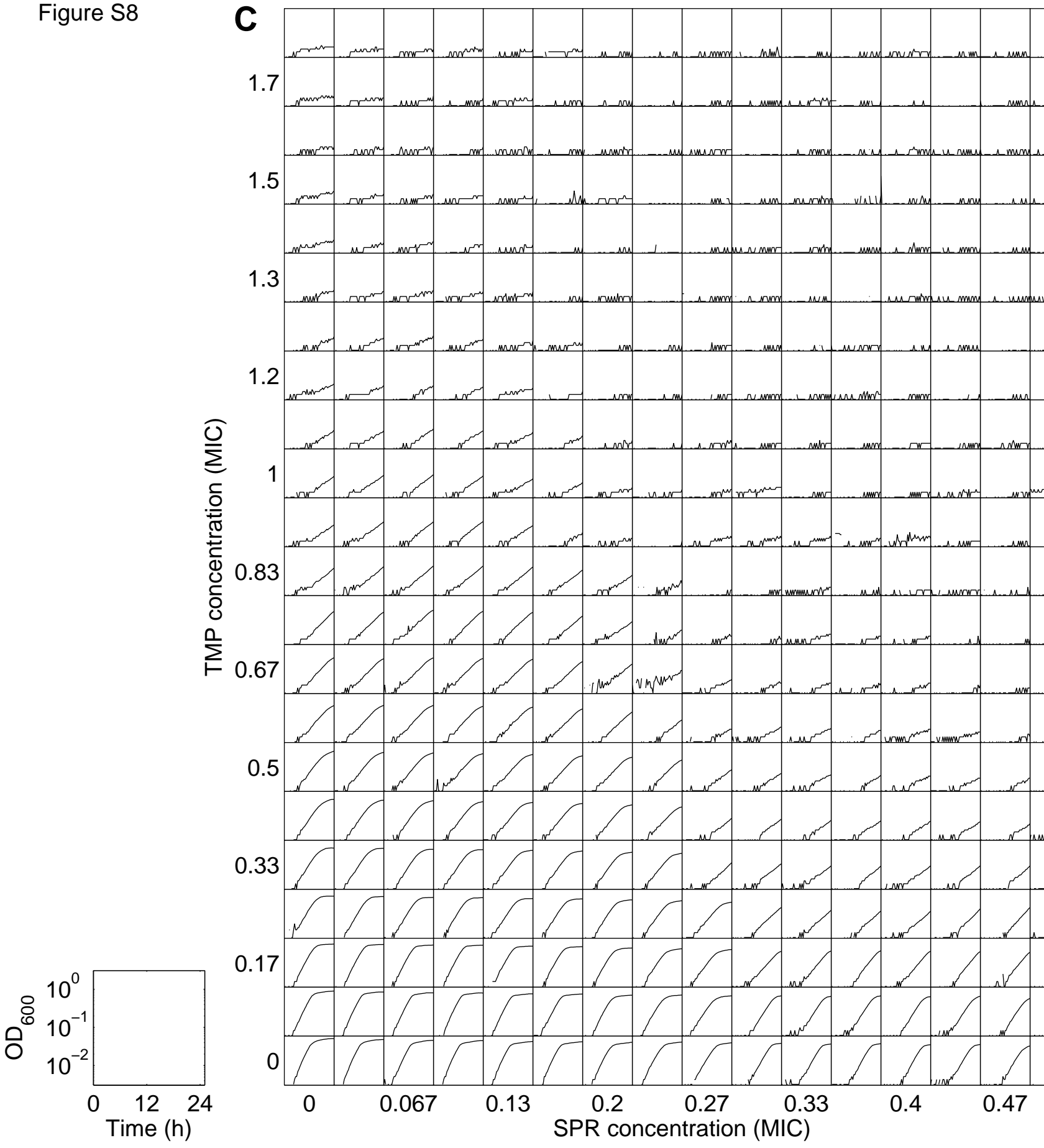


Figure S8



Δ6
LB medium

Figure S9

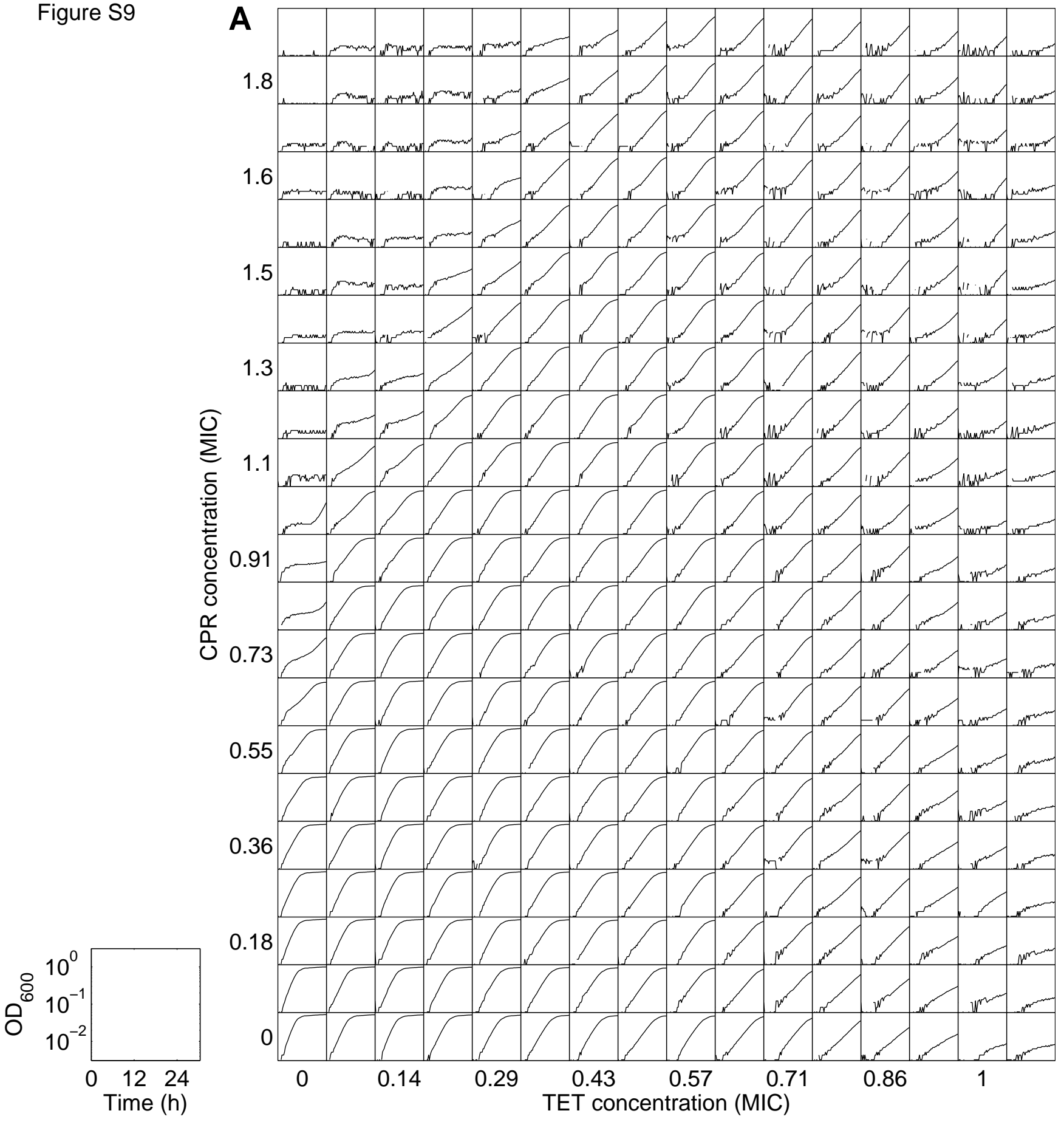
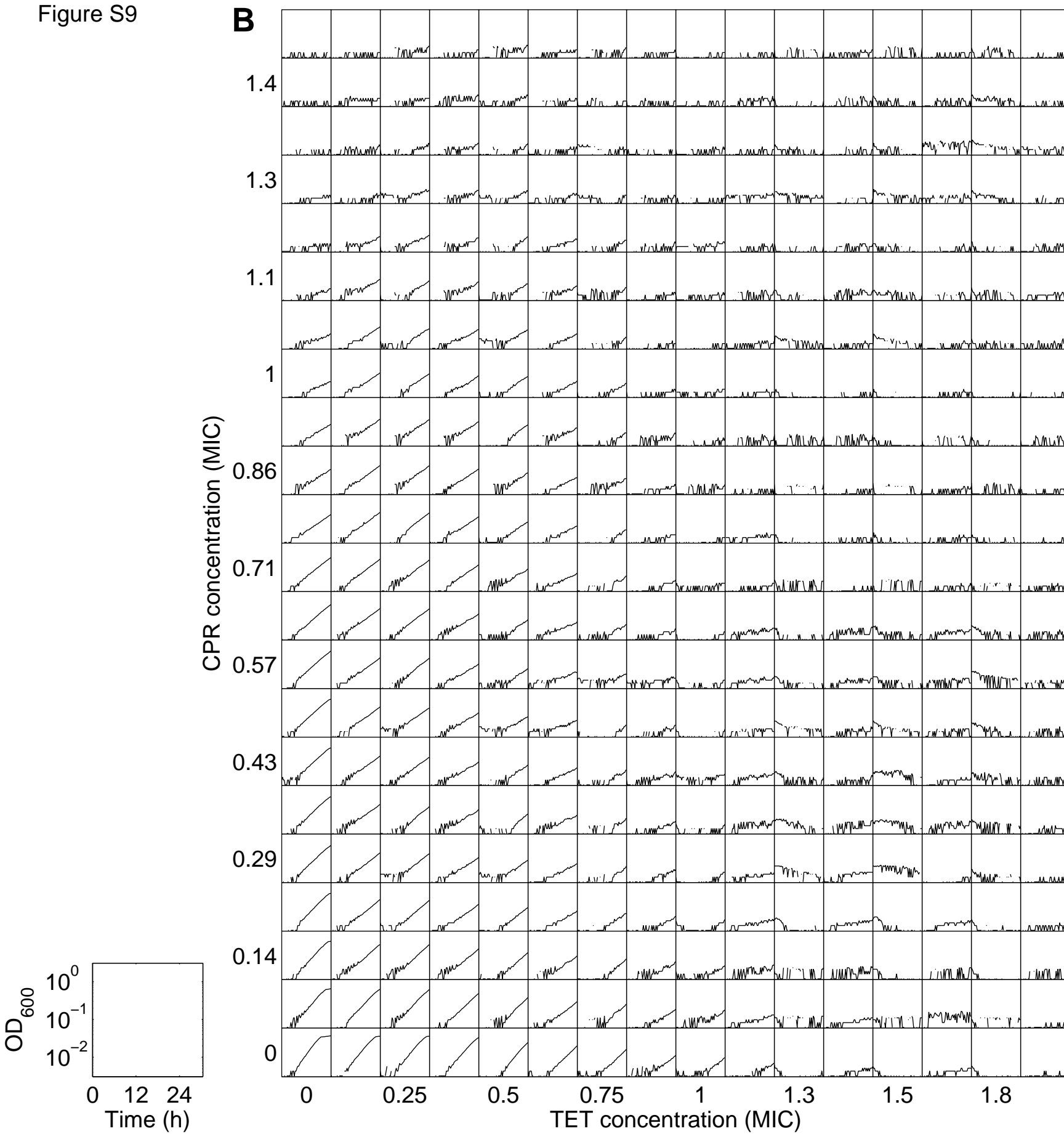
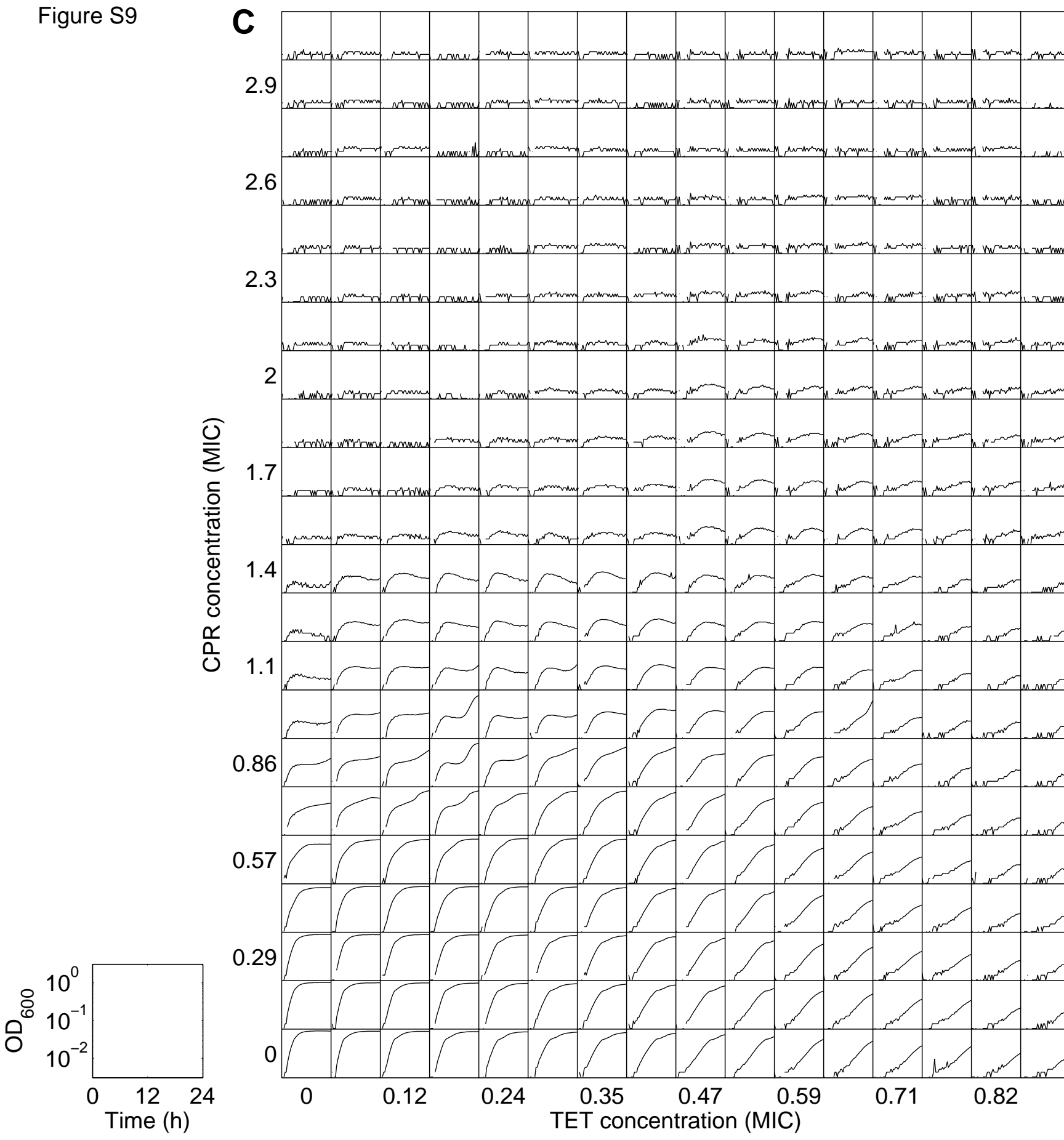


Figure S9

 $\Delta 6$

M9 medium

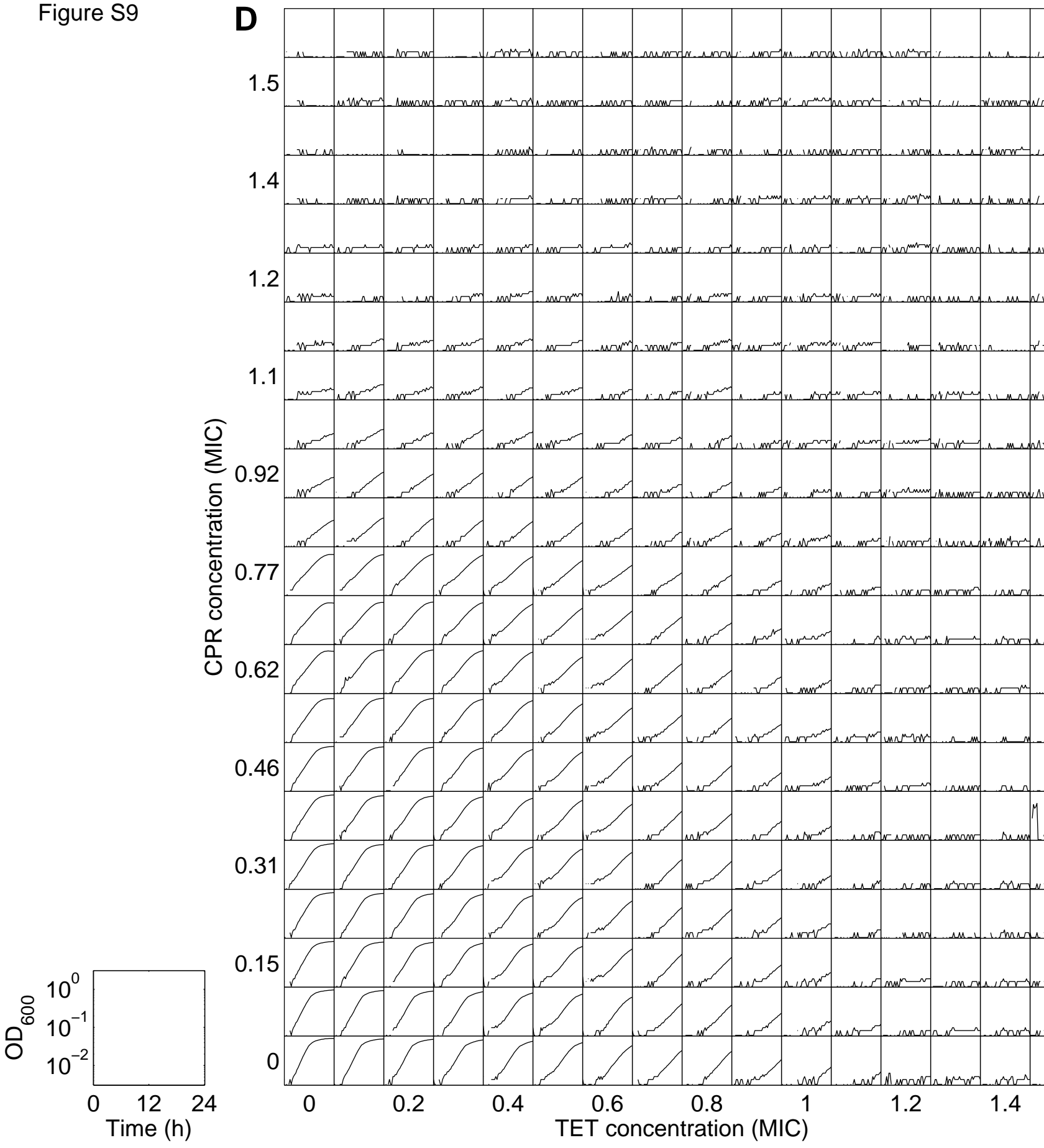
Figure S9



WT MG1655

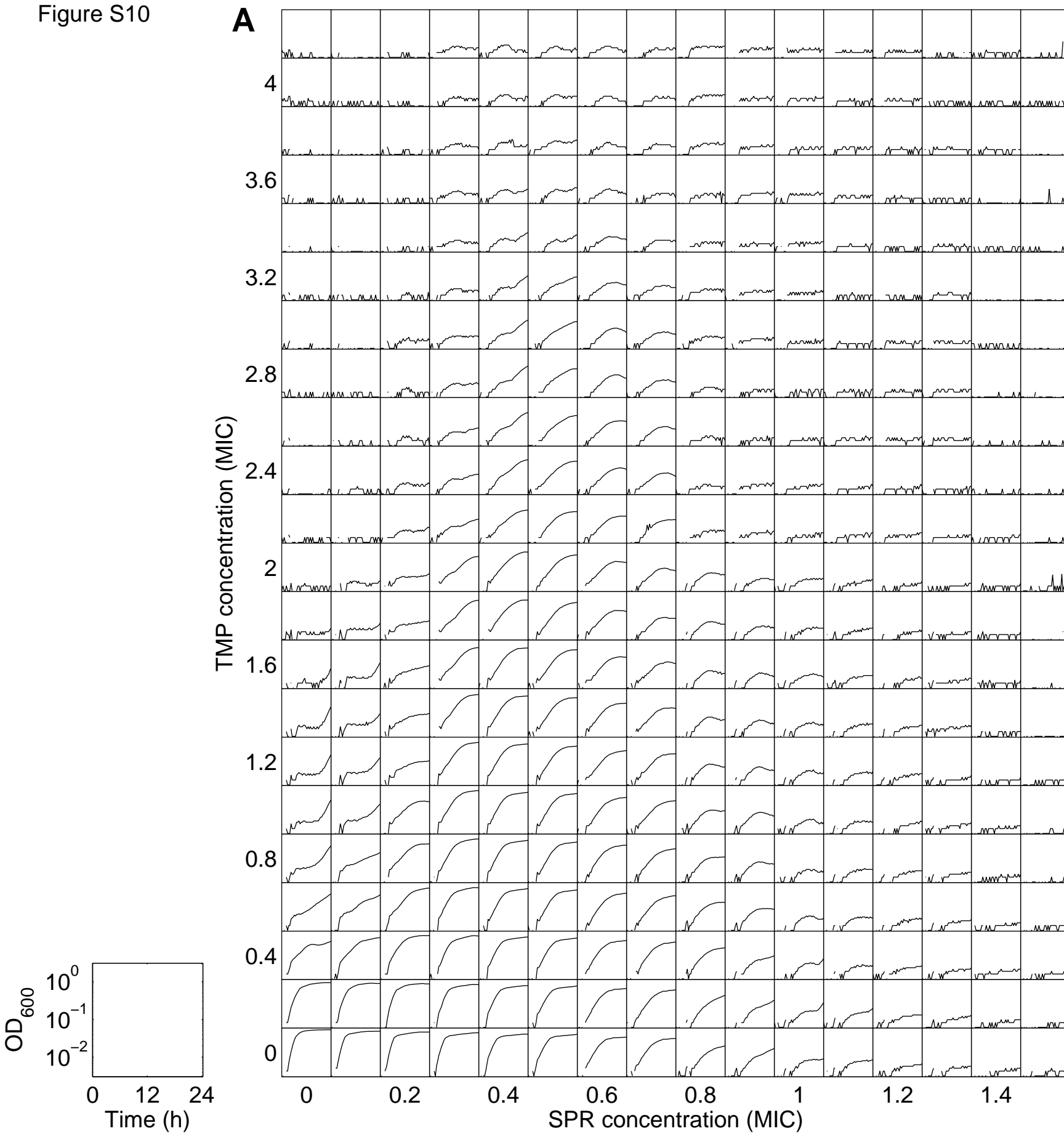
LB medium

Figure S9



Δ6
LB medium

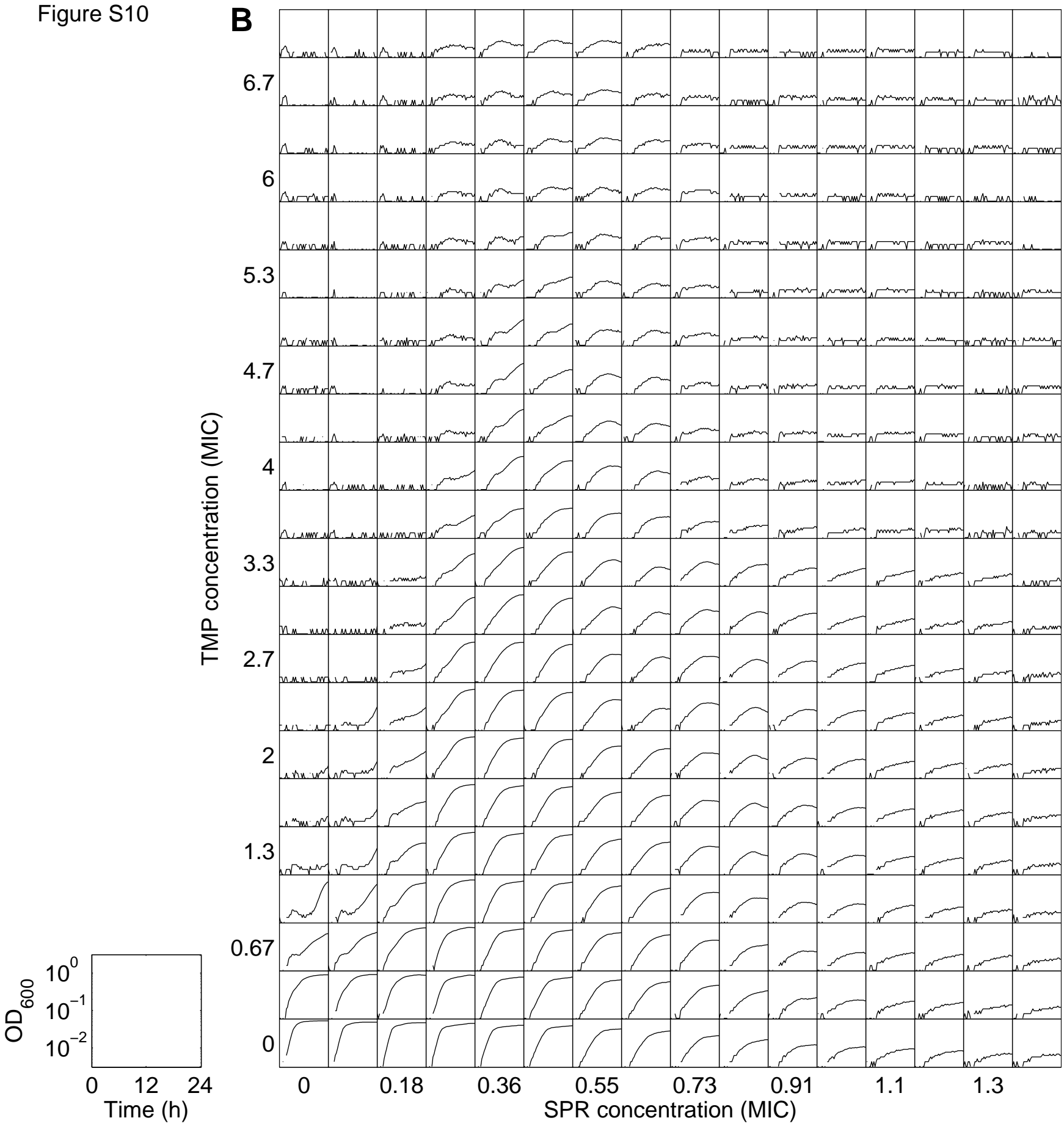
Figure S10



WT MG1655

LB medium

Figure S10



ΔrelA
LB medium

Figure S10

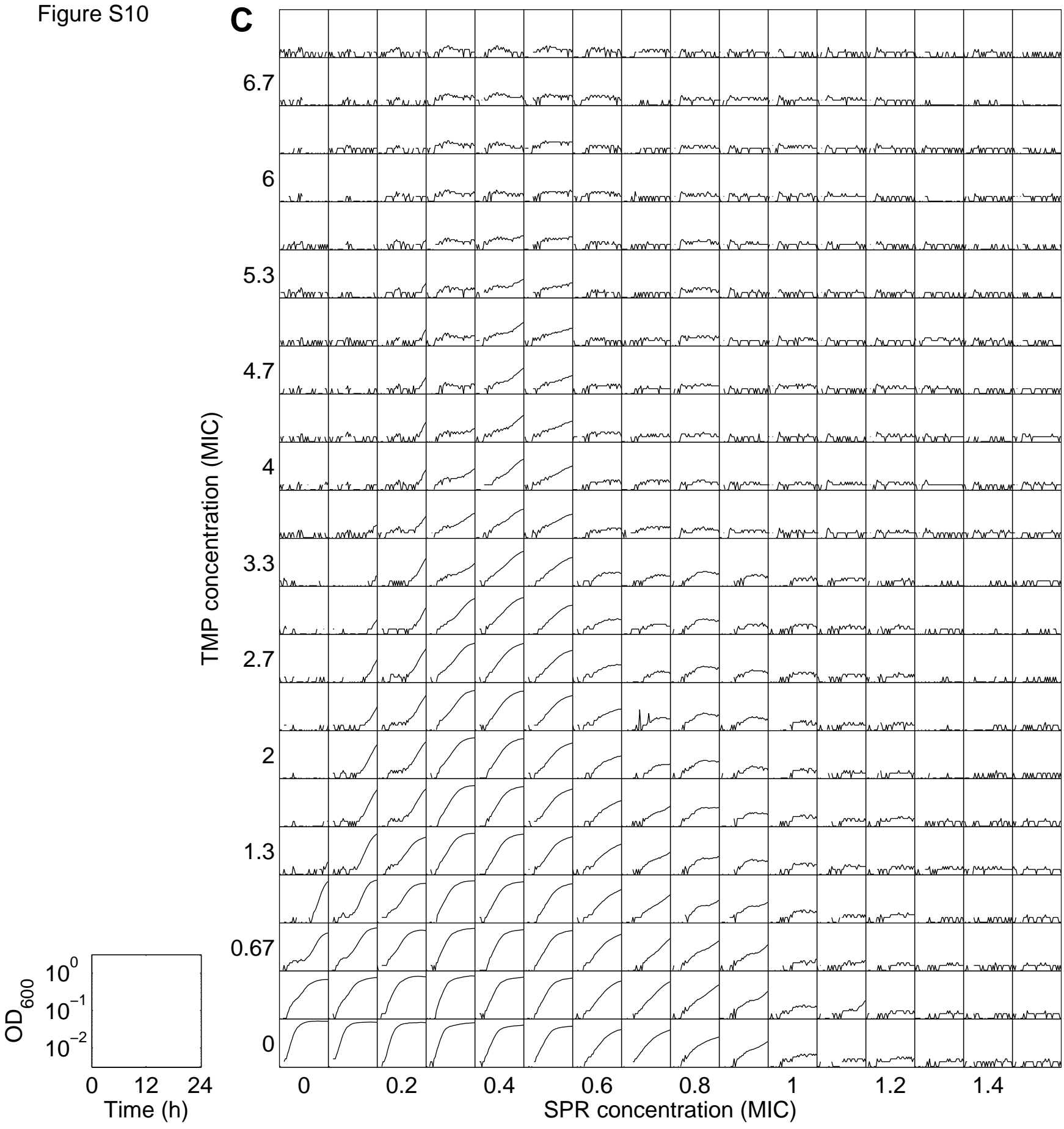
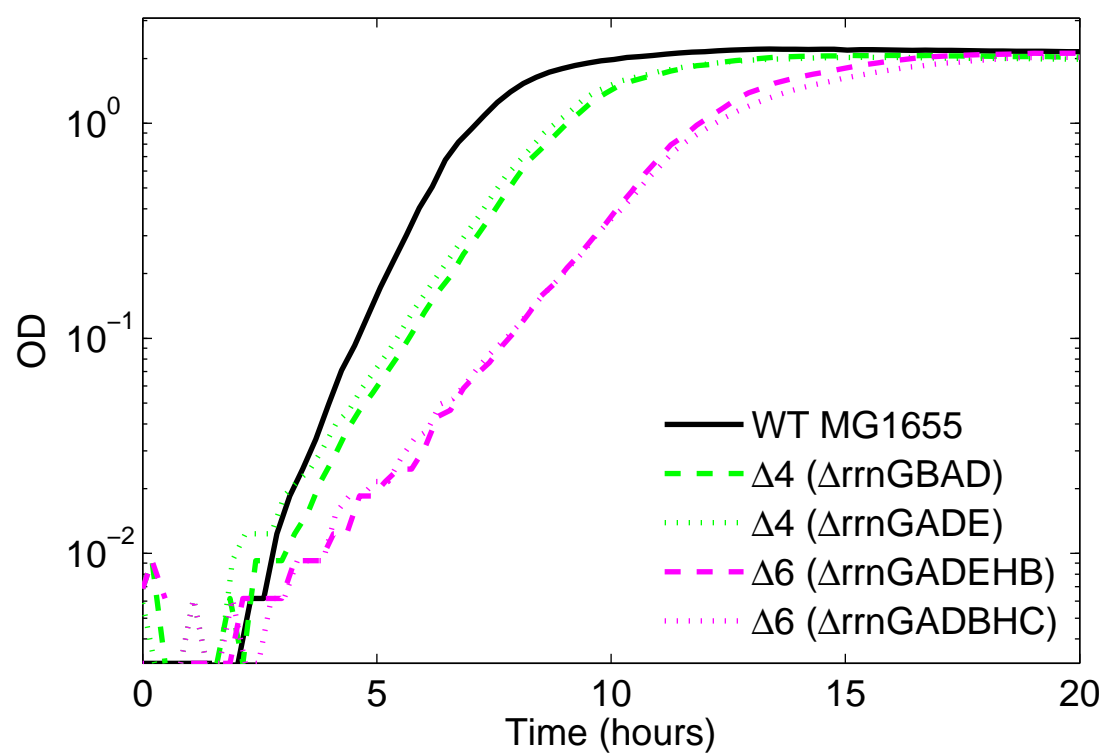


Figure S11

A

No drug

**B**

DNA synthesis inhibitor (CPR)

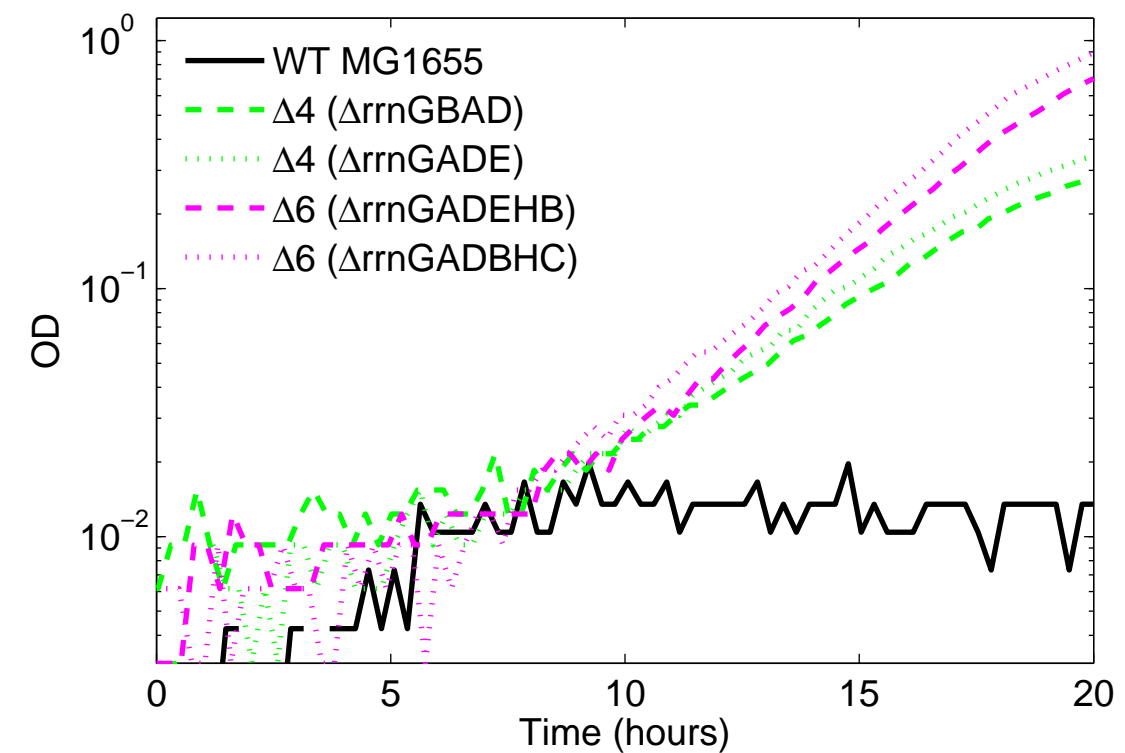


Figure S12

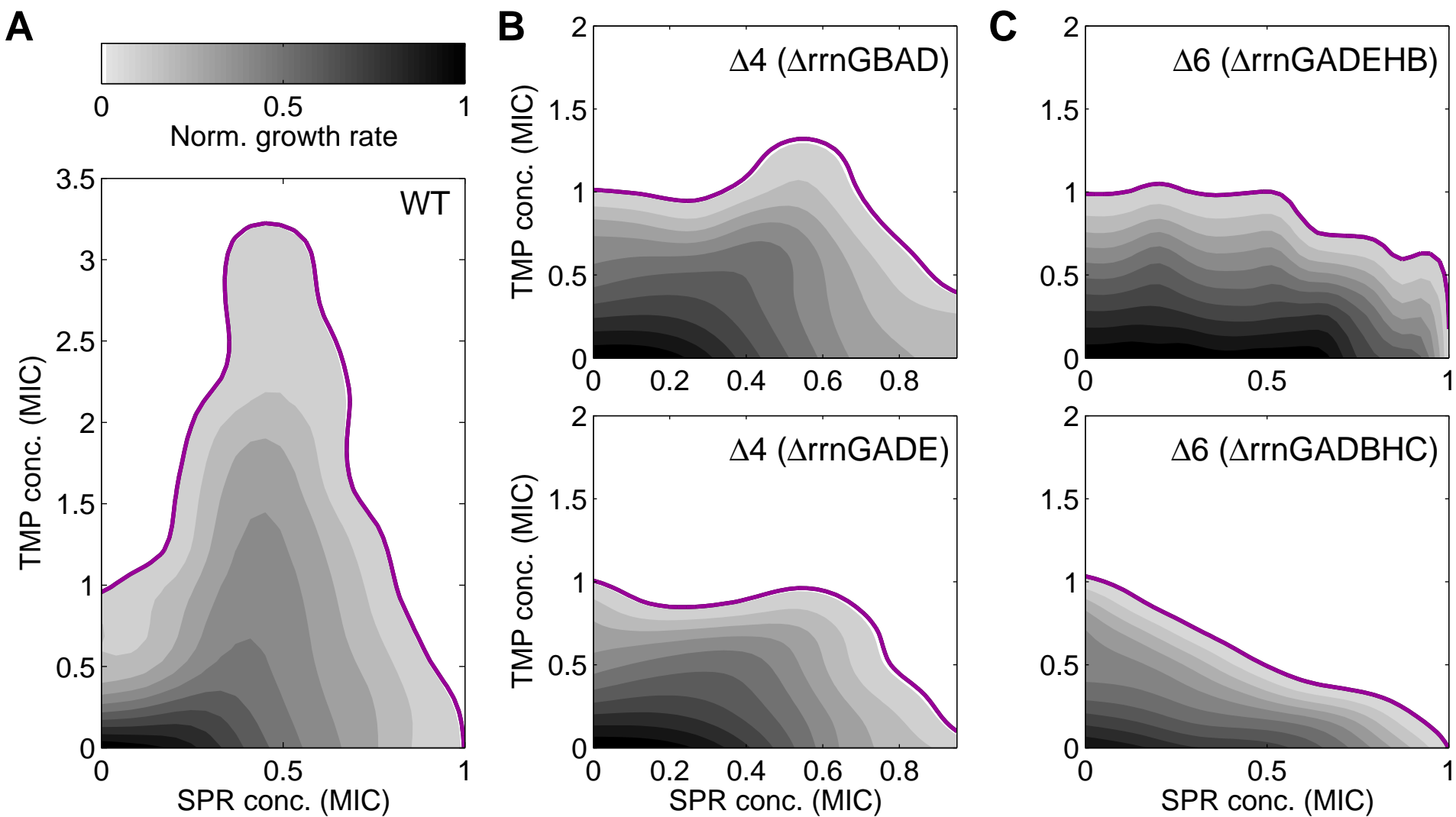


Figure S13

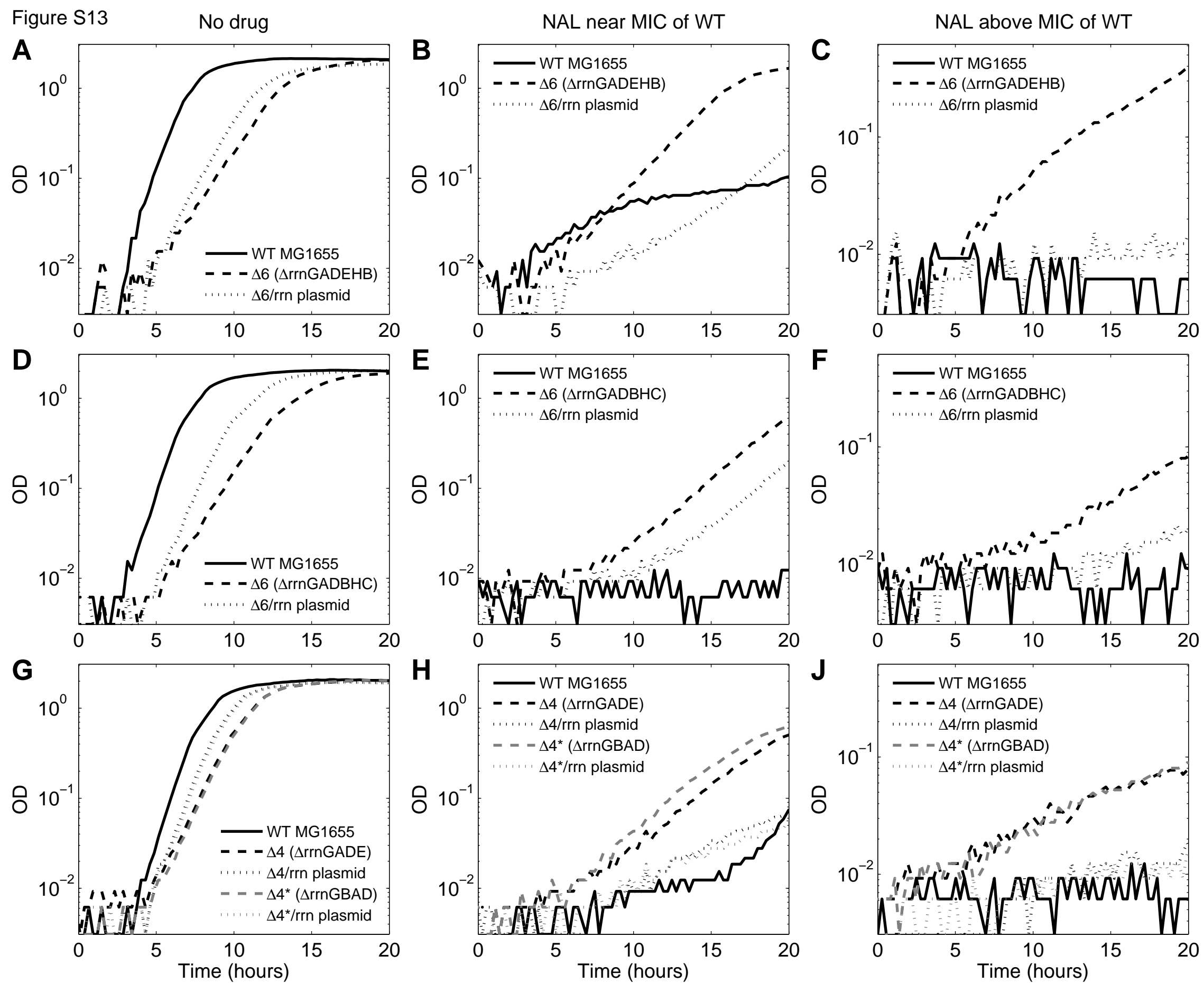


Figure S14

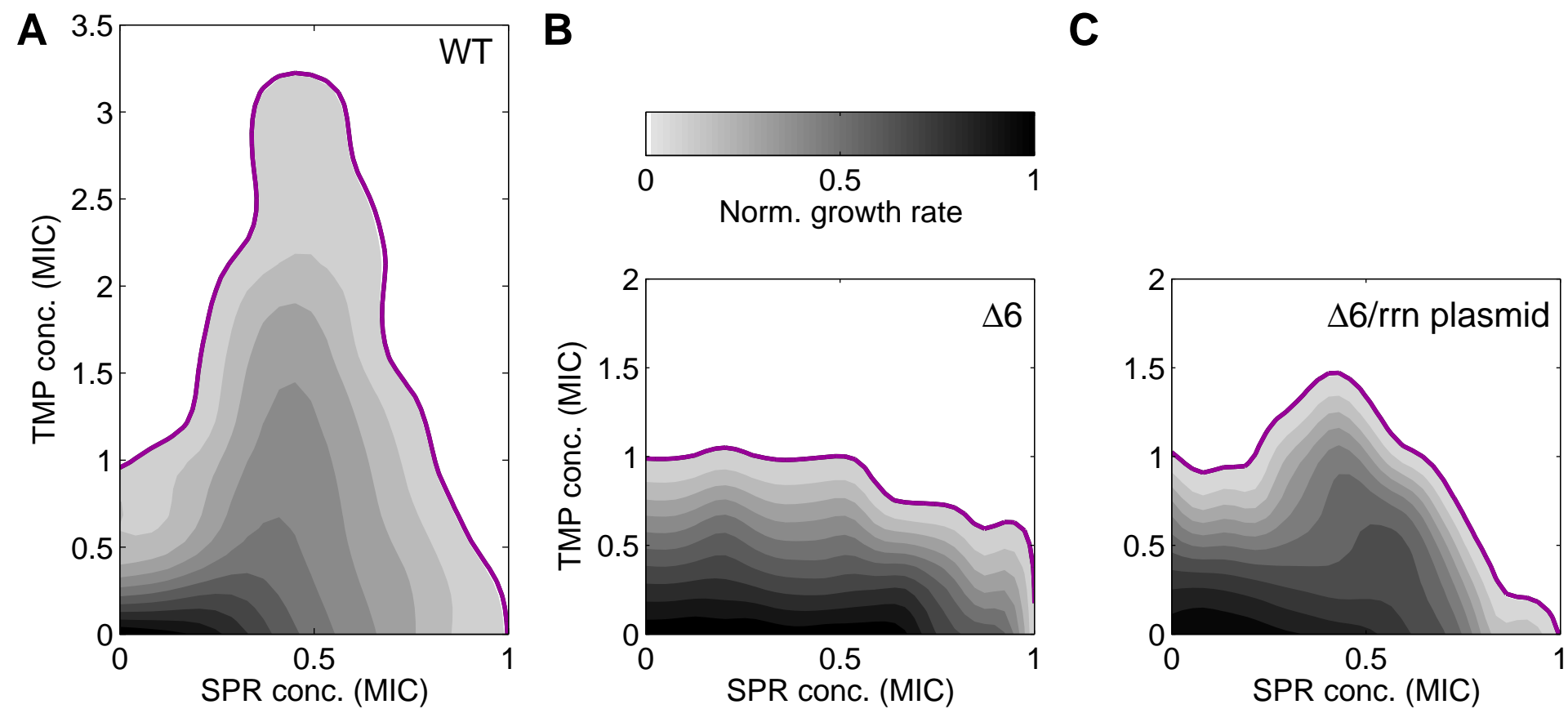


Figure S15

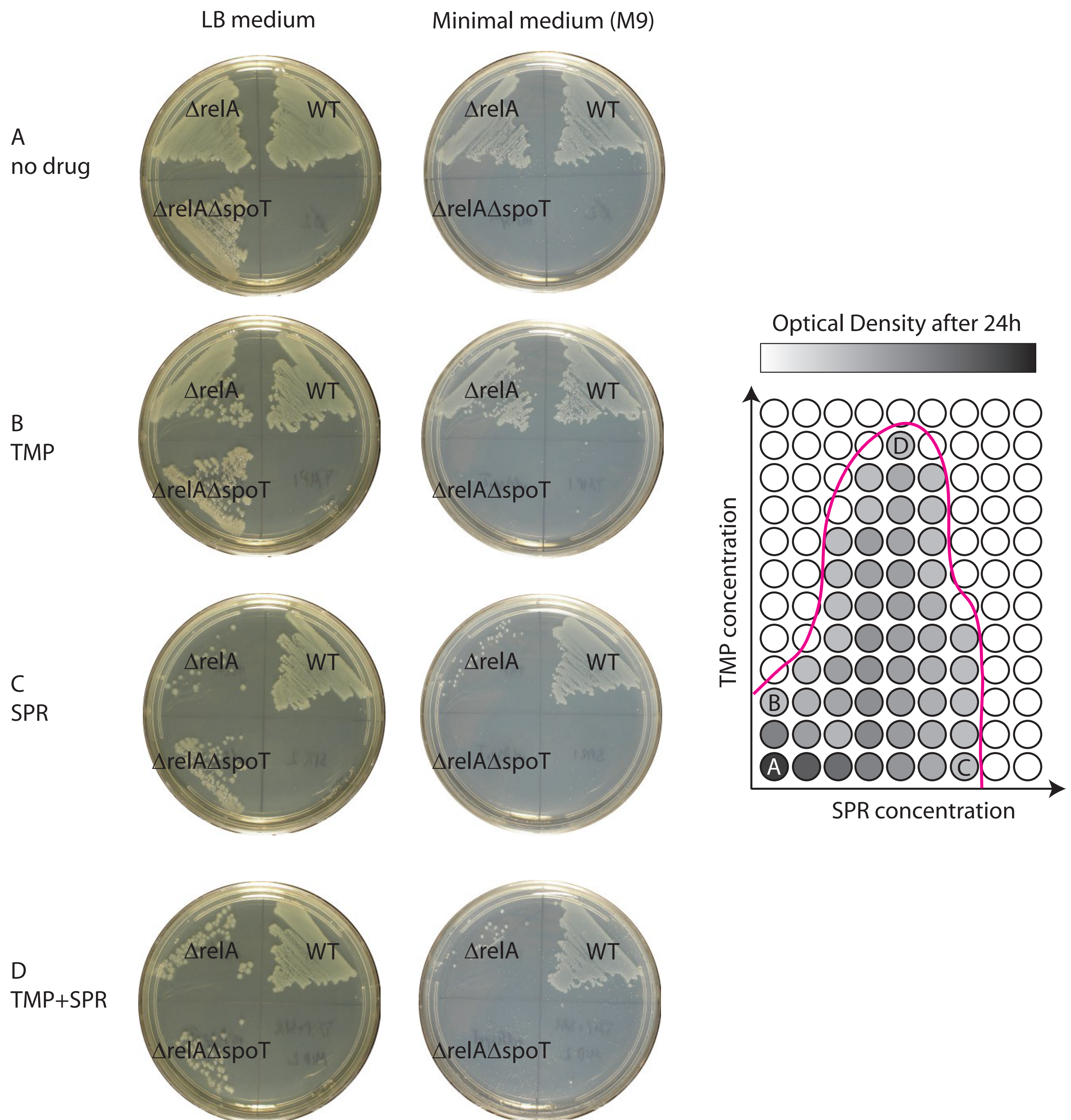


Figure S16

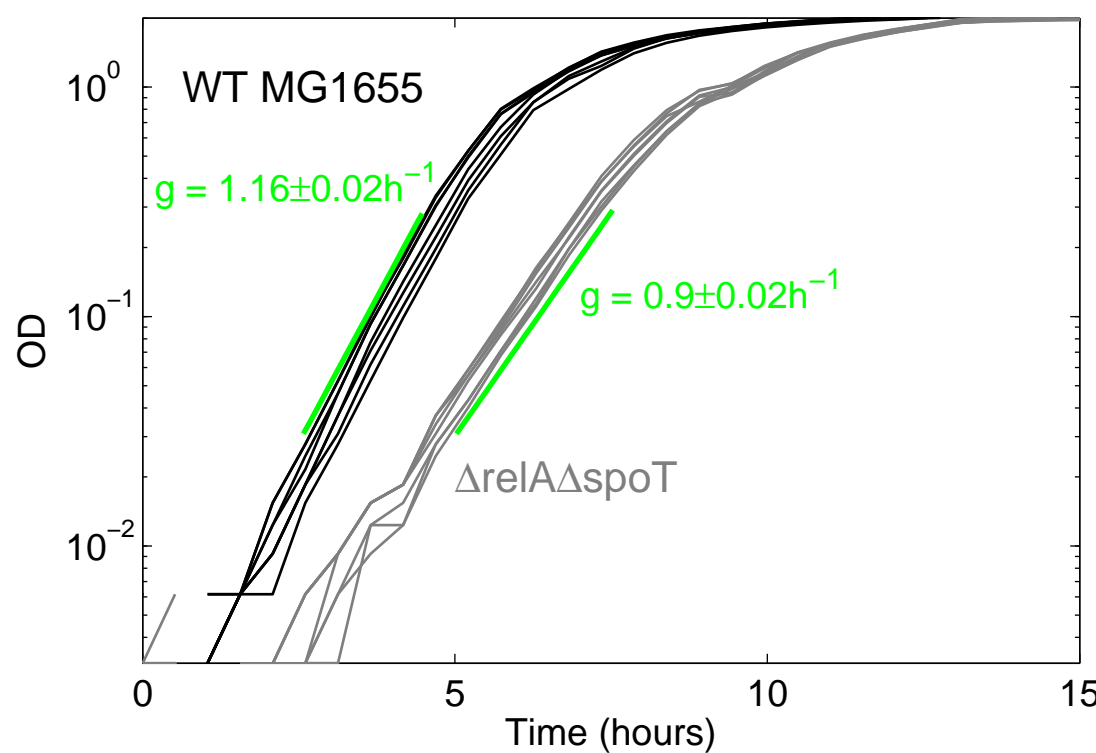
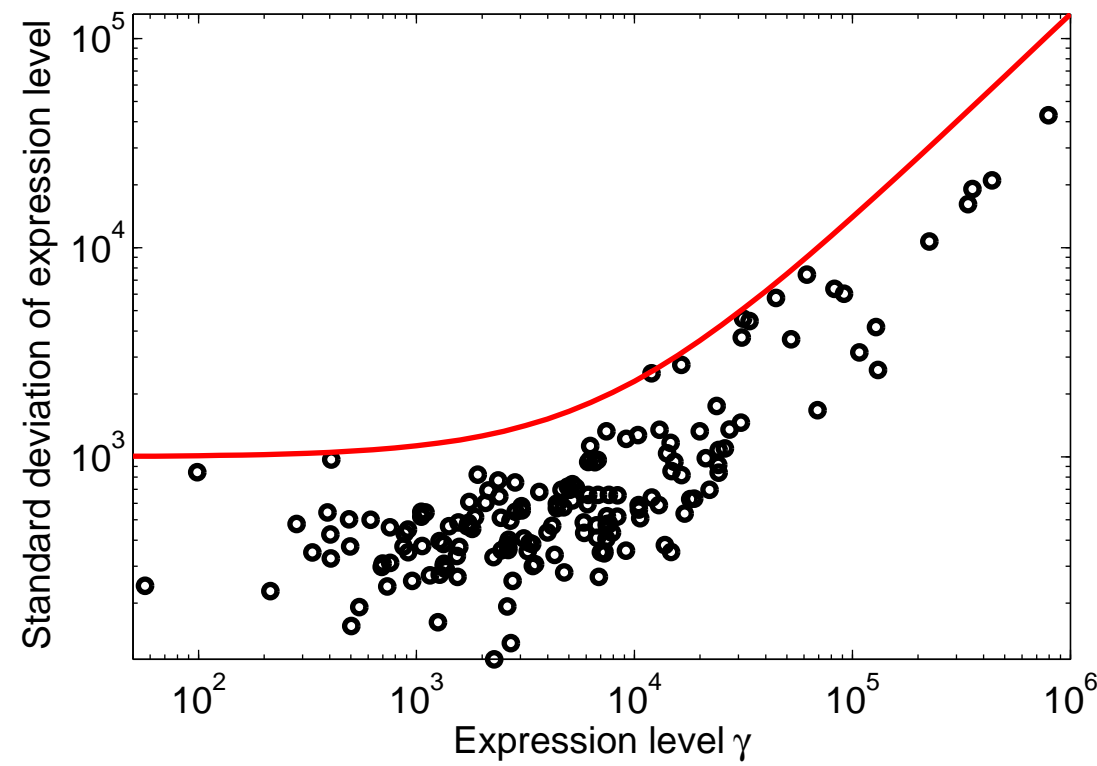


Figure S17



Supplemental Text

1 Introduction to mathematical model of bacterial growth

We discuss a mathematical model of bacterial growth. We use this model to address if the experimental results discussed in the main text and our rationale that the regulation of ribosome synthesis is non-optimal in response to DNA synthesis inhibitors can be reconciled with the paradigm of optimal regulation of ribosome synthesis under no stress conditions.

The model of bacterial growth describes the influx of resources into the cell and the consumption of these resources by the synthesis of proteins, ribosomes, and DNA. The model incorporates Cooper and Helmstetter's classical results about chromosome replication and the cell division cycle of *Escherichia coli* [Cooper & Helmstetter, 1968] as well as Donachie's "initiation mass" mechanism that couples protein synthesis to DNA replication [Donachie, 1968, Donachie & Blakely, 2003] and cell division. The model further captures optimal regulation of ribosome synthesis in different nutrient environments as a function of the intracellular level of resources like amino acids or ATP – a mechanism that is widely accepted as the means by which *E. coli* and other bacteria achieve maximal growth rates in different nutrient environments [Paul et al., 2004]. This regulatory mechanism based on the intracellular resource level applies to many bacterial species while the molecular details of its implementation vary from species to species. In a real cell a large number of different resources like NTPs, amino acids, folic acid, and others are consumed to synthesize DNA, proteins, ribosomes, and other cell components. In our model we simplify this complicated situation by introducing a single effective resource that is consumed in the synthesis of proteins, DNA, and ribosomes. While it does not correspond to any specific actual cellular resource, this effective resource is best thought of as a metabolic precursor that is shared by protein, DNA and RNA synthesis.

2 Kinetic equations

The following dynamical system describes the population averages of the amount of protein p , DNA c , ribosomes r , and resources a per cell in an exponentially growing bacterial culture. The variable p describes all protein in the cell except for ribosomal protein. Proteins, DNA, and ribosomes are synthesized by the cells and are diluted as a result of cell divisions. In addition, resources are consumed in the synthesis of these cell constituents:

$$\begin{aligned} dp/dt &= s_p - gp \\ dc/dt &= s_c - gc \\ dr/dt &= s_r - gr \\ da/dt &= s_a - (g + k_{\text{deg}})a - (\epsilon_p s_p + \epsilon_r s_r + \epsilon_c s_c) \end{aligned} \quad (1)$$

Here, g is the growth rate that leads to dilution of all components as a result of cell divisions and s_p , s_c , s_r , and s_a are the synthesis rates of ribosomes, proteins, DNA, and resources, respectively. These rates depend on the variables p , c , r and a (see below). ϵ_p , ϵ_r , and ϵ_c describe the amount of resources consumed to make one protein, ribosome, and chromosome, respectively. The resource degradation rate k_{deg} captures possible resource instability and resource turnover by processes that are not explicitly captured in the model. This rate k_{deg} could be set to zero without qualitatively changing the conclusions discussed here. In Eq. (1), we neglect protein degradation that only affects a small fraction of the total protein pool in *E. coli*.

Eq. (1) describes the mass and resource balance of the system. To fully define the theoretical description, we specify the synthesis rates s_p , s_c , s_r , and s_a :

$$\begin{aligned} s_p &= (1 - \eta) k_p^0 f_{\text{res}} \rho r \\ s_c &= N_f \times 1/(2\tau_C) \\ s_r &= N_{\text{rrn}} N_o \min(s_r^{\text{opt}}, s_r^0 f_{\text{res}}) \\ s_a &= \nu_a, \end{aligned} \quad (2)$$

with the functions

$$V = k_V (p + p_r r)$$

$$\begin{aligned}
\eta &= p_r s_r / (s_p + p_r s_r) \\
f_{\text{res}} &= \frac{a/V}{M_a + a/V} \\
N_o &= e^{g(\tau_D + \tau_C)} \\
N_f &= 2e^{g\tau_D} (-1 + e^{g\tau_C}) \\
1/\tau_C &= f_{\text{res}} \delta / \tau_C^0 \\
1/\tau_D &= f_{\text{res}} / \tau_D^0
\end{aligned} \tag{3}$$

In the equation for s_p in (2), η is the fraction of ribosomes that translate ribosomal protein and $k_p = k_p^0 f_{\text{res}}$ is the rate of protein synthesis per ribosome. The function $f_{\text{res}}(a/V)$ describes the increase of the translation rate k_p as a function of the intracellular resource concentration a/V . For high resource concentrations, the translation rate saturates at the value k_p^0 . Here, the cell volume V is proportional to the total amount of protein in the cell $p + p_r r$ where p_r denotes the amount of ribosomal protein per ribosome. In agreement with previous studies, we assume that mRNA is always synthesized in sufficient amounts to provide all ribosomes with templates for protein synthesis so that a constant and large fraction of ribosomes (80 percent) are actively translating independent of environmental conditions [Bremer & Dennis, 1996]. Further, ρ is the fraction of ribosomes that are not blocked by a translation inhibitor, i.e. $\rho = 1$ in absence of antibiotics.

In the equation for s_c in (2), N_f is the average number of replication forks per cell, τ_C the average time it takes one replication fork to propagate from the replication origin to the terminus, and τ_D the average delay time between completion of chromosome replication and cell division [Cooper & Helmstetter, 1968]. The average number of replication forks per cell N_f can be calculated from τ_C , τ_D , and the growth rate g using the relation in Eq. (3) [Cooper & Helmstetter, 1968]. We assume that the rate of DNA synthesis $1/\tau_C$ per pair of replication forks increases as a function of the intracellular resource concentration following $f_{\text{res}}(a/V)$ and saturates at a maximal rate $1/\tau_C^0$. The parameter δ with $0 \leq \delta \leq 1$ describes a decrease of the DNA synthesis rate that results from the addition of a DNA synthesis inhibiting antibiotic. In the absence of antibiotics $\delta = 1$.

In general, the resource influx into the cell s_a depends on many factors like membrane proteins involved in nutrient uptake and metabolic processes that convert these nutrients into resources that are usable for protein, DNA, and RNA synthesis. For simplicity, we approximate this resource influx into the cell by a constant ν_a that depends only on the nutrient availability in the environment (growth medium).

Finally, in the equation for s_r in (2), N_{rrn} is the number of *rrn* operons per chromosome ($N_{rrn} = 7$ in the wild type strain), N_o is the average number of replication origins per cell [Bremer & Churchward, 1977], and s_r^0 is the maximal possible ribosome synthesis rate per *rrn* operon. The definition of the function $s_r^{\text{opt}}(a/V)$ that determines the regulation of ribosome synthesis as a function of the intracellular resource concentration a/V is discussed below. In brief, the equation in (2) means that in the absence of antibiotics, s_r is always regulated to the optimal value that ensures maximal growth in a given nutrient environment.

Additional equation that determines the growth rate: We are interested in steady state solutions of Eq. (1). A steady state solution with positive values of the variables p , r , c , and a exists for any growth rate g with $g < k_p/p_r$. The upper boundary of the growth rate k_p/p_r results from the fundamental limit where all ribosomes exclusively translate ribosomal protein. To constrain the value of g in the model, an additional equation is needed. We use

$$s_p = p_0 g N_o. \tag{4}$$

This equation incorporates the mechanism first proposed by Donachie that couples protein synthesis to the initiation of DNA replication and cell division [Donachie, 1968]. In this mechanism, a new round of chromosome replication is initiated whenever the total protein content of the cell per origin of chromosome replication reaches a certain constant value. It follows directly from Eq. (4) that in steady state the amount of protein per replication origin p/N_o is constant and equal to p_0 .

2.1 Optimal regulation of ribosome synthesis in different nutrient environments

Combining Eq. (1) with Eq. (4) yields a closed system of equations and enables us to calculate the optimal ribosome synthesis rate s_r that maximizes the growth rate g in different conditions. For $\rho = \delta = 1$, i.e. in the absence of antibiotics and for given ν_a , we vary the value of s_r and determine the value s_r^{max} at which g is maximal in steady

state. We perform this calculation for a range of values of the nutrient influx ν_a with $\nu_a > 0$ to obtain a set of solutions that describes the effects of different nutrient environments (growth media). The maximal growth rate that can be achieved increases with increasing ν_a . For realistic parameters (discussed in Section 3 below), the steady state cell composition at the optimal ribosome synthesis rate in different nutrient environments resulting from our model is in good agreement with experimentally observed values [Bremer & Dennis, 1996], see Figure S6. This agreement justifies our simplifying assumptions and shows that optimal regulation of ribosome synthesis can be incorporated in a model of bacterial growth in a way that is completely consistent with experimental data.

2.2 Effects of antibiotics

The set of solutions describing growth in the absence of antibiotics determines the optimal rate of ribosome synthesis per *rrn* operon s_r^{opt} as a function of the intracellular resource concentration a/V : It is defined as $s_r^{\text{opt}}(a/V) = s_r^{\max}/(N_{\text{rrn}} N_o)$. Here, we approximate the average number of *rrn* operons per cell by N_{rrn} times the number of replication origins N_o . This is a good approximation because most of the *rrn* operons are located near the replication origin of the chromosome [Blattner et al., 1997]. Below, we will apply the function $s_r^{\text{opt}}(a/V)$ to the case where antibiotics inhibit translation or DNA synthesis.

In presence of a DNA synthesis inhibitor, i.e. when $\delta < 1$, the growth rate can be limited by DNA synthesis which is not captured by Eq. (4). To account for this, we additionally use the equation

$$N_f = N_f^{\text{nd}}(g). \quad (5)$$

Here, $N_f^{\text{nd}}(g)$ is the number of replication forks for the steady state solutions in absence of antibiotics in which g is varied by using different ν_a . Eq. (5) ensures that the inhibition of DNA synthesis is not simply compensated by increasing the parallel replication of the chromosome using an increased number of replication forks; this would lead to a DNA content per cell that increases with increasing DNA synthesis inhibitor which is not observed experimentally [Georgopapadakou & Bertasso, 1991]. This could also be ensured by imposing other equations than (5) without changing the conclusions discussed here. For instance, one could assume that the number of replication forks N_f remains at the steady state value obtained for $\delta = 1$ when δ is reduced below 1. Eq. (5) determines the growth rate in conditions where the limiting factor that determines the growth rate is DNA synthesis and not protein synthesis as in the case described by Eq. (4). Both equations (4) and (5) implicitly define potentially different growth rates g . The actual growth rate is the minimum of the two values capturing that in presence of the different kinds of antibiotics growth is either limited by protein synthesis or by DNA synthesis while in absence of antibiotics, protein synthesis is the limiting factor for growth.

We apply the function $s_r^{\text{opt}}(a/V)$ defined above to the case where antibiotics inhibit translation or DNA synthesis, i.e. where $\rho < 1$ or $\delta < 1$. Figure 7 shows that this approach qualitatively captures changes in the total protein content per cell (Figure 7C), the up- and down-regulation of ribosome synthesis in response to the two different classes of antibiotics (Figure 7D), and the suppressive drug interactions observed between the two classes of antibiotics (Figure 7E). We define the magnitude of suppression in Figure 7E in analogy to the definition used in Figure 6D (Experimental Procedures). To apply this definition, a notion of drug concentration is required. The exact relations between the drug concentrations and the parameters δ and ρ that describe the effects of these drugs are drug-specific and unknown. For simplicity, we thus assume that the DNA synthesis inhibitor concentration is proportional to $1 - \delta$ and the translation inhibitor concentration to $1 - \rho$. Further, since the model does not capture changes in MIC, we use the line of 50 percent growth in the $(1 - \delta)$ - $(1 - \rho)$ plane to quantify suppression.

2.3 Effects of gene deletions

We investigate the effects of the different genetically manipulated strains in the framework of our model.

***rrn* deletions:** Deleting one or several of the *rrn* operons corresponds to simply decreasing N_{rrn} below the wild type value ($N_{\text{rrn}} = 7$) while leaving all other parameters unmodified. Figure 7B shows that these deletions lead to an increase in growth rate under DNA synthesis inhibition ($\delta < 1$) but not in its absence. Further, six deletions ($N_{\text{rrn}} = 1$) strongly decrease the magnitude of the suppressive drug interaction between DNA synthesis inhibitors and protein synthesis inhibitors (Figure 7E) as observed experimentally (Figure 6D).

***relA* *spoT* deletions:** Deleting the genes *relA* and *spoT* leads to over-expression of ribosomes resulting from the removal of guanosine tetraphosphate (ppGpp), a key negative regulator of ribosome synthesis. We capture this effect in the model by adding a small fraction ϕ of the maximal possible ribosome synthesis rate $s_r^0 f_{\text{res}}$ in a given condition to the optimal ribosome synthesis rate: $s_r = N_o N_{\text{rrn}} \min(s_r^{\text{opt}}(a/V) + \phi s_r^0 f_{\text{res}}, s_r^0 f_{\text{res}})$. Here, $0 \leq \phi \leq 1$ describes the over-expression due to absence of ppGpp-dependent regulation. Figure 7E shows exemplarily for $\phi = 0.4$ that the magnitude of the suppressive drug interaction between DNA synthesis inhibitors and protein synthesis inhibitors increases as a result of ribosome over-expression as observed experimentally (Figure 6B,C).

3 Parameter values

The parameters and variables of the model are listed in Table S3. Experimentally measured or inferred values for almost all parameters are available from the literature or online databases [Bremer & Dennis, 1996, Bionumbers, 2009]. Since a does not describe one specific resource for which the molecule number per cell could be measured, the value and scale (units) of this variable can be chosen arbitrarily. We choose the resource scale such that $a = 1$ at 1 doubling/hour.

Using this choice of resource scale, we determine the values of ν_a , ϵ_p , ϵ_r , and ϵ_c from three constraints: (i) the ratios ϵ_p/ϵ_r and ϵ_p/ϵ_c of the parameters ϵ_p , ϵ_r , and ϵ_c that define the amount of resources consumed to synthesize protein, ribosomes, and DNA, respectively, correspond to those for the ATP turnover of these processes. (ii) At a reference growth rate $g = 1$ doubling/hour, the amounts of ribosomes, proteins, and DNA per cell agree with the corresponding literature values [Bremer & Dennis, 1996]. (iii) The growth rate g must be maximal as a function of s_r with all other parameters fixed.

The parameter M_a that determines the resource concentration a/V at which f_{res} is at half maximum was chosen to give good agreement of f_{res} with the relative changes of the peptide and DNA chain elongation rates for different growth rates in different growth media [Bremer & Dennis, 1996], see Figure S6D. This is possible because for the steady state solutions obtained from varying ν_a in absence of antibiotics, a/V increases with increasing g . Finally, a small value for the resource decay rate k_{deg} was chosen to capture possible resource instability and resource turnover by processes that are not captured in the model. This rate k_{deg} could be set to zero without qualitatively changing the conclusions discussed here.

4 Numerical solutions

We performed all numerical calculations using Mathematica 6.0 (Wolfram Research). In particular, steady state solutions of Eqs. (1), (4), and (5) were calculated by integrating the ordinary differential equations forward in time (using the NDSolve function) until a stable fixed point was reached. We verified that this solution does not depend on initial conditions in our numerical calculations. Suppression in the model was quantified from solutions in which δ and ρ were varied on a 17×17 two-dimensional lattice.

| Symbol | Definition | Value | Source |
|------------------|--|------------------------------------|-------------------------|
| g | Cell division rate, growth rate | 0.69h^{-1} | - |
| r | Number of ribosomes per cell | 1.35×10^4 | [Bremer & Dennis, 1996] |
| p | Number of proteins per cell | 2.4×10^6 † | [Bremer & Dennis, 1996] |
| c | Genome equivalents of DNA per cell | 1.8 | [Bremer & Dennis, 1996] |
| a | Number of resources per cell | 1 * | - |
| η | Ribosomal protein fraction ($0 < \eta < 1$) | 0.11 | [Bremer & Dennis, 1996] |
| k_p | Rate of protein synthesis per ribosome | 0.038s^{-1} ◊,† | [Bremer & Dennis, 1996] |
| τ_C | Replication time of chromosome, “C period” | 50min | [Bremer & Dennis, 1996] |
| τ_D | Delay before cell division, “D period” | 25min ▲ | [Bremer & Dennis, 1996] |
| N_f | Number of replication forks | 2.1 | [Bremer & Dennis, 1996] |
| N_o | Number of replication origins | 2.4 | [Bremer & Dennis, 1996] |
| V | Cell volume | $1\mu\text{m}^3$ | [Bionumbers, 2009] |
| ν_a | Resource influx | 2.42h^{-1} | - |
| <hr/> | | | |
| k_{deg} | Resource degradation rate | 0.12h^{-1} | - |
| ϵ_p | Resources consumed to make one protein | 8.1×10^{-7} †,‡ | - |
| ϵ_r | Resources consumed to make one ribosome | 2.2×10^{-5} ‡ | - |
| ϵ_c | Resources consumed to make one chromosome | 0.039 ‡ | - |
| M_a | Resource conc. where chain elongation rates are at half max. | $0.53\mu\text{m}^{-3}$ | - |
| p_o | Protein per replication origin [Donachie, 1968] | 9.9×10^5 | Inferred |
| p_r | Amount of protein per ribosome | 20.7^\dagger | [Bionumbers, 2009] |
| k_V | Cell volume per protein | $3.73 \times 10^{-7}\mu\text{m}^3$ | Inferred |
| k_p^0 | Maximal rate of protein synthesis per ribosome | 0.059s^{-1} † | Inferred |
| s_r^0 | Maximal rate of ribosome synthesis per <i>rrn</i> operon | 72min^{-1} | Inferred |
| τ_C^0 | Minimal replication time of chromosome | 33min | Inferred |
| τ_D^0 | Minimal delay before cell division | 16min ▲ | Inferred |
| N_{rrn} | Number of <i>rrn</i> operons per chromosome | 1 to 7 | [Blattner et al., 1997] |
| ρ | Fraction of functional ribosomes (< 1 with antibiotic) | 0 to 1 | - |
| δ | Relative change of DNA synthesis rate (< 1 with antibiotic) | 0 to 1 | - |

Table S 3: Parameters and variables. Values above the horizontal line depend on the growth rate g and are shown for $g = 1$ doubling/hour which, in the absence of antibiotics ($\rho = \delta = 1$), occurs for a resource influx $\nu_a = 2.42\text{h}^{-1}$. Values for other growth rates which occur for different values of ν_a , ρ , and δ are calculated using the values below the horizontal line, see text.

† assuming an average protein size of 360 amino acid residues

*arbitrarily chosen (see text)

◊based on ribosome efficiency 0.8 and chain elongation rate c_p from Table 3 in [Bremer & Dennis, 1996]

▫for simplicity, we assume $\tau_D = \tau_C/2$ which holds to a good approximation [Bremer & Dennis, 1996]

‡the ratios of ϵ_p , ϵ_r , and ϵ_c correspond to the respective values for ATP molecule turnover to make an average protein, ribosome, and chromosome: $\epsilon_p = 1500$, $\epsilon_r = 4.02 \times 10^4$, $\epsilon_c = 7.23 \times 10^7$ [Bionumbers, 2009]